

INVESTIGATIONS OF THE UV-A PHOTOCHEMISTRY OF THE PESTICIDE AZINPHOS-METHYL

A Thesis

Submitted to the Graduate Faculty

in Partial Fulfilment of the Requirements

for the Degree of

Master of Science

in the Department of Chemistry

Faculty of Science

University of Prince Edward Island

Lovely Yeasmin

Charlottetown, P. E. I.

June, 2006

© 2006. Lovely Yeasmin



Library and
Archives Canada

Published Heritage
Branch

395 Wellington Street
Ottawa ON K1A 0N4
Canada

Bibliothèque et
Archives Canada

Direction du
Patrimoine de l'édition

395, rue Wellington
Ottawa ON K1A 0N4
Canada

Your file *Votre référence*
ISBN: 978-0-494-22834-0

Our file *Notre référence*
ISBN: 978-0-494-22834-0

NOTICE:

The author has granted a non-exclusive license allowing Library and Archives Canada to reproduce, publish, archive, preserve, conserve, communicate to the public by telecommunication or on the Internet, loan, distribute and sell theses worldwide, for commercial or non-commercial purposes, in microform, paper, electronic and/or any other formats.

The author retains copyright ownership and moral rights in this thesis. Neither the thesis nor substantial extracts from it may be printed or otherwise reproduced without the author's permission.

AVIS:

L'auteur a accordé une licence non exclusive permettant à la Bibliothèque et Archives Canada de reproduire, publier, archiver, sauvegarder, conserver, transmettre au public par télécommunication ou par l'Internet, prêter, distribuer et vendre des thèses partout dans le monde, à des fins commerciales ou autres, sur support microforme, papier, électronique et/ou autres formats.

L'auteur conserve la propriété du droit d'auteur et des droits moraux qui protège cette thèse. Ni la thèse ni des extraits substantiels de celle-ci ne doivent être imprimés ou autrement reproduits sans son autorisation.

In compliance with the Canadian Privacy Act some supporting forms may have been removed from this thesis.

While these forms may be included in the document page count, their removal does not represent any loss of content from the thesis.

Conformément à la loi canadienne sur la protection de la vie privée, quelques formulaires secondaires ont été enlevés de cette thèse.

Bien que ces formulaires aient inclus dans la pagination, il n'y aura aucun contenu manquant.

Canada

SIGNATURE PAGES

ii-iii

REMOVED

Abstract

This project focused on the investigation of the photochemistry of the pesticide azinphos-methyl (AZM) using various techniques to explore the kinetics and reaction mechanism of its photolysis with UV-A (290 to <400 nm) light sources in the laboratory and natural environment (in natural water and under direct sunlight). A key aspect of this project was the identification of the intermediate photoproduct involved in the reaction mechanism as well as the final photoproduct(s) of AZM photolysis. Fluorescence spectroscopic techniques were used to study the kinetics of the photodegradation of AZM in a number of solvents. AZM photolysis results with various excitation wavelengths in the fluorimeter showed that complete photodegradation of the pesticide occurred in the aqueous system. In other solvents, complete conversion of the AZM was not observed, at least over the time frame used. On the other hand, kinetic studies using a photoreactor with an excitation wavelength of 350 nm showed AZM to be completely degraded. It was observed that the reaction followed consecutive first-order kinetics ($A \rightarrow B \rightarrow C$) giving a highly fluorescent intermediate B and a relatively non-fluorescent final product(s) C in all the solvents of interest. The solvent polarity effect on the photolysis of the pesticide in protic and aprotic media was examined, which showed no clear dependence on solvent polarity for the growth of the highly fluorescent intermediate ($A \rightarrow B$), but a significant correlation was observed for the further photolysis of this intermediate ($B \rightarrow C$). In aqueous acid buffer solution, AZM photolysis was very slow compare to that in

neutral solution. The observed photolysis of AZM was also observed under direct sunlight in natural water. UV-vis, fluorescence, NMR, HPLC and LFP techniques were used to investigate and identify the intermediate and the final photoproducts. A mechanism of AZM photolysis in the laboratory environment (in water and methanol) is proposed. In this study, N-methyl anthranilic acid was identified as the highly fluorescent intermediate photoproduct. This intermediate photoproduct undergoes further photodegradation processes producing aniline and/or N-methyl aniline, relatively non-fluorescent final product(s). Benzazimide was identified as one of the final photoproducts; it is also relatively non-fluorescent, but is produced by a separate pathway from that producing the N-methylantranilic acid as the highly fluorescent intermediate. It was also proposed that AZM photolysis promoted by sunlight follows the same mechanism found in the laboratory system. The observed photodegradation of AZM by sunlight has important implications for its fate in the environment.

Acknowledgments

In life people meet people. No one remembers every one. But there remain some people whom can never be put out of mind. Certainly, Dr. Brian Wagner is such a respectful person, I would remember forever not only because he is an excellent researcher and a noble teacher but also a great man, a great human. I heard his students often whispering about him "God Chemist." In many occasions I say to myself it is true. A newspaper reports him to be a "radiant researcher". I simply agree. During my research period, I have been with this great scholar as his graduate student. I am lucky. I have a family, two little kids. It was impossible to continue my study if he did not give me freedom. I compiled this freedom into successful results. I found one thing behind Brian that he is so organized towards to manage multiple tasks. He is simple and easy going and whenever I need his help Brian is there and always feel I am the most important out of all. During writing procession of this thesis, I was in Toronto but got every feedback from him. Without such a broaden help this was impossible. THANK YOU.

Is there any way that I can escape Dr. Barry Linkletter without giving thanks? NO! One part of this work is HPLC and Dr. Linkletter allowed me to work in his lab as if I were to be in his group. Thank you. My special thanks goes out to Dr. Norm Schepp of Dalhousie University for doing laser photoflash for this project. I borrowed a photoreactor from Dr. Haines's lab, one of the most important instruments I used and kept it months after months. Thank you Dr. Haines for such an endless help. Thanks to Dawna Lund, the head laboratory technician, and Sharon Martin, secretary of chemistry department for all of your

help and cooperation.

My husband, Shahidur Molla helped me in all respects. Thank you dear. It is my sister Shammi Nasrin, who helped me a lot. Any time I could keep my children with her without any anxiety. She always encourages me. Importantly, I remember you dad and mom for your good wishes and encouragement even being so far from me. Finally, I like to thank every one of my friends and group members. It was a wonderful journey.

Table of Contents

Chapter 1— Introduction

1.1. Azinphos-methyl and Organophosphate Pesticides.....	1
1.2. Organic Photochemistry and the Photodegradation of Pesticides.....	5
1.2.1. Organic Photochemistry.....	5
1.2.2. Photodegradation of Pesticides.....	10
1.2.2.1. Photochemical Pesticide Degradation.....	16
1.3. Literature Review of the Photochemistry of Azinphos-methyl.....	17
1.4. Molecular Fluorescence.....	21
1.5. Project Goals.....	25

Chapter 2— Experimental

2.1. Materials.....	29
2.2. Fluorimeter Based Studies.....	30
2.2.1. Solution Preparation.....	30
2.2.2. Instrumentation.....	30
2.2.2.1. Absorption Spectroscopy.....	30
2.2.2.2. Steady State Fluorescence Spectroscopy.....	31
2.2.3. Kinetic Experiments.....	32
2.2.3.1. Procedure.....	33
2.3. Photoreactor Based Studies.....	34
2.3.1. Solution Preparation.....	34
2.3.2. Instrumentation.....	35

2.3.2.1. Photoreactor.....	35
2.3.2.2. Cuvette Holder Preparation for the Photoreactor.....	35
2.3.3. Kinetic Experiments.....	36
2.3.4. Photoreactor-Based Kinetic Experiment with Acidic Buffer Solution.....	37
2.3.4.1. Solution Preparation.....	37
2.3.4.2. Instrumentation.....	38
2.3.4.3. Procedure.....	38
2.3.5. Identification of the Highly Fluorescent Intermediate.....	38
2.3.5.1. Solution Preparation.....	39
2.3.5.2. Comparison of the Fluorescent Spectra.....	40
2.3.5.3. Kinetic Experiments of Anthranilic Acid and N-methyl anthranilic Acid.....	41
2.3.5.4. Normalization of the Fluorescent Spectra.....	41
2.3.6. NMR Studies.....	42
2.3.6.1. Instrumentation	42
2.3.6.2. Solution Preparation	42
2.3.6.3. Procedure.....	43
2.3.7. HPLC Studies.....	43
2.3.7.1. Instrumentation.....	43
2.3.7.2. Sample Preparation.....	44
2.4. Laser Flash Photolysis Studies.....	44
2.5. Photolysis Studies of Azinphos-methyl under Direct Sunlight using Natural Water.....	45
2.5.1. Sample Collection and Storage.....	45
2.5.2. Solution Preparation.....	45
2.5.3. Procedure.....	45

Chapter 3—Results and Discussion

3.1. Fluorimeter Based Studies.....	47
3.1.1. Analytical Studies of AZM-Methanol Solution.....	47
3.1.2. Analytical Studies of AZM-Water Solution.....	50
3.1.3. Analytical Studies of AZM-(Water-Methanol)Mixed Solution.....	52
3.2. Photoreactor Based Studies.....	54
3.2.1. Kinetic Studies of Azinphos-methyl.....	54
3.2.2. Solvent Polarity Effect.....	67
3.2.3. Acid Buffer Analytical Result.....	70
3.2.4. Identification of the Highly Fluorescent Intermediate and Final Photoproduct(s) of Azinphos-methyl Photolysis.....	72
3.2.4.1. Comparison and Kinetic Results.....	72
3.2.4.2. Normalization of the Fluorescence Spectra.....	75
3.2.5. NMR Studies.....	77
3.2.6. HPLC Studies.....	86
3.3. Laser Flash Photolysis Studies.....	91
3.3.1. Azinphos-methyl Analysis.....	91
3.3.2. Anthranilic Acid Analysis.....	92
3.4. Photolysis of Azinphosmethyl Under Direct Sunlight in Natural Water.....	95
3.5 Proposed mechanism for AZM photolysis.....	99
Chapter 4—Conclusions and Future Work.....	105
References.....	109

List of Figures

Figure 1.1. Structure of azinphos-methyl.....	1
Figure 1.2. Structure of organophosphate insecticides.....	2
Figure 1.3. Spectrum of electromagnetic radiation.....	7
Figure 1.4. Schematic diagram showing possible interactions of an incident light beam (I_0) with matter.....	7
Figure 1.5. The ranges of the electromagnetic spectrum of greatest interest	12
Figure 1.6. The sunlight intensity in the UV.....	14
Figure 1.7. Structure of azinphos-ethyl.....	18
Figure 1.8. Structure of benzazimide.....	19
Figure 1.9. Structure of N-methyl benzazimide.....	19
Figure 1.10. Structure of O, O- diethyl-O (3- methylbenzo[<i>d</i>] [1, 2, 3] triazine-4-yl) phosphate.....	20
Figure 1.11. Structure of N-methyl anthranilic acid.....	20
Figure 1.12. Stylized Jablonski diagram showing various transitions between molecular electronic energy levels.....	23
Figure 3.1. Fluorimeter based photolysis of AZM in MeOH.....	48
Figure 3.2. Photolysis of AZM in MeOH at various wavelengths.....	49
Figure 3.3. Fluorimeter based photolysis of AZM in H ₂ O.....	51
Figure 3.4. Fluorimeter based photolysis of AZM in H ₂ O, MeOH and H ₂ O-MeOH solution.....	53
Figure 3.5. Photoreactor based photolysis of AZM in H ₂ O.....	56

Figure 3.6. Photodegradation kinetics of AZM in H ₂ O.....	57
Figure 3.7. Photoreactor based photolysis of AZM in MeOH.....	59
Figure 3.8. Photodegradation kinetics of AZM in MeOH.....	60
Figure 3.9. Photodegradation kinetics of AZM in deuteriated MeOH.....	61
Figure 3.10. Photodegradation kinetics of AZM in EtOH.....	63
Figure 3.11. Photodegradation kinetics of AZM in cyclohexane.....	64
Figure 3.12. Photodegradation kinetics of AZM in acetonitrile.....	65
Figure 3.13. Solvent polarity effect on k ₁ for H ₂ O, MeOH and cyclohexane.	68
Figure 3.14. Solvent polarity effect on k ₁ for H ₂ O, MeOH, EtOH and cyclohexane.....	69
Figure 3.15. Solvent polarity effect on k ₂ for H ₂ O, MeOH, EtOH and cyclohexane.....	70
Figure 3.16. Kinetic trace and fit of AZM photolysis in acetate buffer (pH 3.0).....	71
Figure 3.17. Kinetic curve for the anthranilic acid	73
Figure 3.18. The kinetic curve of NMAA (concentration 1.0x10 ⁻⁶ M).....	74
Figure 3.19. Normalized fluorescence spectra of AA (1.0 x 10 ⁻⁶ M), NMAA (1.0 x 10 ⁻⁶ M), and photolyzed (6 hours of irradiation) AZM (4.0 x 10 ⁻⁵ M) in methanol.....	76
Figure 3.20. Normalized fluorescence spectrum of AA (1.0 x 10 ⁻⁶ M), NMAA (1.0 x 10 ⁻⁶ M), and photolyzed (6 hours of irradiation) AZM (4.0 x 10 ⁻⁵ M) in water.....	77
Figure 3.21. Structure of AZM showing different types of protons.....	78
Figure 3.22. ¹ H NMR Spectrum of AZM without any irradiation.....	80
Figure 3.23. ¹ H NMR spectrum after 6 hours irradiation.....	81

Figure 3.24. ^1H NMR NMR spectrum for 36 hours irradiation.....	82
Figure 3.25. ^1H NMR for anthranilic acid without any irradiation.....	83
Figure 3.26. ^1H NMR for N-methyl anthranilic acid without any irradiation...	84
Figure 3.27. ^1H NMR for benzazimide without any irradiation.....	85
Figure 3.28. Chromatogram of unphotolyzed AZM (0.25 mM) in water-methanol (60/40).....	88
Figure 3.29. Chromatogram of unphotolyzed anthranilic acid (0.25 mM) in water-methanol (60/40).....	88
Figure 3.30. Chromatogram of unphotolyzed N-methy anthrnilic acid (0.25 mM) in water-methanol (60/40).....	89
Figure 3.31. Chromatogram of unphotolyzed benzazimide (0.25 mM) in water-methanol (60/40).....	89
Figure 3.32. Chromatogram of the mixture of unphotolyzed AA, NMA, BA and AZM (0.25 mM) in water-methanol (60/40).....	90
Figure 3.33. Chromatogram of photolyzed AZM (0.25 mM) in water-methanol (60/40) after 8 hours of irradiation.....	90
Figure 3.34. Transient absorption spectrum of photolyzed azinphos-methyl	91
Figure 3.35. LFP kinetic trace of anthranilic acid at 420 nm.....	93
Figure 3.36. Transient absorption spectrum of photolyzed anthranilic acid..	94
Figure 3.37. Transient spectrum of photolyzed anthranilic acid measured in deoxygenated solution.....	94
Figure 3.38. Photodegradation curve of azinphos-methyl in natural water under direct sunlight.....	97

List of Tables

Table 2.1. Chemicals used in this project..... 29

Table 3.1. Summarized values of k_1 and k_2 for the solvents of interest..... 66

List of Abbreviations

AA	anthranilic acid
AChE	acetylcholinesterase
AZM	azinphos-methyl
AZE	azinphos-ethyl
EPA	Environmental Protection Agency
HPLC	high-performance liquid chromatography
LFP	laser flash photolysis
NMAA	N-methyl anthranilic acid
NMR	nuclear magnetic resonance
OP	organophosphate
UV	ultraviolet
λ	Wavelength
min	minute
m	meter
s	seconds
UV-Vis	ultraviolet-visible
E	energy
h	Planck's constant
ν	frequency
c	speed of light
IR	infrared
Hz	hertz
I_t	Intensity of transmitted light
I_s	Intensity of scattered light
I_a	Intensity of absorbed light
ϵ	molar absorptivity
d	path length
c	concentration
A	absorbance
HOMO	highest molecular orbital

LUMO	lowest molecular orbital
S_0	ground state
S_1	excited state
S_2	excited state
UV-A	ultraviolet-A
UV-B	ultraviolet-B
UV-C	ultraviolet-C
PEST	pesticide
PEST*	pesticide in excited state
F	fluorescence
P	phosphorescence
IC	internal conversion
ISC	intersystem crossing
T_1	triplet state
VR	vibration
I_F	intensity of fluorescence
k_F	rate constant for fluorescence
k_A	rate constant for absorption
k_{IC}	rate constant for internal conversion
k_{ISC}	rate constant for intersystem crossing
t	time
$t_{1/2}$	half-life

Chapter 1

1. Introduction

1.1. Azinphos-methyl and Organophosphate Pesticides

Azinphos-methyl, (Guthion®, AZM) is a nonsystemic organophosphate insecticide, which provides broad spectrum control of non-resistant insects. It is also an acaricide (kills mites). Being a nonsystemic pesticide it is not transported from one plant to another after any application. Its chemical name is O,O-dimethyl-S-[4-oxo-1, 2, 3-benzotriazin-3 (4H)-yl] methyl] phosphorodithioate. Mostly it is applied against leaf-feeding insects as a foliar application. Azinphosmethyl is a colorless crystalline compound. It can be formulated both as a wettable powder and emulsifiable concentrate. It is classified as an organophosphate pesticide because of the presence of phosphorous in its molecular structure, as shown in Figure 1.1.

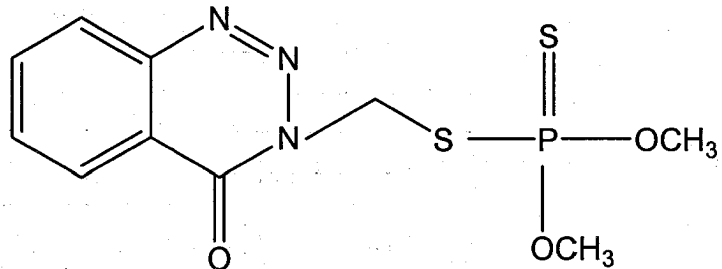


Figure 1.1. Structure of azinphos-methyl

Organophosphates (OPs) are chemical substances originally produced by the reaction of alcohols and phosphoric acid. In the early 1930s Gerhard Schrader, a German scientist, first investigated the insecticide activity of organophosphates. Schrader synthesized a number of organophosphate insecticides; azinphos-methyl being one of the most significant ones.¹ He discovered that the insecticidal activity of this group of pesticides can vary depending on the basic structure (Figure 1.2), which is now known as *Schrader's formula*.¹

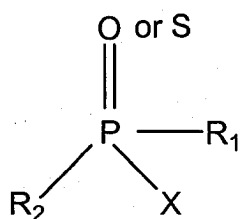


Figure 1.2. General Structure of organophosphate insecticides according to *Schrader's formula*

According to the illustration of the structure shown in Figure 1.2, X is a strong electron withdrawing substituent such as the anion of an organic or inorganic acid (e.g., an aromatic or heteroaromatic, a halogenide, a cyanate, a vinyl group, or other acidic radicals) representing in some cases an effective leaving group; R₁ and R₂ are short chain alkyl, alkoxy (methoxy or ethoxy), or amino radicals.¹

A comprehensive literature survey shows that most of the organophosphates readily undergo conversion from thions (P=S) to oxons

(P=O). In the environment this conversion occurs under the influence of oxygen and light. Oxons are much more toxic than thions, therefore, according to its structure, azinphos-methyl is relatively less toxic than other oxon-based organophosphate insecticides; but oxons break down more readily. Thus, azinphos-methyl is relatively persistent. Ultimately, both thions and oxons are hydrolyzed at the ester linkage, yielding alkyl phosphates and free leaving groups, both of which are of relatively low toxicity.

Organophosphates as a class have become the most frequently used pesticides throughout the world since the decline in the use of organochlorine pesticides in the early 1960s and 1970s; this is mainly because of their rapid breakdown into environmentally benign products. However, they have far more immediate toxicity than DDT and other related insecticides.² There are more than 40 different organophosphate pesticides on the market today, and each of them causes acute and sub-acute toxicity. They are used in agriculture, homes, gardens, and in veterinary practice.

Organophosphate compounds vary greatly in their toxic capabilities and have the advantage over other types of insecticides in that they produce little or no tissue residues. All have a cumulative effect with chronic exposure causing progressive inhibition of cholinesterase.³

AZM, like other organophosphate pesticides, is an acetylcholinesterase (AChE) inhibitor and causes a similar spectrum of symptoms in insects.² This organophosphate reversibly binds to and deactivates the AChE enzyme, inhibiting the breakdown of acetylcholine and

leading to an excess of acetylcholine in cholinergic synapses. This excess acetylcholine initially over-stimulates and then paralyzes cholinergic transmission.³ The bond between the organophosphate and AChE becomes irreversible after a period of approximately 24 to 72 hours, a process referred to as "aging". Toxicity manifests in nicotinic and muscarinic effects in the central and peripheral nervous system.³ AZM, which is a relatively less toxic insecticide being a malathion type of organophosphate, was first used as a pesticide in 1957.⁴⁻⁶ Since then it has proven to be an important pest control tool in agriculture. Today, it is widely used to control the potato beetle and the corn borer, two important potato pests in Canada. The large potato industry in Canada (and in particular Prince Edward Island) is highly dependent upon the use of the pesticide azinphos-methyl. However, in recent years several governmental agencies, including the U.S. Environmental Protection Agency (EPA) have started to reconsider the wide use of AZM and other organophosphorus pesticides due to concern about their effects on the central nervous systems of humans, particularly in children.

The US EPA is currently withdrawing or greatly limiting the use of AZM on a number of crops, fruits and vegetables. In 2001, the Environmental Protection Agency cancelled 28 crops uses of AZM.⁷ This pesticide is highly perilous to fish. In July 2002, AZM was implicated as the culprit of a widespread fish death in Prince Edward Island's Wilmot River and has been linked to fish kills totaling 750,000 by the US EPA.⁸ The usage of azinphos-methyl has recently been restricted on Prince Edward Island.⁹ Seven specific

uses of AZM are being phased-out over four years, and eight crop uses will be allowed to continue with 'time-limited' registration for another four years by EPA. Prior to the expiration of the four year period, the EPA will conduct a comprehensive review of these eight crop uses, based on the latest scientific information, to determine if registration will be allowed to continue. There is no question that a large amount of applied AZM ends up in natural water systems, and has a negative environmental impact.

1.2. Organic Photochemistry and the Photodegradation of Pesticides

1.2.1. Organic Photochemistry

Organic photochemistry is the branch of chemistry concerned with the chemical effects of light on organic compounds. The first law of photochemistry, which is known as the Grotthuss-Draper law, states that light must be absorbed by a chemical substance or matter in order for a photochemical reaction to take place. Therefore, when there is no absorption, no photochemistry can take place.¹⁰ As an illustration, green grass is green because chlorophyll (a green photosynthetic pigment present in plants) absorbs other types of light and reflects green light. To grow a plant under green light (490 nm-570nm) is not possible as the leaves reflect or transmit the light. Hence, no photochemical reaction will occur. The second law of photochemistry, the Stark-Einstein law, states that only one molecule is activated for photochemical reaction for each photon of light absorbed by a chemical system. This is also known as the photo-equivalence law and was

derived by Albert Einstein (and independently by Stark) at the time when the quantum (photon) theory of light was being developed. Only one excited molecule is produced per photon absorbed.¹⁰

Light can be defined as a stream of particles or photons, each with a defined energy, E, and a constant velocity, c, ($3 \times 10^8 \text{ ms}^{-1}$). The energy E can be expressed by the equation,

$$E = h\nu = hc/\lambda$$

where, E = energy, h = Planck's constant, c = velocity of a photon, λ = wavelength, and ν = frequency.

Light is also manifested as electromagnetic radiation, which has wave-like properties that arise from the transverse oscillation of electric and magnetic fields in planes perpendicular to each other and to the direction of propagation of the beam.¹¹

This electromagnetic radiation or light has many forms, some of which are not detectable by the human eyes, such as infrared (IR), radio waves, X-rays, ultraviolet (UV), and gamma rays. The form of electromagnetic radiation that our eyes can detect is called visible or optical light. The spectrum of electromagnetic radiation ranges from low-energy radio waves with long wavelengths to the highly energetic ionizing X-rays and γ -rays on the short wavelength side; this is shown in Figure 1.3.

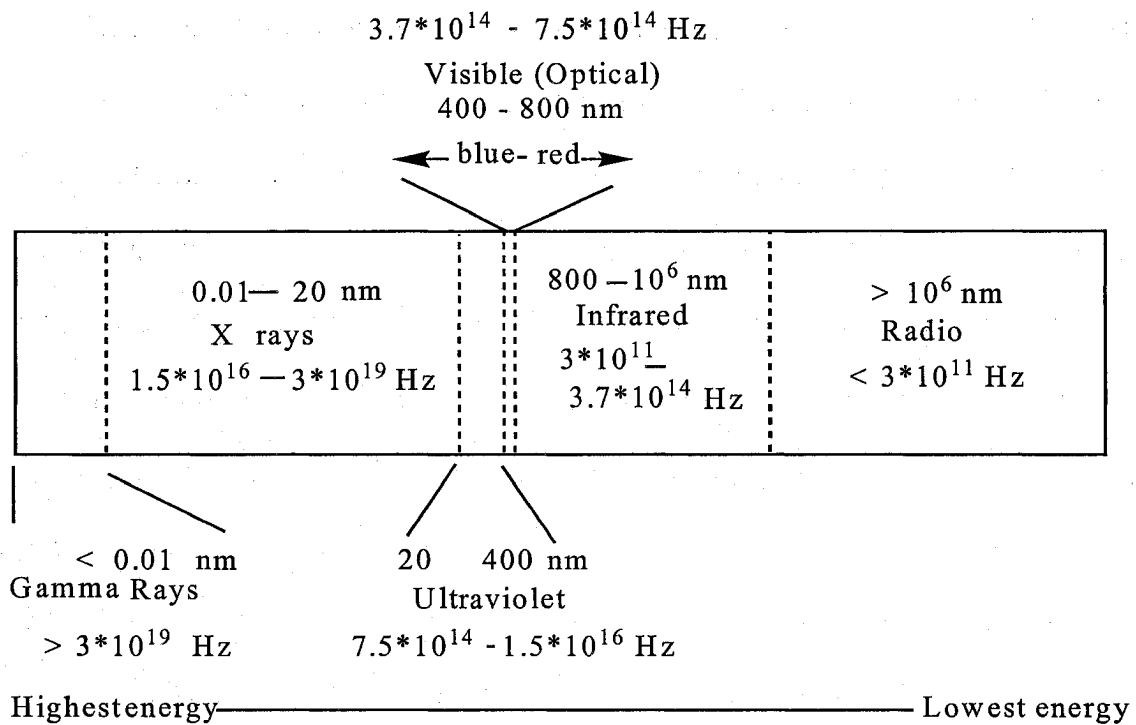


Figure 1.3. Spectrum of electromagnetic radiation

During an interaction of light with matter three events can happen, this is exemplified in Figure 1.4.

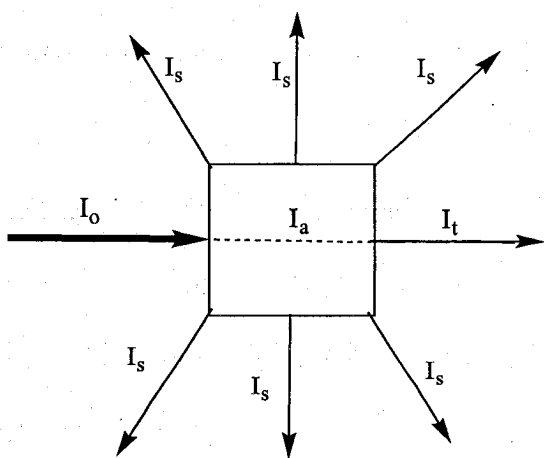


Figure: 1.4. Schematic diagram showing possible interactions of an incident light beam (I_o) with matter

The light can be transmitted (I_t), scattered (I_s), or absorbed (I_a). Only absorption can lead to a photochemical reaction (Grothuss-Draper law). When the incoming light is absorbed by the matter (I_a), the intensity of the incident beam of light (I_o) is reduced resulting in a lower intensity of transmitted light (I_t). This absorption of light is proportional to the number of molecules absorbing light of that wavelength. For monochromatic light, the Beer-Lambert law expresses this relationship for a solution of a compound as follows:

$$I_t = I_o - I_a = I_o \times 10^{-\epsilon cd}$$

$$\log I_o / I_t = A = \epsilon c d$$

where, A = absorbance; ϵ = molar absorptivity of the absorber; c = concentration of absorber and d = path length through which the light beam has passed. According to the Stark-Einstein law, a molecule acquires exclusively well-defined imparted excess energy (photon) after absorption of light. The absorbable portion of light depends firmly on the chemical structure of the molecule that absorbs the energy, and thereby changes from the lowest energetic electronic level, *i.e.*, ground state, to a higher level, the so-called excited state.¹⁰

From a photochemical point of view, the electrons in the highest occupied molecular orbital (HOMO) are of greatest interest. These HOMO electrons exhibit the least attraction to the nucleus because of their distance

from the nucleus and therefore require the smallest amount of energy to be promoted to the next higher energy level, the lowest unoccupied molecular orbital (LUMO). The molecule will absorb that light with exactly this defined HOMO-LUMO transition energy gap (i.e., exactly the right wavelength). If there is no inversion of the spin occurring immediately after the first excitation, the absorbing molecule undergoes a transition to the first singlet excited state (S_1) from the singlet ground state (S_0). The lifetimes of upper excited states (S_2 , etc.) in organic molecules are extremely short, therefore, they usually have no important role in organic photochemistry.

The ability of a molecule to absorb light of defined energy is strictly dependant on its chemical structure. The presence of chromophores, such as aromatic or carbonyl groups, is required for the absorption of light. The specific arrangement of atoms leading to absorption of photons at specific wavelengths is referred to as a chromophore. The chromophore represents the reactive part of an organic molecule in photochemistry, which is primarily responsible for the photochemical activity.¹² As an example, in most organophosphorus pesticides having the Schrader's structure (Figure 1.2), X is a substituted aromatic group; most likely the π -conjugated structure in X will be responsible for the absorption of UV-A light in the solar radiance with wavelength larger than 295 nm.¹³

1.2.2. Photodegradation of Pesticides

Photodegradation of pesticides has been recognized as an important factor in the environmental fate of these xenobiotics. It is obvious that a more comprehensive knowledge of the pesticidal residues found in the environment after the photochemical decomposition of the parent molecule is very important for assessing the potential risks for the health of both humans and animals, during and after the release of the xenobiotics. Pesticides can be applied as liquid spray droplets, or wettable powder. However, after any application on the intended target, i.e. plant or soil, it does not necessarily remain entirely as a surface deposit. There is the possibility that a significant portion of the applied pesticides can go into different regions of environment, such as the atmosphere or surface water. Spray drift, wind or simply volatilization can be responsible for the promotion of the xenobiotic into the atmospheric gas and aerosol phases, where a non-negligible fraction of anthropogenic origin can be made up by pesticides.¹⁴ Leaching because of seasonal rainfall or storms provides the pesticide entrance into the aqueous phases of the environment like surface water, soil moisture and also onto the soil surface. The atmosphere acts as an important transport vector in the dispersal of any pollutant or chemical. Atmospheric current can move pesticides even over long distances to remote areas, e.g., to oceans, deserts or the far regions of the poles.^{14, 15}

Pesticides are very susceptible to external influences when they are released into the environment, which can result in their degradation or

transformation. The physical and chemical properties of the contaminant or of its microenvironment can control the rate and the course of these conversions. Enzymatic or metabolic decomposition of a pesticide is predominant in microorganisms, and also, after uptake, in animal and plant organisms when they are in water, moist soil, or plant surfaces. In inanimate nature, hydrolysis, oxidation, reduction, and above all photochemical processes contribute to a great extent to the chemical transformation of pesticides in the environment.

Chemical changes of the parent molecule do not always result in a "less toxic compound". For example, the best known organophosphorus insecticide, parathion, is rapidly photooxidized on soil and dust surfaces to the more toxic paraoxon.¹⁶ Another example is photodieldrin, which is the photoproduct of an organochlorine insecticide dieldrin, and is more active against flies than the parent compound.

Negative ecological consequences of pesticide use depend significantly on the persistence of the pesticide in the environment after its application. To minimize this negative impact of pesticidal residues, they need to be decomposed after the necessary residence time in the environment required for pest control. Sunlight photolysis can be one of the significant pathways for the destruction of pesticides inside either aerosol particles or residues¹⁷. Solar radiation between 290 nm and 800 nm can penetrate the earth's atmosphere; this radiation in this region is responsible for the photochemistry of pesticides. When sunlight passes enters the atmosphere

its intensity becomes weakened because of molecular and aerosol scattering and also absorption by atmospheric gases. Figure 1.5 shows a more detailed description of the relevant portion of the electromagnetic spectrum, showing in particular the subregions of the UV particularly important to this project. They are the UV-C (200-280 nm) , UV-B (280-320 nm), and UV-A (320- 400 nm).

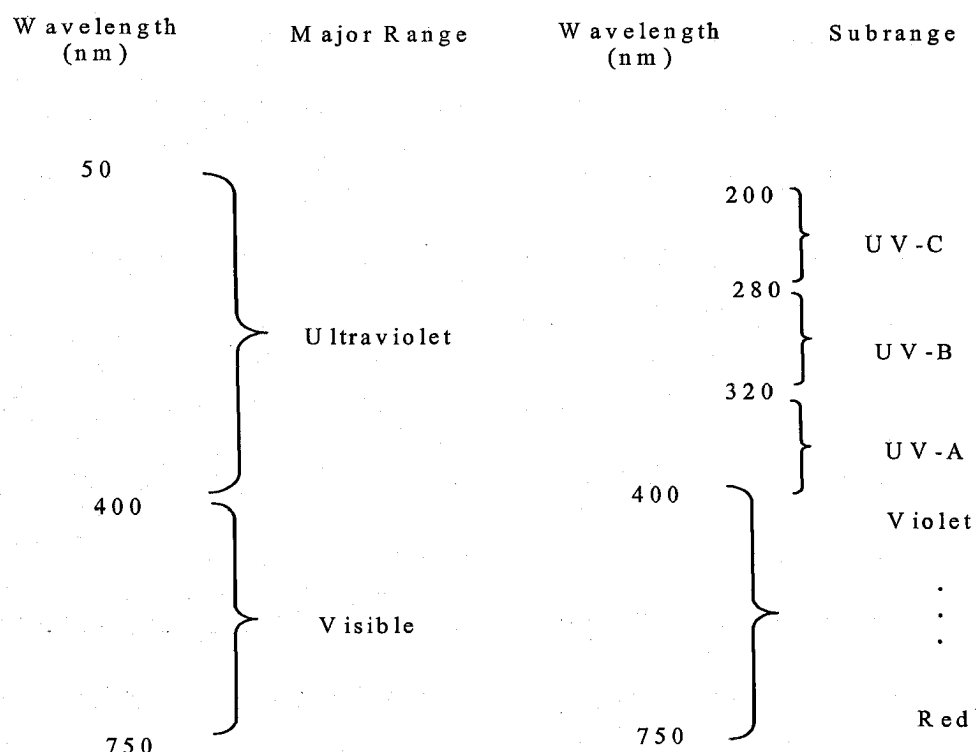


Figure 1.5. The ranges of the electromagnetic spectrum of greatest interest.

Stratospheric ozone, aided to some extent by O_2 , absorbs ultraviolet light at the shorter wavelength ranges 220-290 nm, which overlaps the 200-280 nm region known as UV-C.¹⁸ Ozone can absorb almost all photons

between 280 and 320 nm; as a result the intensity of UV-B radiation sharply decreases at the earth's surface.¹⁹⁻²¹ The lowest wavelength of sunlight that can reach the earth's surface was recorded as 286.3 nm.²¹ Therefore, wavelengths <290 nm can be considered as non-significant for the photochemistry induced by sunlight on earth. On the other hand, wavelengths greater than 800 nm do not have sufficient energy to break chemical bonds of ground state molecules.²¹

UV-A light, that ranging from 320-400 nm, is designated as the least biologically harmful region of ultraviolet light, but it does penetrate to the Earth's surface much more than the more harmful UV-B. The reason is that UV light in this region is not absorbed significantly by ozone, O₂, or other constituents of the clean atmosphere. The sunlight intensity in the UV region and in part of the visible region, which were measured outside the atmosphere and at the Earth's surface is shown in Figure 1.6. The curve at the left corresponds to the intensity of light received outside the Earth's atmosphere, whereas the curve at the right corresponds to the light that is transmitted to the troposphere, i.e. to the surface; the vertical separation at each wavelength between the curves corresponds to the amount of sunlight that is absorbed in the stratosphere and outer regions of the atmosphere.

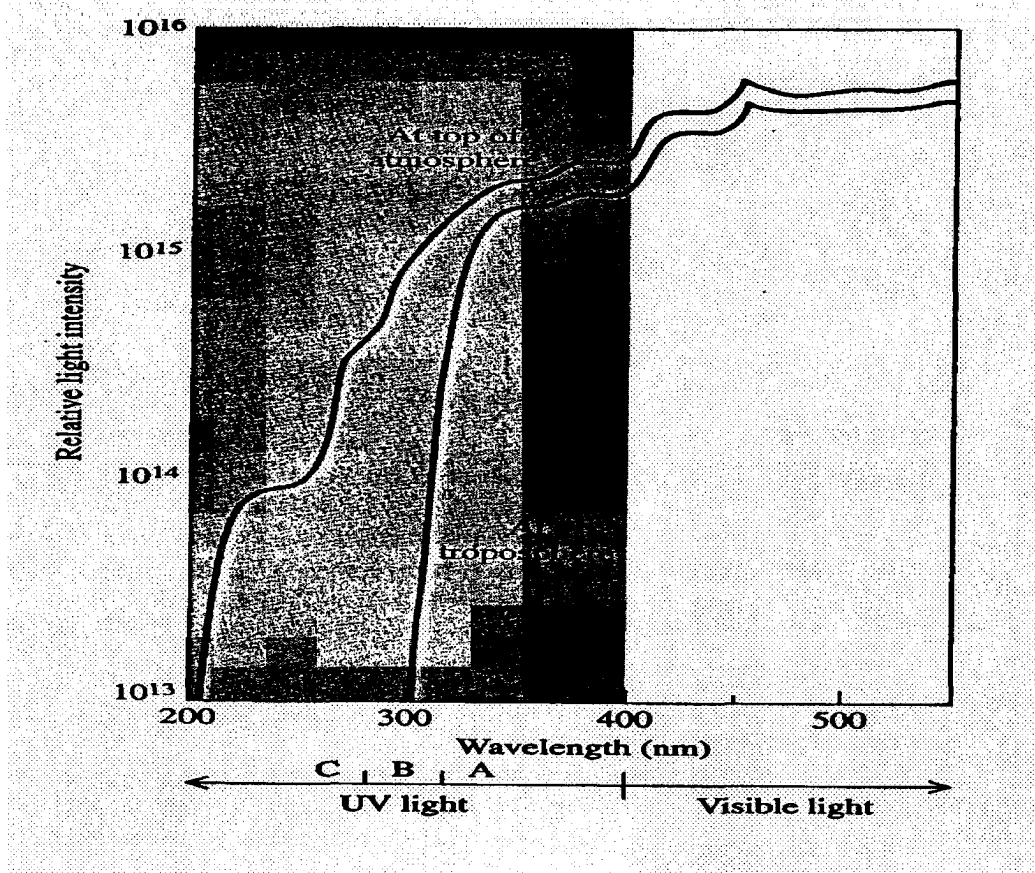


Figure 1.6. The sunlight intensity in the UV and in part of the visible region measured outside the atmosphere and at the Earth's surface. (Reproduced from reference 18).

Various factors are responsible for the spectral distribution of sunlight and the resulting intensity spectrum. For example, the thickness of the ozone layer depends on the season, the angular height of the sun at different period of time, i.e., midday –sunset, summer-winter, and the latitude. Other factors may also be involved, such as the geographical altitude and the clearness of the sky.

Like the spectral distribution and intensity of the exciting radiation, the surrounding medium also influences the photochemical behavior of a

molecule.²³ In pure media such as distilled water, direct photolysis is predominant after intrinsic absorption of light energy of a molecule.²⁰ In natural waters, incident light is strongly attenuated to a much lower intensity depending on the depth of water and the degree of turbidity, e.g. photodegradation can take place in about the first 30 m in ocean water; this is referred to as the photic zone.²⁴

A significant portion of the solar radiation which penetrates the water body is absorbed by various naturally occurring substances, like aquatic humic substances and other natural photosensitizers. Hence, resultant electronically excited molecules (e.g., O_2^- , H_2O_2 , 1O_2 , etc) can react with aquatic pollutants. Therefore, photodegradation can occur even though the molecules are stable to sunlight in distilled water.²⁵⁻²⁷ The various photochemical processes already mentioned are very important in elucidating their risk assessment for environmental contamination. The chemistry of the interaction of various environmental compartments with pollutants is very complex and still mostly unknown. Photochemical investigation under natural environmental conditions is extremely difficult and to some extent impossible due to the dependence of the spectral distribution and intensity of the sunlight on time, location and other factors, as mentioned above. Therefore, oversimplified laboratory modeling and experiments under a limited range of controlled and reproducible conditions may serve to understand the photochemical behavior of a pesticide in a selected medium (e.g., aqueous,

organic, etc.) and can also provide very useful data that can be transferable to natural conditions.

1.2.2.1 Photochemical Degradation of Pesticides

Photochemical methods can be considered for pesticide degradation in two distinct processes:

1. Direct photolysis and;
2. Indirect photolysis.

Direct photolysis of pesticides is a two-step process in which UV-A light is the source of irradiation, $h\nu$:

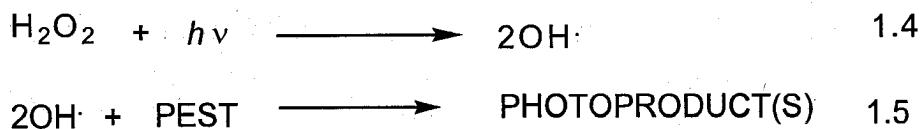


with PEST = pesticide in the ground state; PEST* = pesticide in the electronically excited state. A third step, which is competitive with step 1.2, may occur:



with X = solvent, pesticide or other molecule present in the solution.

The indirect photochemical method is based on the photolysis of H_2O_2 by UV light. It leads to the formation of OH^- radicals, which react subsequently with pesticides:



1.3. Literature Review of the Photochemistry of Azinphos-methyl

The properties of azinphos-methyl have been studied since 1959.²⁸ Since then, a number of studies of its photochemistry have been reported. Kuriharaha and Crosby in 1966 reported that an abstraction of hydrogen from the solvent could be possible during AZM photolysis under UV light.²⁹ Crosby in 1969 reported another experimental approach to AZM photodecomposition.³⁰ In his approach the photolysis of azinphos-methyl in hexane was described, with the formation of benzazimide and trimethyl phosphorodithioate as photoproducts. They also reported the formation of small amounts of anthranilic acid and a cholinesterase-inhibiting polymer in both hexane and methanol. Schulz and coworkers investigated the persistence and degradation of azinphos-methyl in soils in 1970.³¹ An investigation was performed by Liang and Lichtenstein to elucidate the

photochemical characteristics of azinphos-methyl, using ^{14}C substituted AZM in 1972.^{32, 33}

There have been no more recent investigations of the photochemistry of AZM. However, Abdou and coworkers investigated the photochemical behavior of the ethyl analogue of AZM, azinphos-ethyl (AZE, shown in Figure 1.7) in 1987.³⁴ Thus both AZM and AZE, two triazine derivatives, exhibit a number of photochemical reactions on exposure to both UV light and sunlight. This is contradictory to the related 3-alkyl substituted 4-oxo-benzo[d][1,2,3]triazines, which have been reported to be generally stable to UV light irradiation in the photochemical literature.³²

Since most of the AZM work has been done with soils, the most relevant literature work to this project is that on the AZE analog (Figure 1.7). This work will be discussed in detail here.

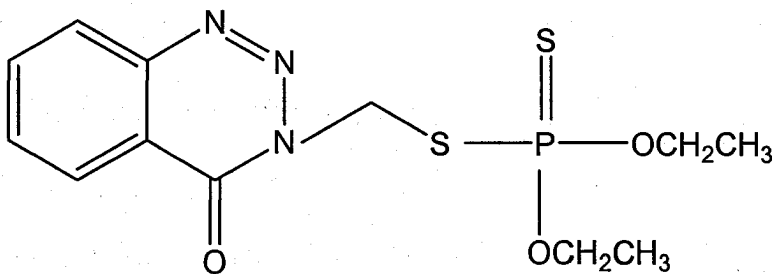


Figure 1.7. Structure of azinphos-ethyl

Abdou and coworkers³⁴ used 313 nm radiation to irradiate AZE in chloroform, using a Pyrex photoreactor. They could separate four crystalline products of

the photoreaction, besides elemental sulfur. One of them was benzazimide (Figure 1.8) and another one was N-methyl benzazimide (Figure 1.9).

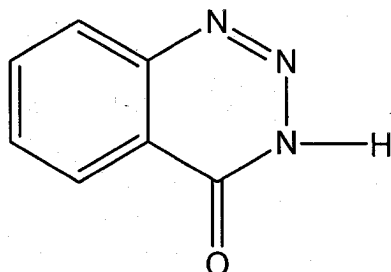


Figure 1.8. Structure of benzazimide

Both of these products were also found by Liang and Lichtenstein in their AZM work.^{32,33} The formation of these two compounds was explained by homolytic cleavage of the side chain, either of CH₂-S- or N-CH₂- bond (Figure 1.7) and hydrogen transfer from the solvent.

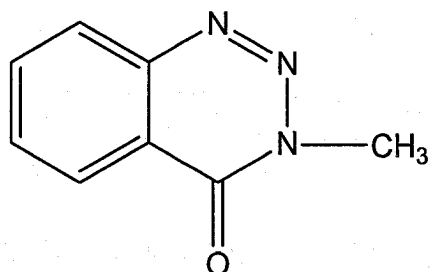


Figure 1.9. Structure of N-methyl benzazimide

A well-documented reaction pathway in the photochemistry of various sulfides and sulfoxides is initial photochemical desulfuration, which is followed by intramolecular rearrangement of the resulting radical and P=S to P=O

oxidation mentioned earlier. Initial photochemical desulfuration was the proposed reaction pathway by these authors to lead to the third photoproduct, O, O-diethyl-O (3-methylbenzo[*d*] [1, 2, 3] triazine-4-yl) phosphate (Figure 1.10). This photoproduct was clearly different from an oxygen analogue of azinphos reported in the first paper of Liang and Lichtenstein.³²

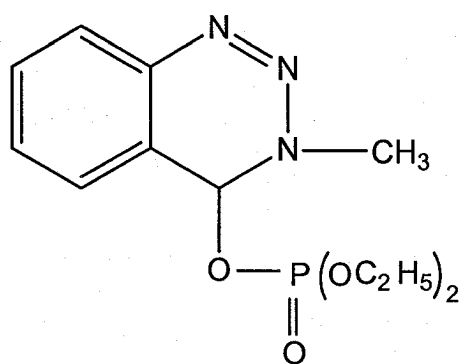


Figure 1.10. Structure of O, O-diethyl-O (3-methylbenzo[*d*] [1, 2, 3] triazine-4-yl) phosphate

Another photoproduct was the solvent dependent photochemical generation of N-methyl anthranilic acid (Figure 1.11) that was preceded by the homolytic cleavage of the triazine moiety and extrusion of nitrogen. The mechanism was previously reported in some publications of Ege *et al.*³⁴

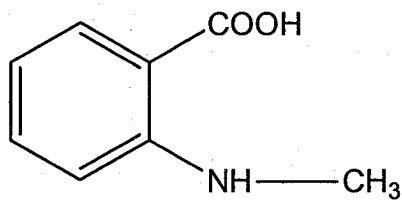


Figure 1.11. Structure of N-methyl anthranilic acid

Again, all of these studies were performed in solution with chloroform solvent. Using methanol as solvent these authors could identify methyl N-methyl anthranilate, which is formed by the same mechanism as N-methyl anthranilic acid.

1.4. Molecular Fluorescence

Molecular fluorescence is the physical process involved in the optical emission from molecules that have been excited to higher energy levels due to absorption of electromagnetic radiation. Because of the absorption of a photon by an organic molecule the transformation of an electron occurs from an occupied bonding molecular orbital to an upper unoccupied (higher energy) orbital. If the resulting excited state has two unpaired electrons with opposite spins, it is called a singlet and when the spins are parallel, it is termed as a triplet. In the absence of chemical reactions, the electronic deactivation or relaxation can occur in one of two ways, either (1) radiatively by the emission of a photon of light, or (2) non-radiatively with the release of the excitation energy as heat. Molecular fluorescence is the emission of light by an electronically excited molecule during an electronic transition between states of the same spin multiplicity. Therefore, fluorescence (F) is a radiative transition. Another type of radiative transition is phosphorescence (P), in which emission of the light occurs from a molecule during an electronic transition between states of different spin multiplicity. The two major non-

radiative transitions are internal conversion (IC) and intersystem crossing (ISC). Internal conversion involves relaxation to a state of the same multiplicity; on the other hand, intersystem crossing involves relaxation to a state of a different multiplicity. Thus, these are the non-radiative analogues of fluorescence and phosphorescence, respectively.³⁵ Phosphorescence and intersystem crossing are spin forbidden, as they require a change in state multiplicity. Hence they tend to have rate constants which are orders of magnitude smaller than those for fluorescence and internal conversion.³⁵

The well-established Jablonski diagram provides a convenient illustration of these various radiative and non-radiative transitions, as shown in Figure 1.12.³⁶ This diagram shows the ground (S_0) and first excited singlet (S_1) and triplet (T_1) states as well as vibrational levels of each electronic state. This diagram also shows the transitions between these states with radiative transitions indicated by solid arrows and non-radiative transitions indicated by wavy arrows. The other non-radiative process that is shown in the diagram is vibrational relaxation (VR). This is an extremely rapid process by which vibrationally excited states relax to the ground vibrational level within an electronic state.³⁶ This is very a rapid relaxation process (ranges from femtosecond to picosecond time scale) of vibrational excitation within an electronic level, and consequently all electronic transitions occur from the lowest vibrational level of an electronic state. In the case of fluorescence, the most important consequence of this is that the energy of the emitted photon is always less than or equal to the energy of the absorbed photon. Therefore, in

the case of the transition between the ground vibrational levels of the S_0 and S_1 states ($v=0$ to $v'=0$) the photon energies are equal. Thus, the fluorescence spectrum for a given transition occurs at lower energy, or longer wavelengths in comparison to the absorption spectrum. Vibrational relaxation is also involved in both internal conversion and intersystem crossing, which are in fact isoenergetic process between vibrational levels of different electronic states, followed by rapid vibrational relaxation to the lowest vibrational level of the lower excited state.³⁶ These two processes are shown together in Figure 1.12 by the single vertical wavy arrow as a single step for convenience in the case of internal conversion, but is shown as the two step mechanism in the case of intersystem crossing.

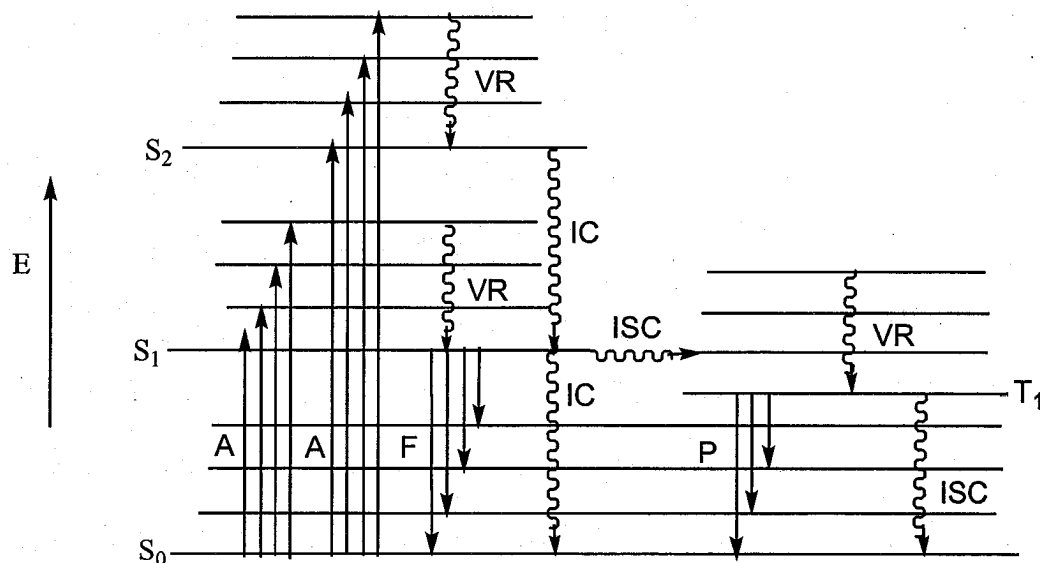
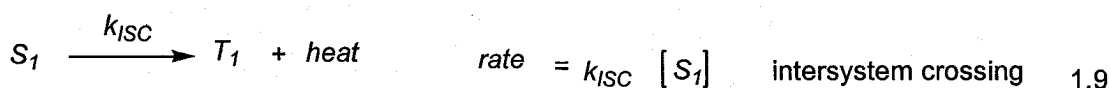
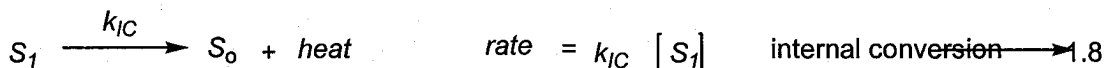
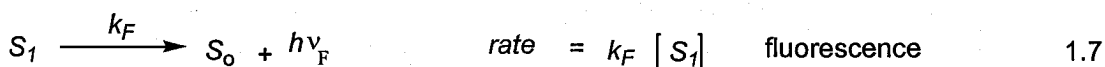
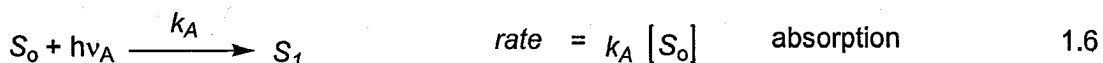


Figure 1.12. Stylized Jablonski diagram showing various transitions between molecular electronic energy level.

The processes illustrated in Figure 1.12 can all be described kinetically as first order processes. The rate law for each of these processes is therefore expressed as the product of a rate constant and the concentration of the initial electronic state. The following equations are the relevant expressions of the mechanism related to fluorescence emission.³⁷



The fluorescence intensity, i.e., number of photons per second emitted can be expressed by the following equation.

$$I_F = k_F [S_1] \quad 1.10$$

Thus, the intensity of fluorescence provides a measure of the number of molecules in S_1 , and thus, the concentration of the fluorophore itself.

Fluorescence is most commonly measured by the steady-state fluorescence spectroscopy technique. According to this technique, the solution containing the fluorescent molecule is continuously illuminated by a stable excitation light source. Since the excitation light is maintained at a

constant intensity, this results in a constant rate of absorption, k_A of the molecule and hence, a constant rate of formation of the first excited singlet state, S_1 , as given by equation 1.6. The rates for the three relaxation processes shown in equations 1.7 to 1.9 are also constant, which results in a very rapid establishment of steady state condition, where the rate of relaxation or decay of the S_1 population is exactly the same as the rate of its formation. This results in a constant S_1 population meaning that under these conditions, the rate of fluorescence emission (Equation 1.7) is constant as both $[S_1]$ and k_F are constant. Since $[S_1]$ is proportional to $[S_0]$, this gives the relationship to fluorophore concentration. The experimental details for the measurement of the resulting fluorescence in this project will be discussed in the Experimental section (Chapter 2).

1.5. Project Goals

The literature review described in Section 1.3 shows that studies of the photolysis of azinphos-methyl was confined to the identification of the degraded final photoproducts, and there have been no published reports on the reaction mechanism, nor on any intermediates that might be involved. As described in Section 1.3, the only relevant description of a photolysis mechanism was that of Abdou and his co-workers³⁴, who proposed reaction mechanisms for the identified photoproducts of azinphos-ethyl (AZE) UV-photolysis. Recently, Wagner's group³⁸ discovered that continuous exposure of AZM to a UV source results in its significant fluorescence enhancement,

presumably via formation of a more fluorescent photoproduct(s). Interestingly, this UV exposure was performed directly in the fluorimeter, using the excitation lamp! The mechanism for the photolytic degradation of AZM, and the identity of the highly fluorescent photoproduct, remained unknown. This is the major goal of this thesis. The achievement of this goal is important not only for the fundamental understanding of the photochemistry of AZM, but also for the information that such a study may provide on the environmental fate of this pesticide, as it does indeed enter natural water systems due to its use in the agricultural sector.

Specifically, the integrated goals of this current project are:

- 1) To photolyze AZM in the laboratory and in the natural water environment under direct sunlight, and study the kinetics of this process;
- 2) To determine if the highly fluorescent photoproduct previously observed is itself stable to UV exposure;
- 3) To identify the highly fluorescent photoproduct (or intermediate if it is photoreactive) and other relatively non-fluorescent final photoproduct(s) of AZM photolysis;
- 4) To determine the mechanism of the UV-A photochemistry of AZM;

- 5) To photolyze AZM in natural water samples under direct sunlight, to investigate its potential photolysis in the environment.

With respect to the final goal, to the best of our knowledge no previous work has been reported on the photolysis of AZM in aqueous media in the environment, nor on the role of photolysis by sunlight on its environmental fate.^{29-34, 39}

These goals will be achieved by experimental studies involving first photolyzing solutions of AZM using various sources of UV light (fluorimeter excitation lamp, a UV photoreactor, or sunlight) for fixed periods of time, then monitoring the progress of the reaction by measuring the fluorescence spectrum of the reaction mixture. This takes advantage of the fluorescence enhancement work on AZM solutions upon UV exposure previously reported by our group.³⁸ This project also involves the identification of the highly fluorescent intermediate(s) or photoproduct(s) and relatively non-fluorescent final product(s) using NMR spectroscopy, UV-vis absorption spectroscopy, fluorescence spectroscopy, high-performance liquid chromatography (HPLC), and laser flash photolysis (LFP) techniques. It is interesting to note that the previous study by Wagner *et al.* reported that the fluorescence of AZM in aqueous solution is also enhanced by increasing the pH to 12.0, by a huge factor of 300, and that previous studies by other researchers established this

to be the result of base hydrolysis of AZM to anthranilic acid, which is indeed a highly fluorescent compound. This is therefore also a likely suspect in these photolysis reactions. Finally, it is our aim that these studies will lead to a much greater understanding of the chemistry and photochemistry of this very important pesticide, and thereby to a greater understanding of its fate upon entering the environment.

Chapter 2

2. Experimental

2.1. Materials

Chemical compounds used in this project are listed in Table 2.1 with source and grade. The pesticide was used as received and without further purification. In addition to these commercial compounds, a natural water sample was collected from a selected location (Rolling Pond stream in North Rustico, PEI) in a plastic flask and was stored in the freezer.

Chemical	Source	Grade
H ₂ O	UPEI Chemistry Research Lab	Deionized
Methanol	Aldrich	HPLC
Ethanol	Aldrich	Absolute
Acetonitrile	Aldrich	HPLC
Cyclohexane	Aldrich	HPLC
Methanol-d ₄	CDN Isotopes	99.9% D
Acetic Acid	Aldrich	Reagent
Sodium Acetate	Aldrich	Reagent
Azinphos-methyl	Aldrich	Pesticide grade
Anthranilic Acid	Aldrich	Reagent
Benzazimide	Aldrich	Reagent
N-methyl anthranilic acid	Aldrich	Reagent

Table 2.1. Chemicals used in this project

2.2. Fluorimeter-Based Studies

2.2.1. Solution Preparation

Different solutions of azinphos-methyl pesticide were prepared using methanol, distilled deionized water and various water-methanol mixtures for the photolysis of AZM in the fluorimeter. The concentration of the pesticide in each solvent was 4.0×10^{-5} M; this gave an appropriate absorbance for the fluorescence studies. This solution was prepared by dissolving 0.0012 g of AZM into 100 mL of each solvent. In methanol, AZM was found to be readily dissolved. It required one hour of sonication in the case of distilled water solution because of its poor solubility in aqueous media. In addition, solutions (4.0×10^{-5} M) in water-methanol mixtures of different proportions (1:1, 3:1, and 9:1) were prepared. In each case, preparation of these mixed solutions also required sonication for a period of time depending on the solvent used. All of the solutions were kept sealed in a dark cupboard in the laboratory at room temperature.

2.2.2. Instrumentation

2.2.2.1. Absorption Spectroscopy

During the course of this project, the initial absorption spectra were recorded for all solutions. The absorption wavelength of interest in this fluorimeter-based study was 315 nm. This wavelength was chosen on the basis of the previous work in our laboratory.⁴⁰ In this project, a Cary 50 Bio

UV-vis spectrophotometer was used to measure the absorbance of all solutions.

2.2.2.2. Steady State Fluorescence Spectroscopy

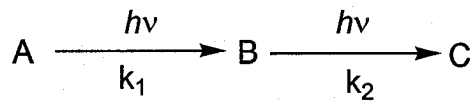
The steady-state fluorescence technique described in Section 1.4 was used to measure the fluorescence spectra of the pesticide in this study. A Perkin Elmer LS-55 fluorimeter was the instrument used for this purpose. This fluorimeter is equipped with a Xe lamp excitation source, 1 cm² quartz cuvette as a sample cell, monochromator, and a photomultiplier tube as the fluorescence detector. Molecules in solution are excited with UV light from the xenon lamp. Broadband excitation light from the lamp passes through a monochromator, which allows for selection of the wavelength of interest (with a spectral width determined by the monochromator slit widths, typically 3-5 nm). Then the fluorescence is collected at right angles to the incident light, dispersed by another monochromator and detected by a photomultiplier tube.

In this study, the fluorescence enhancement, I/I_0 was determined as the ratio of the intensity under the fluorescence spectrum (I_F versus λ_F) of the AZM solution after and before photolysis, where, I is the intensity after photolysis and I_0 is the intensity before photolysis, both measured at the emission maximum. UV photolysis was monitored by plotting the curves of fluorescence enhancement, I/I_0 , versus UV irradiation time (t_{irr}) at the analytical excitation and emission wavelengths of the pesticide. The

experimental data was recorded and collected using the software for the fluorimeter and analyzed using Fig-P® Version 2.7 software.

2.2.3. Kinetic Experiments

The fluorimeter-based kinetic study of azinphos-methyl photolysis was carried out using the UV source of the fluorimeter to do the photolysis. Excitation/photolysis wavelengths of 300, 315 and 320 nm were used. Kinetic plots of I/I_0 versus irradiation time (t_{irr}) were constructed from the above-described fluorescence data. Kinetic fits were performed using the non-linear curve fitting capability of the commercial Fig-P software program, based on the following kinetic model for the photolytic reaction of AZM (as described in Section 3, a two-step process involving an intermediate was observed):



This is a well-known kinetic model (consecutive first order reactions), for which the following equation can be derived.⁴¹

$$I_F(t) = A \times k_1 / (k_2 - k_1) (e^{-k_1 t} - e^{-k_2 t}) \quad 2.1$$

where, $I_F(t)$ = fluorescence intensity at irradiation time t ; A = pre-exponential factor; k_1 = rate constant of the reaction $A \rightarrow B$; and k_2 = rate constant of the reaction $B \rightarrow C$.

The fluorescence intensity (I_F) of AZM (Equation 2.1) due to the exposure to UV light at various wavelengths was measured as a function of time. The values of k_1 , the growth rate constant, and k_2 , the decay rate constant of the photoproduct(s) (Equation 2.1) were determined by plotting the data as enhancement, I/I_0 , versus time. The following solvent systems were used for the photolysis of AZM: methanol, distilled deionized water, and various ratios of methanol-water mixtures. Samples of the different AZM solutions were exposed to the UV light at 315, 320 and 300 nm excitation wavelengths using the fluorimeter light source and monochromator. The slit widths of the monochromator were adjusted to 2.5 nm for the emission and 15.0 nm for the excitation wavelength. The same set of fluorimeter parameters was used for each kinetic trial with various solvents.

2.2.3.1. Procedure

The prepared solution of AZM in a number of solvents mentioned above was withdrawn from the solution flask (Pyrex glass) and pipetted into a 1 cm², 3 mL quartz cuvette. The absorption spectrum of the sample prior to any exposure to UV light in the fluorimeter was recorded. The cuvette was then placed in the cuvette holder of the fluorimeter and the sample was exposed to the UV light of the fluorimeter for a total of 48 hours in each case.

The initial emission was recorded before any irradiation. The fluorescence spectrum during the photolysis reaction was recorded at an interval of every 120 minutes irradiation to the UV source using the kinetic scan mode of the fluorimeter. The absorption spectrum was recorded after the total irradiation of the AZM pesticide. The maximum wavelength emission for analysis was chosen to be 405 nm. The kinetic curves for each solvent trial were fit to Equation 2.1 using the Fig-P software.

2.3. Photoreactor Based Studies

2.3.1. Solution Preparation

The azinphos-methyl pesticide solution was prepared in distilled water and five different organic solvents, namely: methanol, cyclohexane, acetonitrile, methanol-d₄, and ethanol, to perform the kinetic experiments and to investigate any solvent polarity effect. The concentration of the pesticide in all cases was 4.0×10^{-5} M. In a flat bottom volumetric Pyrex glass flask 0.0012 g of AZM was weighed and solvent of interest was poured into the flask for the required concentrated solution preparation. All organic solvents were HPLC grade except ethanol. Absolute ethanol was used because of the unavailability of higher grade ethanol at the time. The water solution of AZM required sonication for one hour because of poor solubility, as in the fluorimeter-based studies. In other solvents used, the pesticide readily dissolved. All solutions were sealed and stored in a dark cupboard of the laboratory at room temperature.

2.3.2. Instrumentation

2.3.2.1. Photoreactor

All photochemical experiments were performed at room temperature using a photoreactor with 350 nm excitation wavelength. The emission of a set of sixteen Xenon lamps (maximum emission at 350 nm) arranged in a circular pattern within the photoreactor was used as the UV-A source. There was an insignificant rise in temperature observed during the course of photolysis experiment; this was minimized using a cooling fan to control the temperature rise during a long run time. At the top of the reactor, a cardboard box was used to protect researchers from UV light exposure out of the reactor. A special cuvette holder (details in Section 2.3.2.2) was placed on the bottom of a Pyrex measuring flask, placed upside down at the middle of the reactor. Therefore, the distance of the cuvette holder from each UV lamp was the same, and reproducible from sample to sample.

2.3.2.2. Cuvette Holder Preparation for the Photoreactor

A cuvette holder was needed in the photoreactor to place the sample for the UV exposure of the pesticide. The clamp in the photoreactor for the holding purpose was not appropriate for the small, 1cm^2 fluorescence cuvette. Therefore, a special cuvette holder was prepared in our laboratory using a waxy material, Epoxy Putty, an aluminum plate and a 3 mL disposable plastic cuvette. The Epoxy resin and fixer were poured into the aluminum plate and thoroughly mixed (until the color was consistent and fully blended). The

disposable plastic cuvette was wrapped with aluminum foil and set in the middle of the mixed epoxy resin to form a square hole to hold the experimental cuvette once the epoxy was set. The cuvette was left in the waxy putty-coated aluminum plate for one day for the epoxy to be dried and hard. After drying the disposable cuvette was removed and discarded, leaving a usable cuvette holder. The waxy putty was stable at the insignificant temperature rise during the photolysis experiments.

2.3.3. Kinetic Experiments

2.3.3.1. Procedure

The steady-state kinetic experiments with AZM solutions were performed by withdrawing a 3 mL aliquot of solution from the volumetric Pyrex glass flask and pipetting it into the quartz cuvette, which was then placed in the photoreactor ($\lambda = 350$ nm). The total course of irradiation of the pesticide sample in distilled water was 36 hours, whereas a 31 hour exposure time was used for each of the organic solvents. The UV-irradiated sample was then placed into the fluorimeter at the fixed excitation wavelength of interest (315 nm) to measure the intensity of the emission spectrum of the irradiated pesticide after each 60 minute period of exposure to UV light in the photoreactor. The exposure of the sample to the 315 nm fluorimeter excitation source for the few minutes required to record the fluorescence was judged to be insignificant compared to the high intensity within the photoreactor. The slit widths of the fluorimeter were adjusted to 2.5 nm for the emission and 10.0

nm for the excitation wavelengths. The kinetic parameters of the experiment were determined following the same procedure as described in the section 2.2.3.1. The kinetic curve fits were plotted using the kinetic model equation 2.1. The rate constant values (k_1 and k_2) for each of the five solutions (other than acetonitrile) were calculated using the Fig-P software. To examine the solvent polarity effect plots were obtained of the natural logarithm values of k_1 and k_2 versus dielectric constant (ϵ) of the solvents. In addition, half-lives ($t_{1/2}$) were determined; these correspond to the period of time at which the pesticide concentration is equal to half of the initial concentration, and is given by the equation $t_{1/2} = \ln 2/k$ (for first order reactions). All kinetic experiments were performed at room temperature.

2.3.4. Photoreactor-Based Kinetic Experiment with Acidic Buffer

Solution

2.3.4.1. Solution Preparation

An AZM solution was prepared in an acetate buffer (acetic acid plus sodium acetate in deionized water); the pH of this buffer was measured to be 3.0. The concentration of both the acetic acid and sodium acetate was 50 mM.

2.3.4.2. Instrumentation

The pH of the acid buffer solution was measured using the Fisher Scientific Accumet pH meter 910.

2.3.4.3. Procedure

In this experiment, 3 mL of AZM buffer solution was withdrawn from the volumetric solution flask, pipetted into the quartz cuvette and irradiated in the same photoreactor with 350 nm excitation. At each one hour of irradiation, the fluorescence spectrum was recorded and the process was continued for 31 hours keeping the fluorimeter parameters the same as for the kinetic experiments mentioned above. Using Fig-P software, the analyzed data was plotted to obtain the kinetic curve of fluorescence enhancement (I/I_0) versus time. The kinetic data and fit were plotted using the same kinetic model (Equation 2.1). The experiment was performed at room temperature.

2.3.5. Identification of the Highly Fluorescent Intermediate and Relatively Non-fluorescent Final Photoproduct of Azinphos-methyl Photolysis

A number of solutions were prepared to help in the identification of the intermediate and final photoproducts of AZM photolysis (see Chapter 3)

2.3.5.1. Solution Preparation

Anthranilic Acid : A stock solution of anthranilic acid was prepared with a concentration of 4.0×10^{-5} M. A four-fold diluted anthranilic acid was prepared with a concentration of 1.0×10^{-5} M using this stock solution. From this diluted solution, a further ten-fold diluted solution was prepared with a concentration of 1.0×10^{-6} M. Both methanol and distilled water were used as solvents. These solutions were used for normalization and kinetic studies. The solutions were kept in the dark at room temperature.

N-methyl anthranilic Acid: A stock solution of N -methylanthranilic acid in methanol and distilled water was prepared at a concentration of 1.0×10^{-5} M. A portion of each of the stock solutions was diluted to a concentration of 1.0×10^{-6} M by adding required amount of solvents. All solutions were stored at room temperature in a dark place.

Benzazimide: An amount of 0.0006 g benzazimide was transferred into a 100 mL volumetric flask and required amount of methanol was added in order to prepare a solution with a concentration of 4×10^{-5} M. The solution was left in the dark at room temperature.

2.3.5.2. Comparison of the Fluorescence Spectra of AZM, Anthranilic Acid and N-methylanthranilic Acid

A comparison study between the fluorescence spectrum of the pesticide AZM (4.0×10^{-5} M) and anthranilic acid, AA (4.0×10^{-7} M) was carried out in methanol. Experimental evidence showed that the intensity of the fluorescence spectrum of anthranilic acid at a concentration of 4.0×10^{-5} M was off the scale since this species was found to be highly fluorescent. In order to rectify this situation, the solution of AA was diluted by one hundred-fold with respect to AZM. The fluorescence intensities were 2.49 and 280.30 for the above solutions of 4.0×10^{-5} M and 4.0×10^{-7} M solutions of AZM and AA, respectively. The calculated ratio of the concentration of AZM and that of AA was 1:100 whereas, the calculated ratio of fluorescence intensity of AZM and that of AA was 1:113. It was therefore found that fluorescence of AA was around 11,000 times more intense than that of AZM.

In order to test whether the observed intermediate in the AZM photolytic reaction is anthranilic acid, the absorption and fluorescence spectra of commercial AA were obtained. In addition, the comparison between the fluorescence spectra of AZM and another candidate for the observed intermediate, N-methyl anthranilic acid (NMAA) was performed following the same procedure. The concentration of AZM was 4.0×10^{-5} M and the concentration of NMAA was 1.0×10^{-5} M. The concentration of NMAA was 4 fold diluted compared to that of AZM because of its high fluorescence intensity, which made it difficult to measure in the fluorimeter. The calculated

ratio of the fluorescence intensity of AZM and NMAA was 1:33. Therefore, the fluorescence intensity of the NMAA was approximately 130 times higher than that of AZM.

2.3.5.3. Kinetic Experiments on Anthranilic Acid and N-methyl Anthranilic Acid

Kinetic studies on anthranilic acid and N-methyl anthranilic acid in methanol were carried out following the same procedure mentioned in the section 2.3.3. In both the cases, the concentrations of the two products were kept the same (1.0×10^{-6} M). Solution preparation has already been mentioned above. The photodegradation rates of AA and NMAA in methanol followed a first order kinetic decay curve, $C_t = C_0 \exp^{(-kt)}$, where, C_t and C_0 represent the concentration of the compound at time t , and initial concentration of the compound, respectively and k is the rate constant. The Fig-P software was used to calculate the value of k .

2.3.5.4. Normalization of the Fluorescent Spectra for the Identification of the Highly Fluorescent Intermediate Photoproduct of AZM

The normalization of the fluorescence spectrum of the intermediate photoproduct of AZM to that of anthranilic acid and N-methyl anthranilic acid was performed. The data points obtained for the spectra of AA, NMAA and photoexposed AZM (intermediate) in distilled water and methanol solution were plotted on the same graph using Fig-P software. The fluorescence spectrum of benzazimide and that of irradiated AZM (after total course of

irradiation) obtained both in methanol solution were also measured and normalized for comparison. The initial concentration of AZM and benzazimide was 4.0×10^{-5} M.

2.3.6. NMR Experiment for the Determination of Intermediate and Final photoproducts of AZM

2.3.6.1. Instrumentation

^1H NMR spectra of methanol-d₄ solutions were obtained on a Bruker Avance 300 MHz ultra-shield instrument with tetramethylsilane (TMS) as an internal standard.

2.3.6.2. Solution Preparation

The solution concentration of the AZM for NMR study was chosen to be 1.5×10^{-3} M. To prepare this solution, 0.0014 g of solute was measured into the 3-mL quartz cuvette and methanol-d₄ was added to make up the volume. The solution concentration of the anthranilic acid for NMR study was 3.6×10^{-3} M, which was prepared by dissolving 0.0015 g of AA in 3.00 mL of methanol-d₄ in the quartz cuvette. Solutions of benzazimide (3.6×10^{-3} M) and NMAA (3.6×10^{-3} M) were prepared by dissolving 0.0016 g of the each solute in methanol-d₄ in 3-mL quartz cuvette.

2.3.6.3. Procedure

A required amount of solution was pipetted into a NMR tube after the preparation and the ^1H NMR spectrum of the AZM without any irradiation was measured. The solution was then poured back into the quartz cuvette from the tube and the cuvette sample was exposed to the UV light in the photoreactor. Following this procedure, the NMR spectrum of AZM irradiated sample to UV light for 6 hours (to determine the trace amount of intermediate photoproduct) and again after 36 hours (to determine the final photoproducts) were obtained. In the same way, ^1H NMR for anthranilic acid and benzazimide were recorded for both the initial one and for 8 hours irradiated sample. The ^1H NMR signals obtained were very weak for the N-methyl anthranilic acid without any exposure to UV light at a concentration of 3.6×10^{-3} M (section 2.3.6.2.1). Therefore, a relatively higher concentrated solution of NMAA was prepared by adding more solute. The solution was then transferred to an NMR tube and the ^1H NMR obtained for this sample was very sharp and clear.

2.3.7. HPLC Studies for the Identification of Intermediate and Final photoproducts of AZM

2.3.7.1. Instrumentation

HPLC analysis was performed with a Varian 400 auto sampler system. The column used was a PursuitTM C₁₈ reversed-phase column, and the solvent was 60/40 water-methanol (v/v). A 325 UV/VIS dual wavelength detector

used was used, and the pump was a Prostar 210]. 20 μ l of the sample was injected for each analysis. Optimal separation of the peak was achieved with 20 min run time. In order to compare retention time of the photoproducts with the standards, the instrument, the column and the detection wavelength were the same as for the qualitative analysis.

2.3.7.2. Sample Preparation

The solutions of azinphos-methyl, anthranilic acid, N-methyl anthranilic acid and benzazimide were prepared in water-methanol (60/40% v/v) solvent system. The concentration of each solution was 0.25mM. The mixture of AZM, AA, NMAA and BA was obtained by withdrawing 1 ml of each 0.25 mM concentrated solution in a 5 ml vial manually. All samples were prepared and stored at room temperature in the dark.

2.4. Laser Flash Photolysis Studies

The laser flash photolysis studies were performed at Dalhousie University in Halifax by Professor Norm Schepp, using a home-built laser flash photolysis system. A XeCl excimer laser with 308 nm emission was used as the excitation source. The absorbance at 308 for both samples (AZM and AA) was ca. 0.4 over a 7 mm path length. The kinetic trace and the spectra were plotted using the MS-Excel program. The time windows for the spectra were 1.5, 2.4, 7.8 and 13 microseconds after the laser pulse.

2.5. Photolysis Studies of Azinphos-methyl under Direct Sunlight using Natural Water

2.5.1. Sample Collection and Storage

Natural water sample with no previous treatments such as filtration or sterilization, were previously collected from a stream near Rollings Pond in North Rustico on Prince Edward Island. The water sample was collected in May 2004 and preserved in the freezer prior to use.

2.5.2. Solution Preparation

The natural water solution of the azinphos-methyl pesticide was prepared for irradiation under direct sunlight at a concentration of 4.0×10^{-5} M. Since AZM was found to be poorly soluble in water, two hours of sonication was required for its dissolution. The pesticide concentration in water was sufficient to carry out the kinetic studies using the fluorimeter.

2.5.3. Procedure

Outdoor experiments were carried out in a capped quartz cuvette on the balcony of the K.C. Irving Chemistry Center in August 2004. The concentration of the pesticide solution was 4.0×10^{-5} M, which was the same as the distilled water solutions in the laboratory experiment. The steady-state kinetic study was performed following the same experimental procedure as for distilled water. The prepared natural stream water sample was irradiated

under direct sunlight for 12 hours (morning to evening) and the fluorescence spectrum was recorded at intervals of two hours using the fluorimeter. The fluorimeter parameter setup was the same as that for the kinetic experiment for the distilled water solution (section 2.3.4.3). A dark, controlled experiment was also conducted by keeping a quartz glass cuvette in the dark place of the cupboard in our laboratory preventing exposure to any light source. The analyzed data plot was used to obtain the photodegradation curve using Fig-P software.

The irradiance of UV by the sun was variable, depending on the day time (height of the sun) and although sunny days were chosen, there were occasional clouds blocking the sun. The temperature also varied (maximum at 23⁰ C). Therefore, this was purely a qualitative experiment.

Chapter 3

3. Result and Discussion

3.1. Fluorimeter- Based Studies

The first approach taken for this study of AZM photolysis was to expand on the previous fluorimeter-based photolysis in water reported by Wagner *et al.*,³⁸ using different excitation wavelengths and various solvents to change the reaction medium. In this way, the products and mechanism for this photochemical reaction can be studied.

3.1.1. Analytical Studies of AZM-Methanol Solution

At the first stage, methanol was chosen as the solvent for photolysis of AZM in the fluorimeter. Since AZM is highly soluble in organic media, but poorly soluble in water, methanol allowed a higher AZM concentration in solution. Another reason behind the selection of methanol was to study the reaction using NMR, by dissolving the product in the deuterated version of the solvent in order to elucidate the structure of photoproduct(s). The optimum excitation wavelength (315 nm) for the UV light in the fluorimeter was used based on the previous reports.⁴⁰

A graphical plot of the ratio of I_F/I_0 versus time is shown in Figure 3.1. Interestingly, at least over the time frame used, there was no well-defined maximum fluorescence intensity recorded, indicating complete conversion of the AZM was not attained. These results also suggest that the highly fluorescent photoproduct itself is stable to UV irradiation. It is also strange that the increase itself increases with time (the plot shows upward curvature).

For each trial the initial absorbance (without any exposure to UV source) of the solution was measured and compared to the final absorbance after a total irradiation time of 48 hours. It was found that the absorption of the solution decreased with the irradiation by the UV light. This result supports the idea that the observed increase in the fluorescence of AZM upon UV exposure is due to its photolysis.

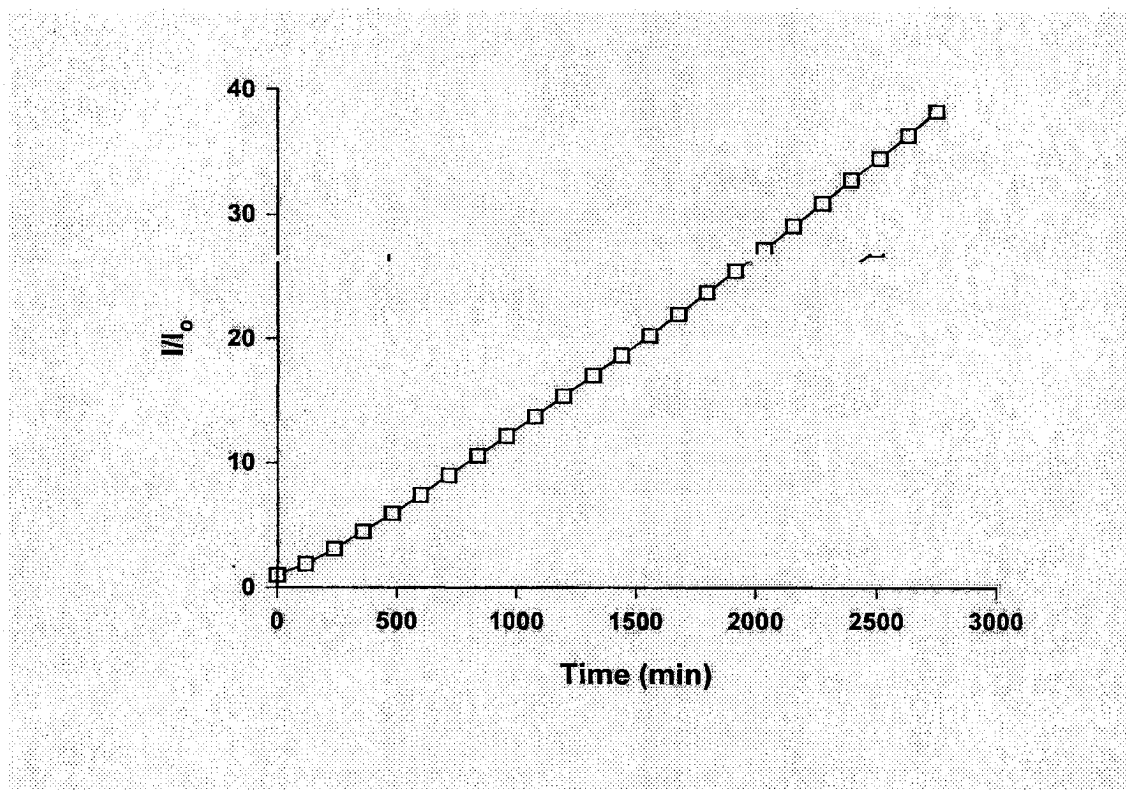


Figure 3.1. Fluorimeter based photolysis of AZM in MeOH

It is well known that the wavelength distribution and intensity of light might influence the photodegradation of the pesticide. Therefore, the same experiment was performed exposing the AZM-methanol solution at 300 nm

and 320 nm excitation wavelength to compare the results among various wavelengths. The conditions of the irradiation of the sample in the fluorimeter were the same for each experiment. In all cases, the emission was measured at 405 nm. The curves found for AZM photolysis at various wavelengths are shown in Figure 3.2.

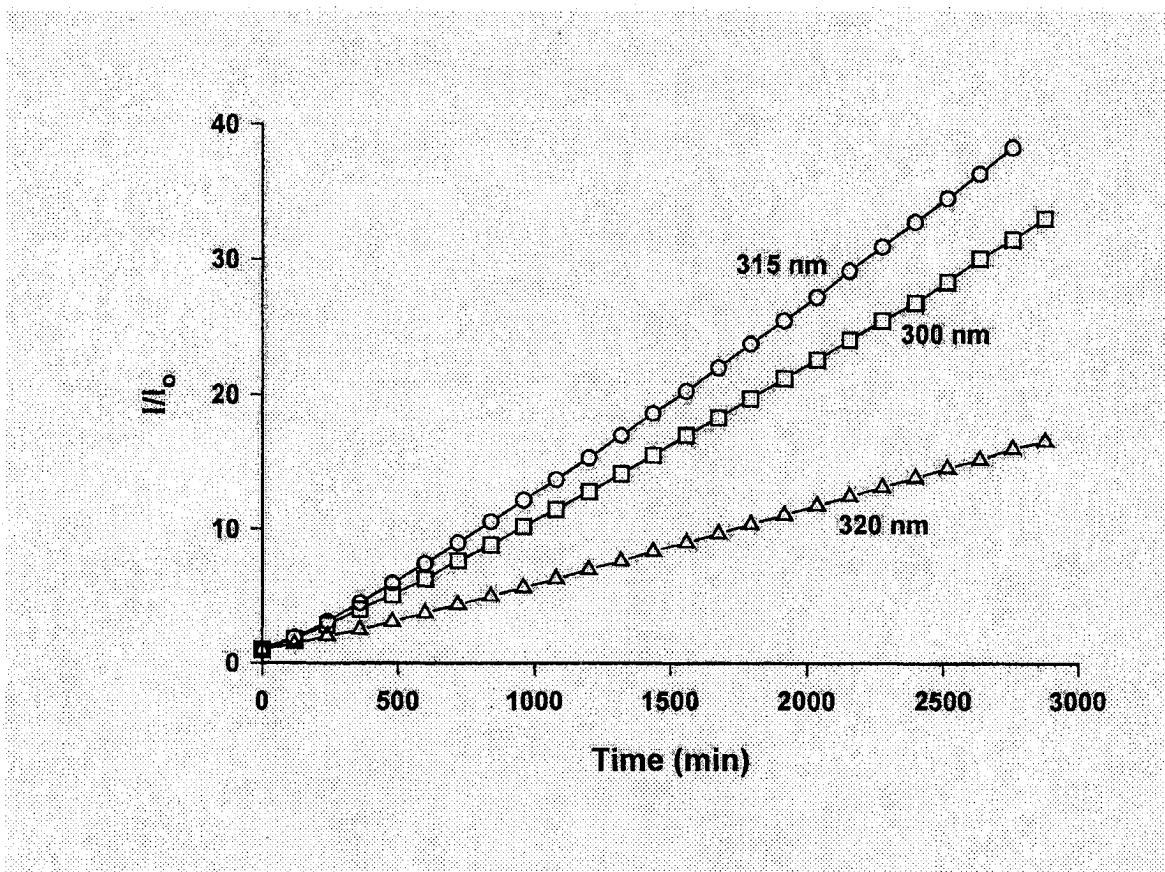


Figure 3.2. Photolysis of AZM in MeOH at various wavelengths

The results found in the Figure 3.2 show that 315 nm excitation gave the largest effect, and interestingly, the enhancement effect dropped off significantly at 320 nm. The reason is still ambiguous but the phenomenon is reproducible.

3.1.2. Analytical Studies of AZM-Water Solution

To model an environmental fate for AZM, it was necessary to have a laboratory model using water. Therefore, a kinetic study of AZM in deionized water solution was performed in the laboratory environment. Previous work by our lab showed that during the AZM photolysis using the fluorimeter in aqueous media up to 7 hours total irradiation time, the fluorescence enhancement of this pesticide increases until 5 hours of exposure, then starts to level off followed by a slight decrease of fluorescence intensity. In our case AZM photolysis was performed for 48 hours total irradiation period to better observe the maximum and subsequent decrease in fluorescence. A continuous increase of fluorescence enhancement of AZM was observed up until 6 hours and then the enhancement began to decrease after hitting a maximum value. This confirms the previous report, and indicates the growth of a highly fluorescent intermediate photoproduct of AZM photolysis which is itself subsequently photolyzed. During the total irradiation period the enhancement decreases nearly to the base line meaning that the further photodegradation of the photochemically unstable intermediate results in relatively non-fluorescent photoproducts.

The kinetic curves in Figure 3.3 suggest that the photodegradation of azinphos-methyl in distilled water follows consecutive first order reactions of a growth followed by decay of an intermediate. This result shows that the maximum enhancement effect was largest at 300 nm excitation, which is interestingly the reverse of that in methanol. The fluorescence enhancement

dropped off at 320 nm excitation wavelength; this effect is a similar effect to that observed in methanol. This observed complete photodegradation in aqueous media at various wavelengths using the fluorimeter has very significant importance for the determination of the mechanism of AZM photolysis, although the equation for the kinetic model involving stepwise first order reactions mentioned in chapter 2 (Equation 2.1) did not fit these curves.

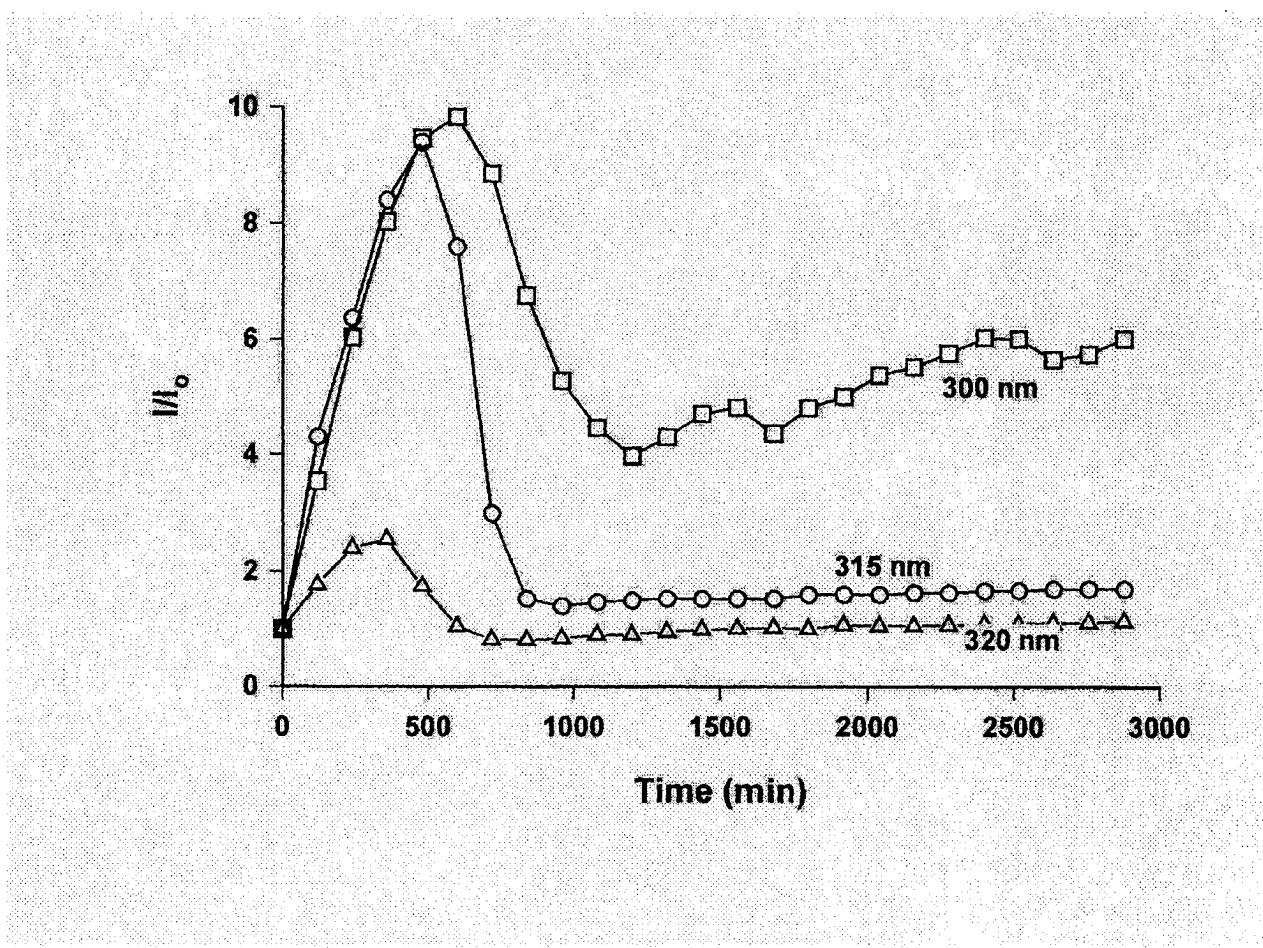


Figure 3.3. Fluorimeter based photolysis of AZM in H₂O

3.1.3. Analytical Studies of AZM-(Water-Methanol) Mixed Solution

The photolysis of AZM in methanol solution did not show any maximum intensity, *i.e.*, the enhancement continuously increased with exposure time resulting in a continuously increasing curved line, indicating a stable highly fluorescent photoproduct rather than a kinetic photodegradation curve. However, in water a maximum was obtained, followed by loss of fluorescence, indicating a second step photolysis reaction of the highly fluorescent intermediate. Thus, it was decided to irradiate mixed water-methanol solutions of AZM to further investigate this solvent dependence, and to see if this increase followed by decrease could be seen in methanol in the presence of water. Various ratios of the water-methanol mixed solutions were used, namely 1:1, 3:1 and 9:1 (v/v). Figure 3.4 shows the kinetic curves of AZM after the same course of total irradiation to UV light in these different water-methanol mixtures as well as in distilled water. No well defined maximum intensity was found for any water-methanol mixtures (1:1, 3:1 and 9:1) (v/v); the results were all similar in shape to that in pure methanol. However, in water, the photolytic degradation of AZM was very significant since the reaction started approximately within seven hours, whereas no such evidence was observed in the case of other solvent systems even after UV exposure up to two days.

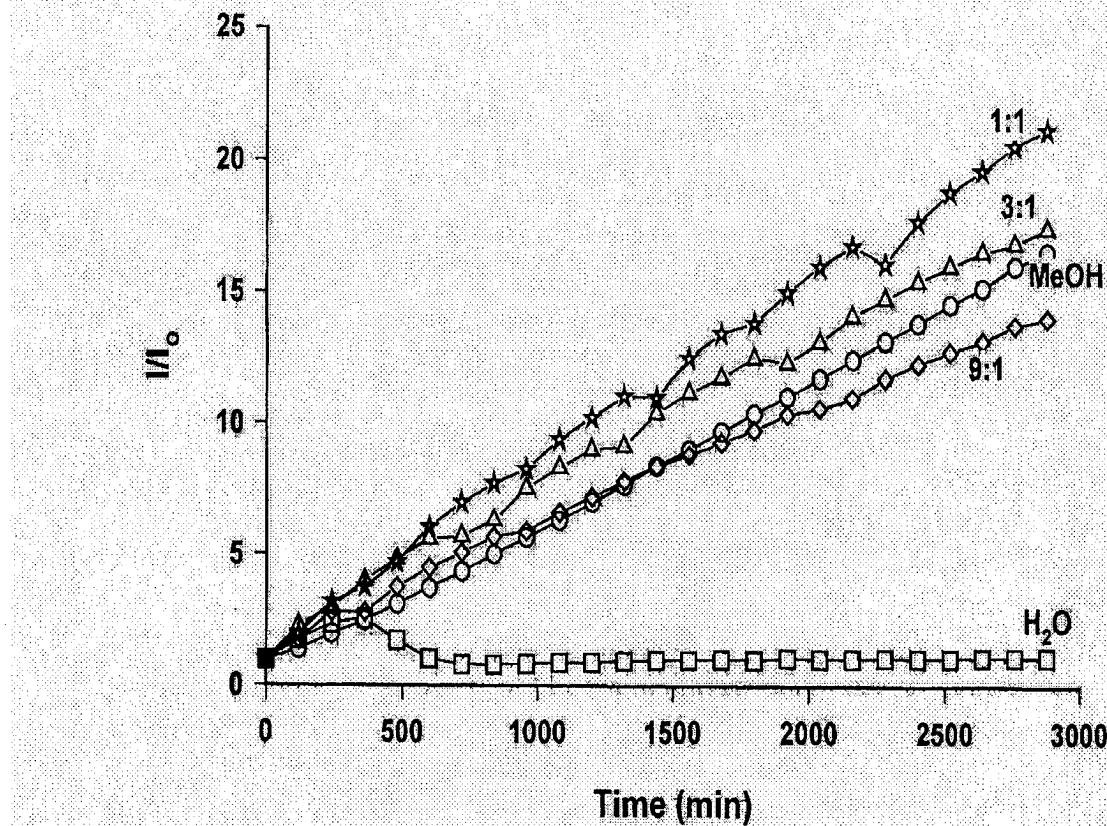


Figure 3.4. Fluorimeter based photolysis of AZM in H_2O , MeOH and H_2O - MeOH solution

In aqueous solution, the maximum fluorescence enhancement was observed followed by a decrease in fluorescence. This suggested that the highly fluorescent photoproduct was actually unstable to UV irradiation in aqueous solvent, but not in the presence of methanol. In the case of methanol, the photoproduct was either stable, or its subsequent photolysis was too slow to observe on the experimental time scale. This result indicates

a significant role of water as a reactant in the second step, the photolysis of the highly fluorescent intermediate. It is very strange however that this does not occur if even 10% methanol is present in these fluorimeter studies.

3.2. Photoreactor Based Studies

3.2.1. Kinetic Studies of Azinphos-methyl

The photodegradation results of the fluorimeter-based kinetic studies were rather frustrating and puzzling, especially the observation of an intermediate in water but not in methanol or methanol-water mixtures. Therefore, it was decided to use a photoreactor equipped with a UV source of fixed excitation wavelength at 350 nm. This photoreactor has UV lamps all around the sample to be photolyzed. This gives the advantage of a much higher UV intensity, which should speed up the photolysis reaction.

Furthermore, the use of 350 nm as excitation wavelength is an excellent model for UV exposure in the environment. As discussed in the introduction, the UV part of the solar spectrum which reaches the Earth's surface becomes very low below 340 nm. Such a high wavelength could not in fact be used in the fluorimeter-based experiments, because of the low intensity of the lamp coupled with the low absorption of AZM at this wavelength. Thus, the switch to the photoreactor to do the AZM photolysis provides for much better control of UV exposure, much higher intensity, and a better model for photolysis of this pesticide in the environment.

The kinetics of azinphos-methyl photolysis was studied in a number of organic solvents as well as distilled water, with the goal of studying the effect of polarity on the reaction kinetics. This could for example indicate the polarity of the transition state, and any role of proton transfer from the solvent. In this project, AZM was photolyzed in the photoreactor at 350 nm excitation in the following six solvents: water, methanol, deuterated methanol, ethanol, cyclohexane and acetonitrile. AZM was found to be photodegraded in all of the above solvent systems. The results showed that for certain period of consecutive irradiation of AZM, the intensity increased and then reached a maximum enhancement point, followed by subsequent photolytic decay. In all cases, after the total period of photolysis, a relatively non-fluorescent photoproduct(s) was produced. All kinetic traces obtained in each of these solvents of interest fit to the model equation 2.1 based on the consecutive first order reaction ($A \rightarrow B \rightarrow C$) with the interesting exception of acetonitrile.

Figure 3.5 shows the comparable results of the fluorescence enhancement due to the AZM photolysis in aqueous system. The photolysis was carried out for 36 hours of total irradiation by the 350 nm UV source in the photoreactor. In Figure 3.5, the spectrum **a** represents the weak fluorescence of the pesticide AZM in distilled water solution, *i.e.* prior to any exposure to UV light in the photoreactor; the spectrum **b** represents the maximum enhancement after 8 hours of irradiation, whereas spectrum **c** represents the final product(s) after a total irradiation period of 36 hours. The results showed that after UV exposure for 8 hours a highly fluorescence

intermediate photoproduct had been produced (spectrum b). On the other hand, it took 6 hours in the fluorimeter to reach the maximum enhancement showing the formation of the highly fluorescent intermediate, which may be due to the intensity difference of the UV lamp in the fluorimeter and excitation wavelength difference. However, this intermediate undergoes further photolysis and spectrum c shows that the intensity of the end product(s) was greater than that of AZM, but much less than that of the intermediate. Hence we refer to these as the relatively non-fluorescent (*i.e.* compared to the intermediate) final product(s).

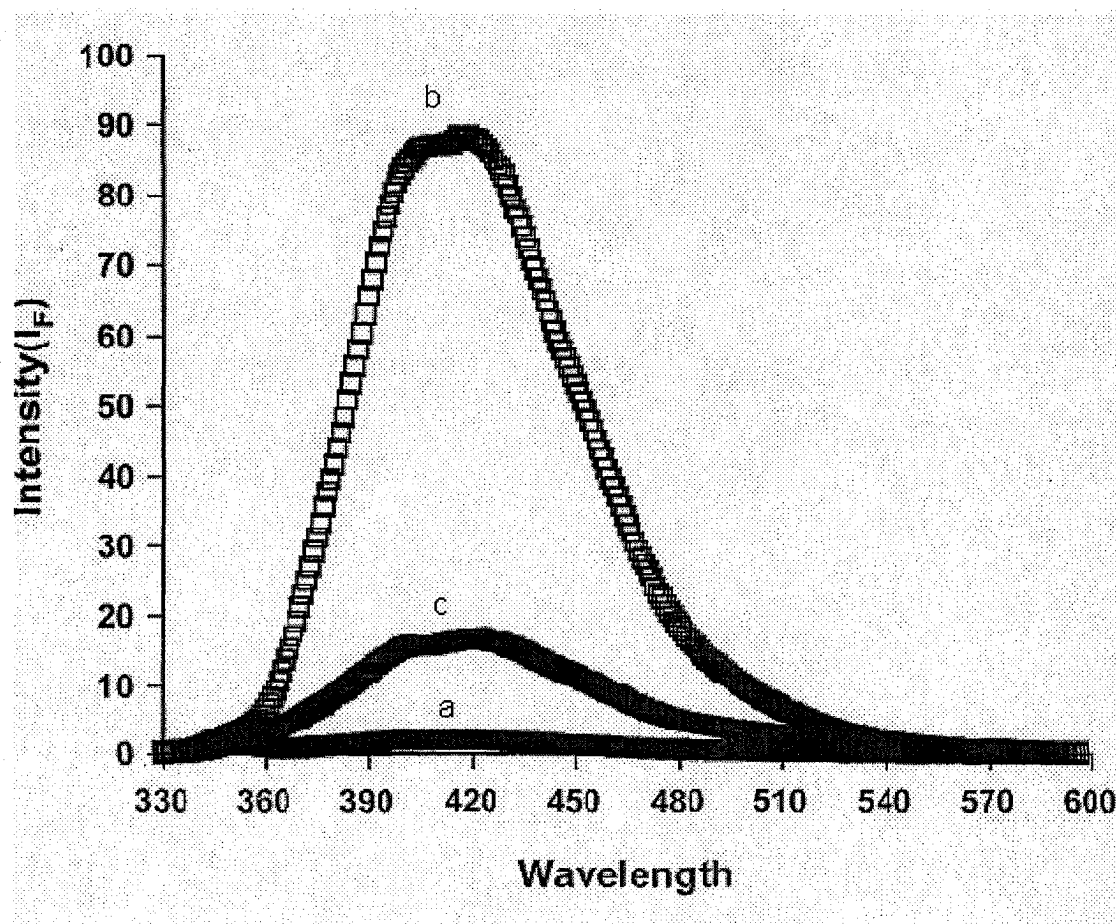


Figure 3.5. Photoreactor based photolysis of AZM in H₂O

The kinetic fit of the photolysis of AZM in distilled water to Equation 2.1 (Figure 3.6) showed an excellent fit (correlation coefficient, $r = 0.999$), confirming that the photodegradation of azinphos-methyl follows this model based on the consecutive first order reactions ($A \rightarrow B \rightarrow C$).

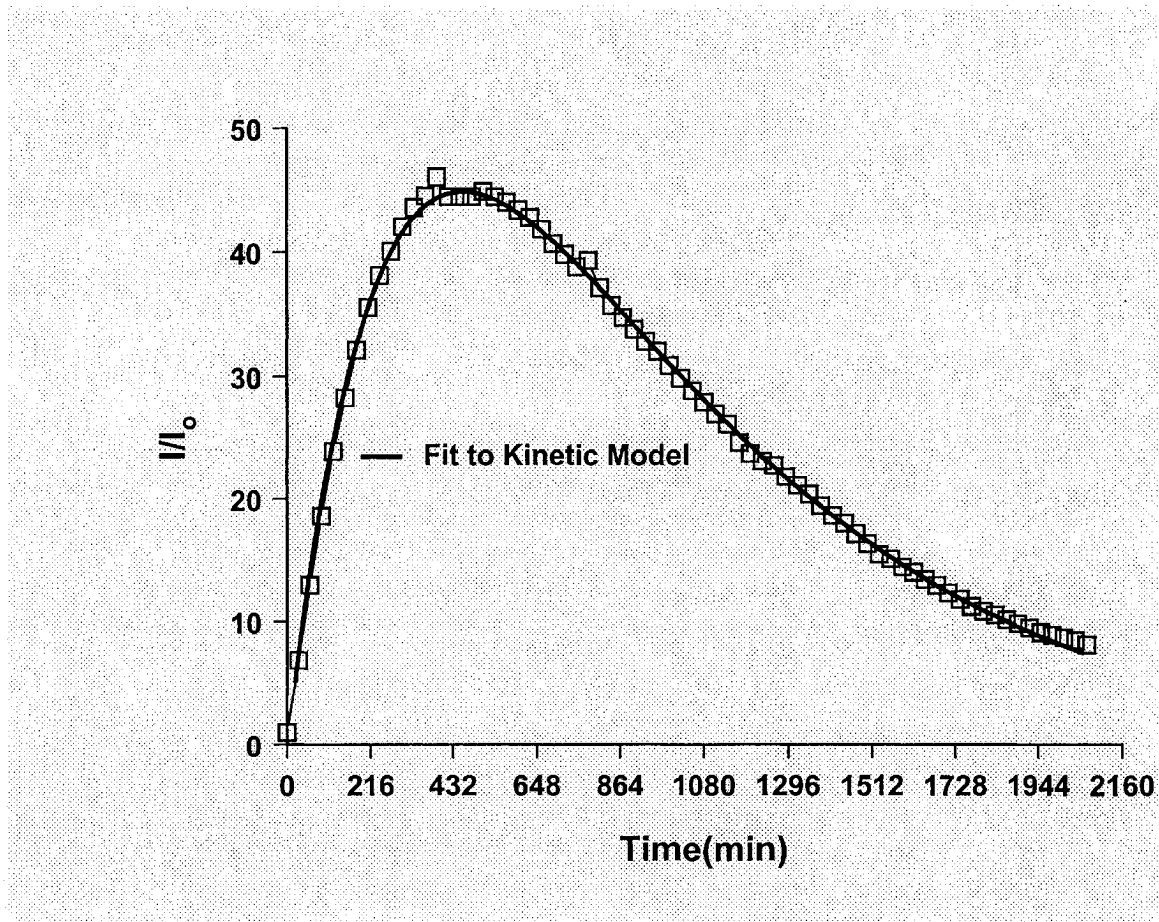


Figure 3.6. Photodegradation kinetics of AZM in H_2O

The growth rate constant k_1 was $1.5 \times 10^{-3} \text{ min}^{-1}$, while the decay rate constant, k_2 was found to be $3.1 \times 10^{-3} \text{ min}^{-1}$. It must be noted that the kinetics are being followed in terms of the intermediate concentration, since it is by far the most fluorescent species. This explains the observed shape of the kinetic

traces of a first order growth followed by a first order decay. The half-life for the growth was 7.7 hours, whereas by comparison the half-life of the decay was 3.7 hours.

Figure 3.7 shows the comparable results for the fluorescence of AZM photolysis in methanol. The total course of irradiation was 31 hours. The obtained result shows that during the exposure of AZM to the UV source in the photoreactor, a growth of a highly fluorescent but photolytically unstable intermediate was observed, which again undergoes further photodegradation producing a relatively non-fluorescent photoproduct(s). This result is significantly and also surprisingly contradictory to the previous results of AZM photolysis in methanol or water-methanol mixed systems obtained in the fluorimeter. In Figure 3.7, (a) represents the initial spectrum without any irradiation; (b) represents the maximum enhancement for the highly fluorescence intermediate and (c) represents for the spectrum after the total irradiation for the final product(s). The shape of the intermediate spectrum was different from that of the distilled water system; this indicates either a solvent effect on the intermediate fluorescence spectrum or in fact a different intermediate being produced.

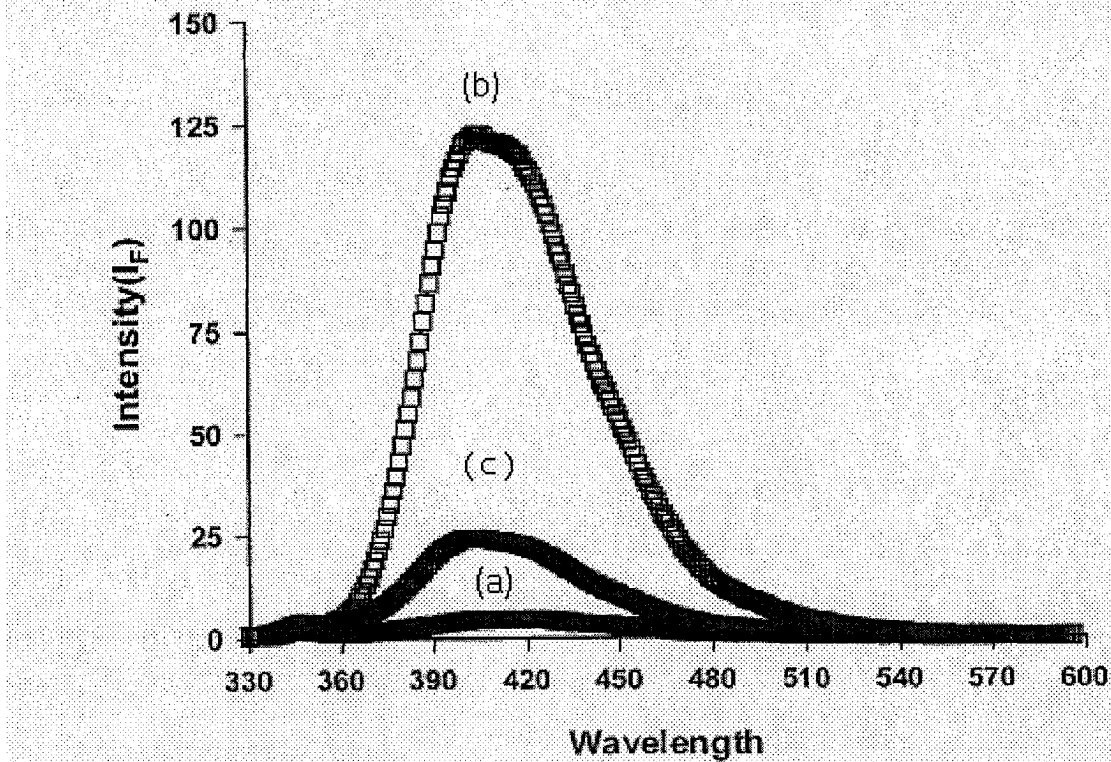


Figure 3.7. Photoreactor based photolysis of AZM in MeOH

Figure 3.8 shows the kinetic trace and fit to equation 2.1 for the AZM photodegradation in methanol, which again followed the model based on consecutive first order kinetics. The growth rate constant k_1 was $4.5 \times 10^{-3} \text{ min}^{-1}$ and the decay rate constant k_2 was recorded to be $4.4 \times 10^{-3} \text{ min}^{-1}$; these were significantly higher than the corresponding values in the distilled water system. The half-life for both the growth and decay was 2.6 hours, which were significantly lower than the values found in the case of deionized water. Thus, both photolysis reactions occur faster in methanol as compared

to water. In methanol, AZM was exposed to the UV light for as long as 31 hours. At that point, the data plot showed that the decay curve had leveled off nearly to the base line; therefore, no further irradiation was carried out.

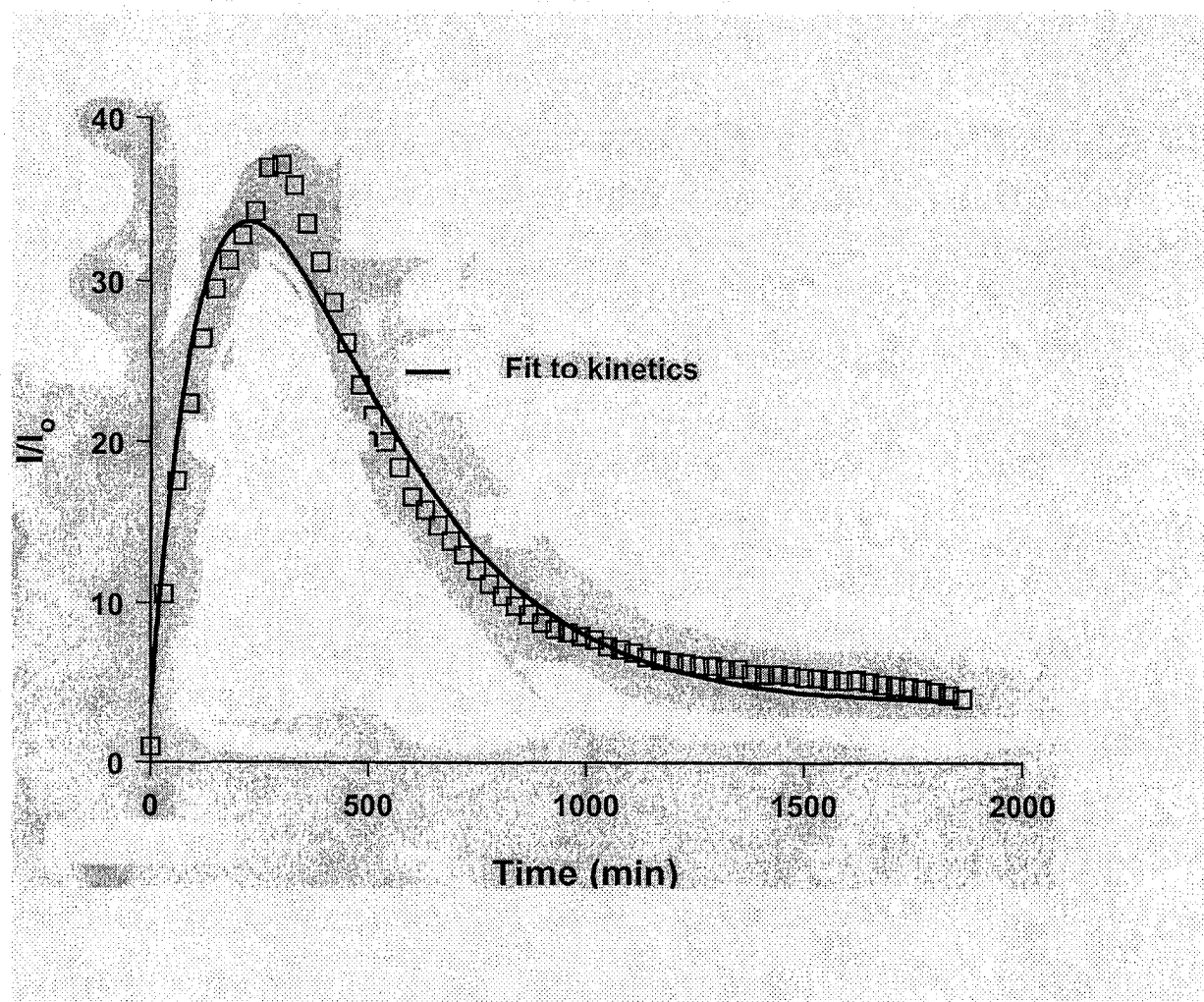


Figure 3.8. Photodegradation kinetics of AZM in MeOH

To determine the role of protonation in this reaction in methanol, the experiment was also performed in deuterated methanol, with the results shown in Figure 3.9.

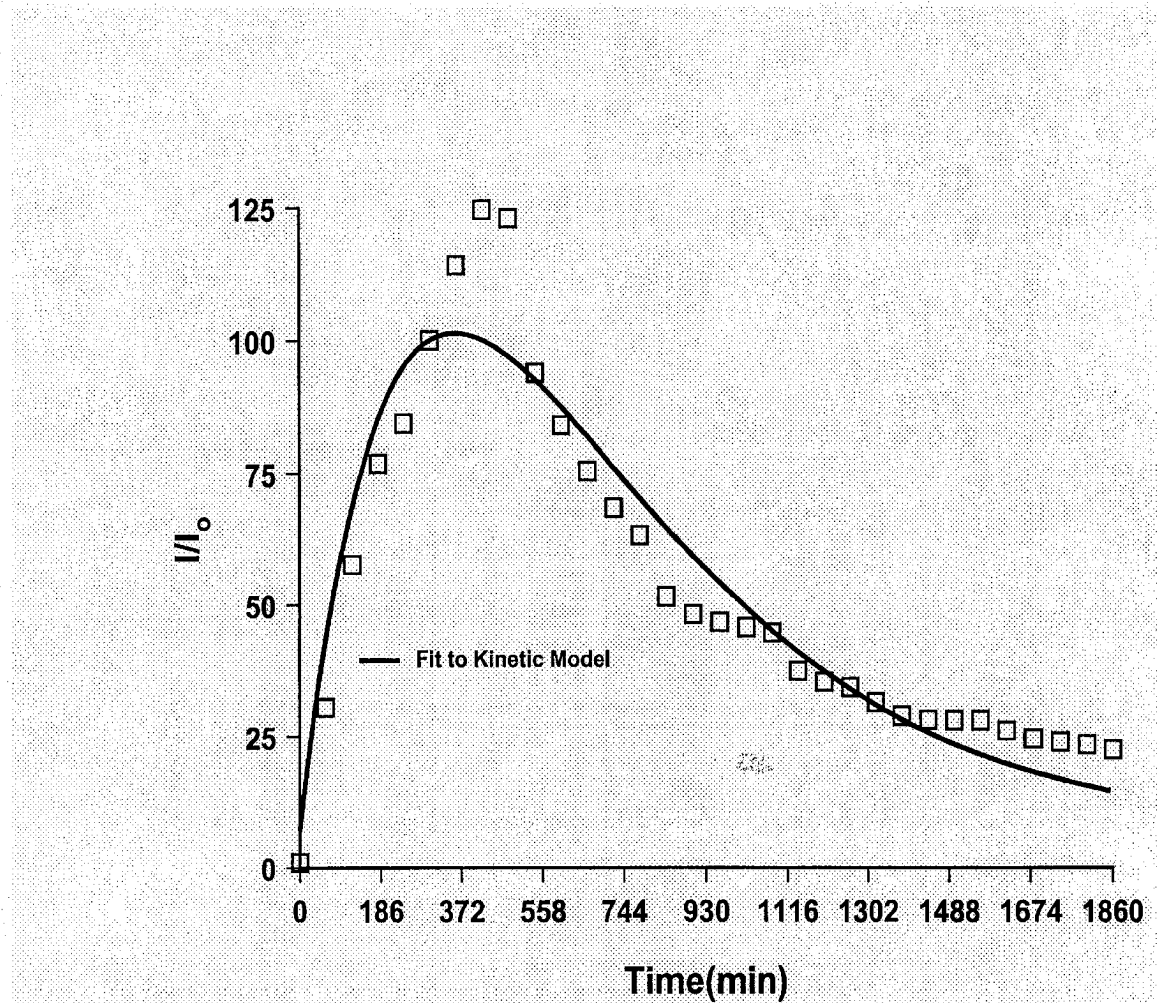


Figure 3.9. Photodegradation kinetics of AZM in deuterated MeOH

According to the kinetic fit also shown in Figure 3.9, the growth rate constant for the kinetic reaction, k_1 was $4.6 \times 10^{-3} \text{ min}^{-1}$, essentially identical to that of methanol solvent system. The half-life for the growth was 2.5 hours, again very close to that in methanol. The decay rate constant k_2 was $1.7 \times 10^{-3} \text{ min}^{-1}$;

this is significantly lower than that of k_2 in methanol. This is very clear from the half-life for the decay, which was 6.8 hours, significantly higher than that in methanol. This gives an experimental deuterium isotope effect for the decay of $k_H/k_D = \sim 3$, which is an indication of a primary effect. This result suggests that there was no role of hydrogen atom transfer in the formation of the intermediate species, but a significant role in the photodegradation of the intermediates species. This is important in terms of elucidating the mechanism, which will be discussed later.

In ethanol solution, UV irradiation was performed for 31 hours, the same period as was for the case of the other organic solvents. The results showed consecutive first order kinetics (Figure 3.10) like the other solvents mentioned above.

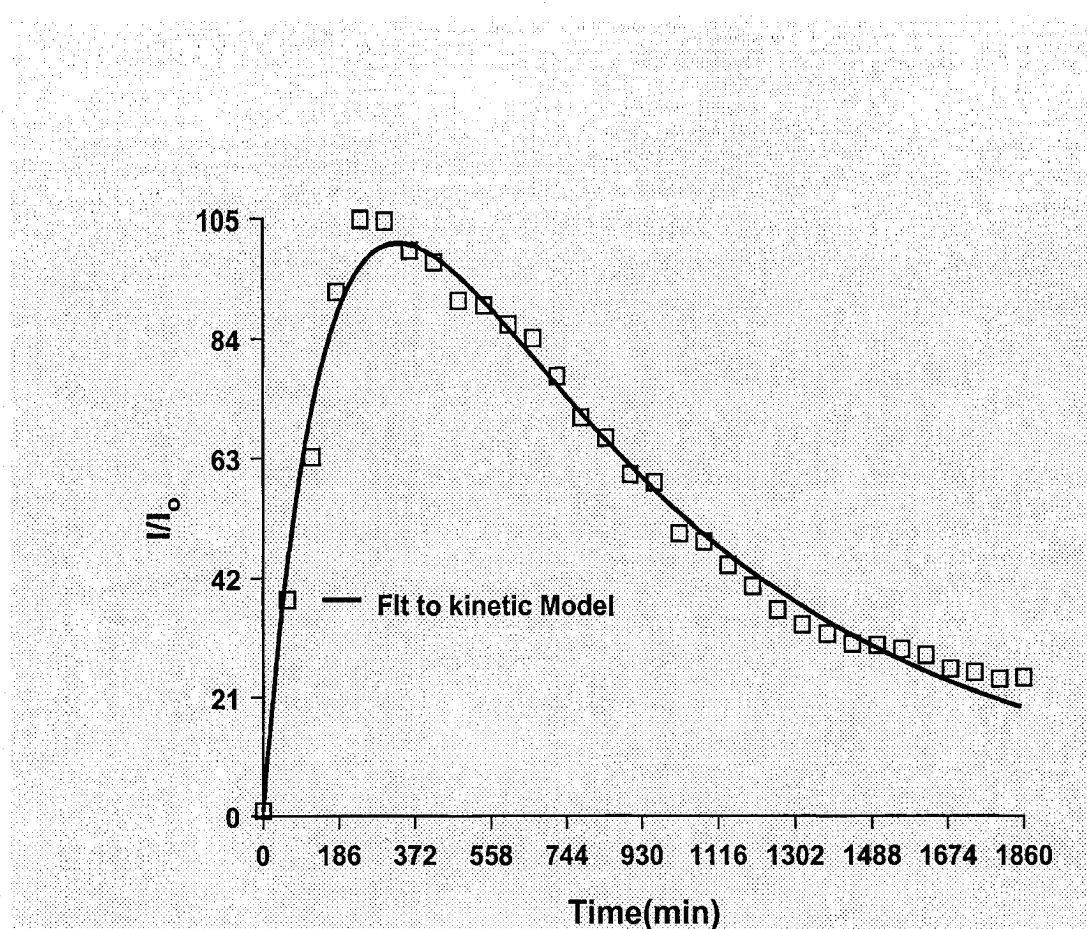


Figure 3.10. Photodegradation kinetics of AZM in EtOH

In this kinetic reaction, the growth rate constant was $1.2 \times 10^{-3} \text{ min}^{-1}$ and the rate constant of decay was $4.6 \times 10^{-3} \text{ min}^{-1}$, giving a half-life of 10 hours for the growth and 2.5 hours for the decay. This kinetic result in ethanol system shows a surprising contribution in the solvent polarity effect on the AZM photolysis which will be discussed later.

In cyclohexane solution, AZM was exposed to UV light again up to 31 hours. The emission maximum was found to occur at 390 nm, shifted slightly from that in the other system. The emission might be shifted because of the very large polarity difference with solvent, and its effect on the emission

spectrum of the intermediate. It could also be due to a different intermediate being formed in this aprotic solvent. The reaction was observed to follow the same model, *i.e.* consecutive first order reactions, as shown in Figure 3.11. The growth rate constant, k_1 for this case was $1.1 \times 10^{-2} \text{ min}^{-1}$ and the decay rate constant, k_2 was $9.5 \times 10^{-3} \text{ min}^{-1}$; these are very large compared to the other solvents. The decay half-lives were very short, 1.0 and 1.2 hours for the growth and decay, respectively. The reaction was by far the fastest in this aprotic, nonpolar solvent.

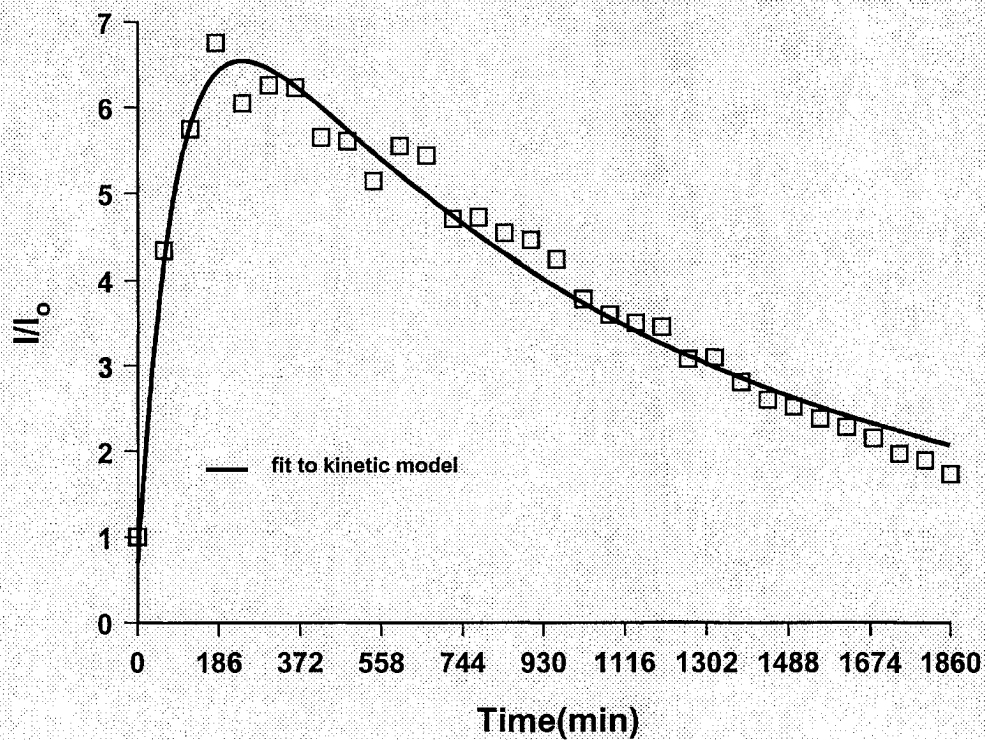


Figure 3.11. Photodegradation kinetics of AZM in cyclohexane

The photolysis of the pesticide in acetonitrile solution was carried out for up to 31 hours like for the other organic solvents. After 13 hours irradiation, the pesticide started to be degraded and its enhancement slowly declined as shown in Figure 3.12. The data points did not fit the consecutive first order kinetic model. A possible reason for this unexpected result could be because of a direct chemical reaction taking place between AZM and acetonitrile, giving a completely different mechanism than that in the other solvents. This will not be examined further, as the emphasis and interest is on the photolysis of AZM in aqueous (and other protic) media.

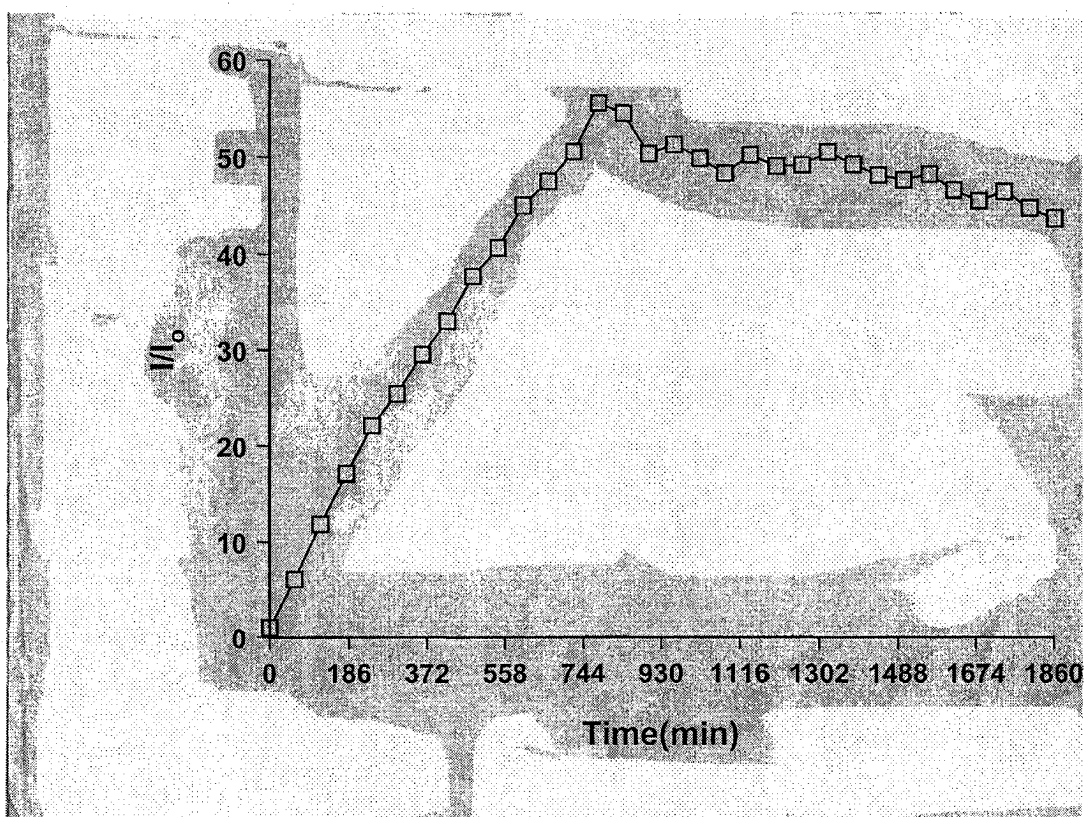


Figure 3.12. Photodegradation curve of AZM in acetonitrile

All the kinetic fit results (except acetonitrile system) mentioned in this section are compiled in tabular form in Table 3.2, and the solvent effects will be described in the next section. In all cases, a second trial was performed to check on the reproducibility of these results. It should be noted that error limits have not been provided, since those obtained from the FigP fitting program were not useful (all being very small relative to the recovered fit values), and standard deviations could not be determined based on two measurements. It was deemed reasonable to report the rate constants to two significant figures.

Solvent	Trial	$k_1(\text{min}^{-1})$	Average k_1 (min^{-1})	$k_2(\text{min}^{-1})$	Average k_2 (min^{-1})
Water	1.	0.0015	0.0019	0.0031	0.0027
	2.	0.0023		0.0023	
Methanol	1.	0.0045	0.004	0.0044	0.0038
	2.	0.0036		0.0033	
Deuterium Methanol	1.	0.0046	0.0041	0.0017	0.0017
	2.	0.0035		0.0018	
Ethanol	1.	0.0013	0.0012	0.0059	0.0053
	2.	0.0012		0.0046	
Cyclohexane	1.	0.011	0.010	0.0095	0.011
	2.	0.0086		0.012	
Acetonitrile	1.	-	-	-	-
	2.	-		-	

Table 3.1. Summarized value of k_1 and k_2 for the solvents of interest

3.2.2. Solvent Polarity Effect

From the kinetic results of the photolysis of AZM in the various solvents (except acetonitrile) compiled in Table 3.2, it is possible to explore solvent polarity effects on the kinetics of the photodegradation of AZM, to provide information about the mechanism.

In order to investigate the role of solvent polarity on each of these two steps (intermediate growth and decay) in the mechanism, the kinetic values of k_1 from water, methanol and cyclohexane are plotted, against solvent dielectric constant ϵ in Figure 3.13. This shows a significant correlation, with a r value of 0.967. This indicates that for this set of solvents, there is a significant polarity effect on the first step of the reaction, i.e., production of the intermediate. This reaction rate is seen to be significantly increased as the solvent polarity is decreased (the fastest kinetics were observed in cyclohexane, the least polar solvent).

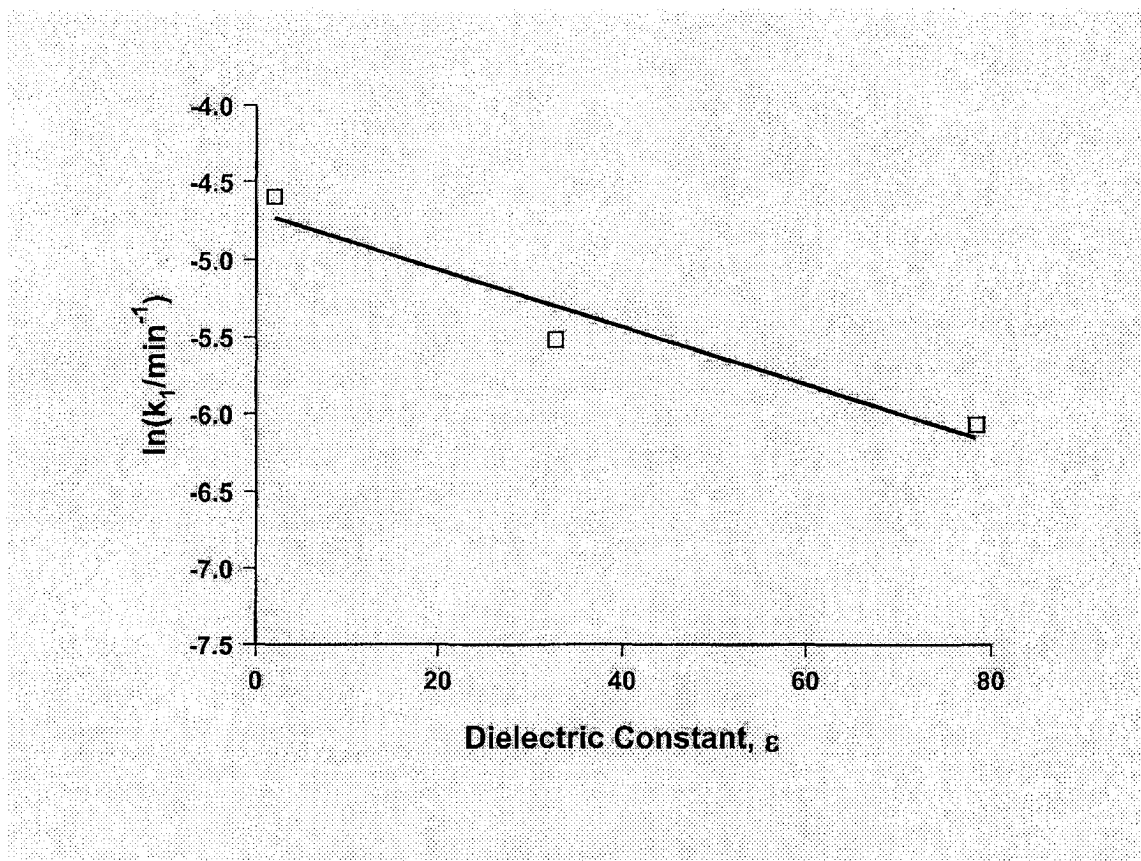


Figure 3.13. Solvent polarity effect on k_1 for H_2O , MeOH and cyclohexane

However, if the value of k_1 in ethanol solution is included in the plot, the correlation drops to 0.404 (Figure 3.14). Therefore, the results for the four solvents show a much less convincing dependence on solvent dielectric constant.

However, the results of the k_2 value for these four solvents shows a decent correlation with solvent polarity, as shown in Figure 3.15. For the four solvents, there was a correlation of 0.913. Thus, there seems to be a dependence of the rate of the second step (photolysis of the intermediate) on solvent polarity, with a clear trend of increased rate constant with decreased

solvent polarity. It must be noted, however, that the mechanism itself might be different in the different solvents.

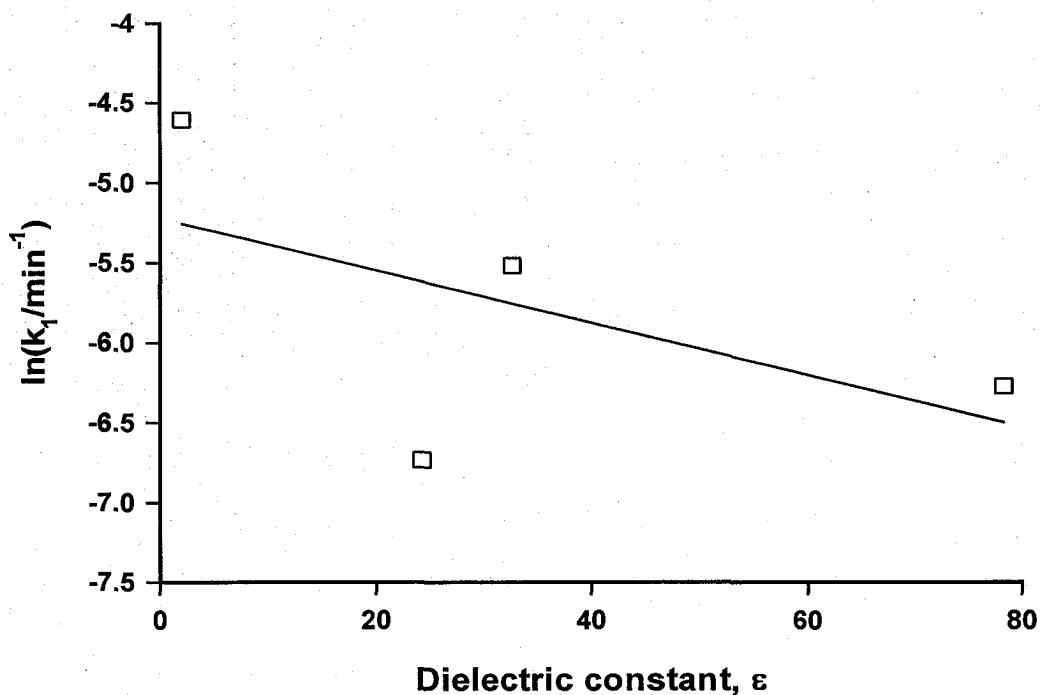


Figure 3.14. Solvent polarity effect on k_1 for H_2O , MeOH , EtOH and cyclohexane

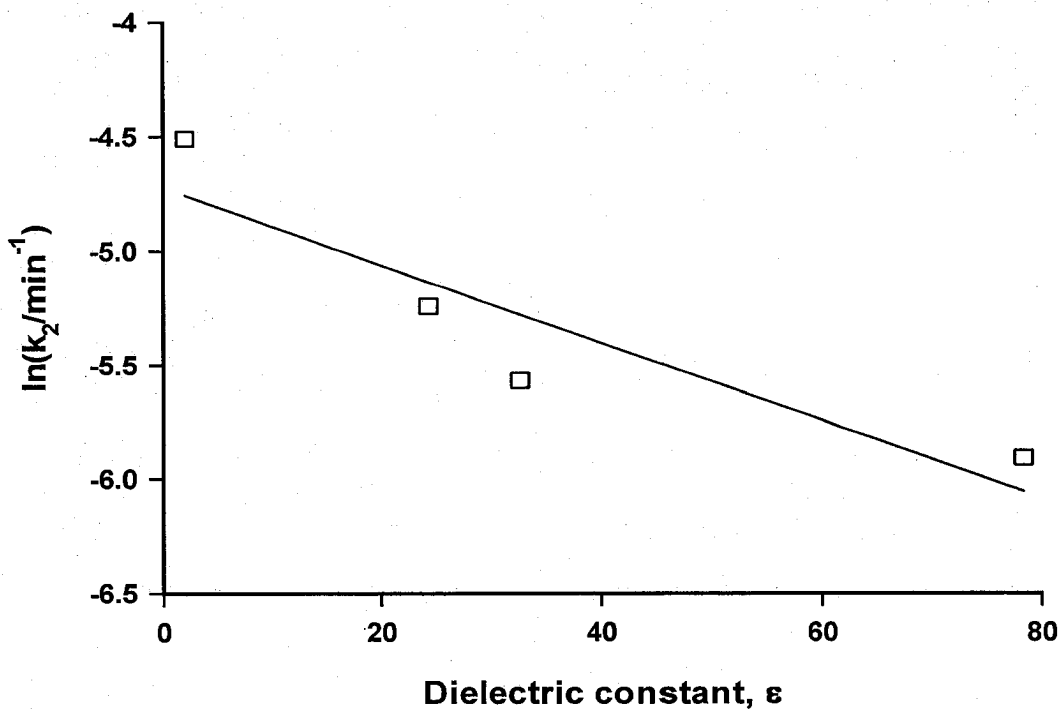


Figure 3.15. Solvent polarity effect on k_2 value for H_2O , MeOH , EtOH and C_6H_{12}

3.2.3. Acid Buffer Analytical Result

The deuterated methanol result showed a clear role of hydrogen atom transfer from solvent in the second step of the reaction in methanol. To investigate the possible role of proton transfer in water, an acid buffer experiment was performed. The photolysis of AZM was carried out in acetate buffer in aqueous media at pH 3.0 to observe the direct protonation effects on the kinetics of AZM in water. Figure 3.16 shows the kinetic trace and fit to the model equation 2.1. It is not clear why the fit line in Figure 3.16 does not go through the data points. The correlation coefficient r was 0.990, which is very

good, and indicative of a good fit. It is possible that there was a plotting error for this fit line. The results of the fit gave the rate constant k_1 and half-life for the growth was $1.3 \times 10^{-4} \text{ min}^{-1}$ and 88 hours respectively. The decay rate constant k_2 was $2.4 \times 10^{-3} \text{ min}^{-1}$ and half-life for the decay was 4 hours. It is also possible that this was not in fact a good fit, perhaps due to the small amount of decay part of the kinetic trace. However, even without using these fit results, it can be seen in comparing the shape of the data in Figure 3.16 to that obtained in neutral water (Figure 3.6) that both the growth and decay are much slower at this lower pH. Thus neither reaction is acid-catalyzed, and there is no role of proton transfer in aqueous solution. It is not understood however why the rate constants in fact decreased under acidic conditions.

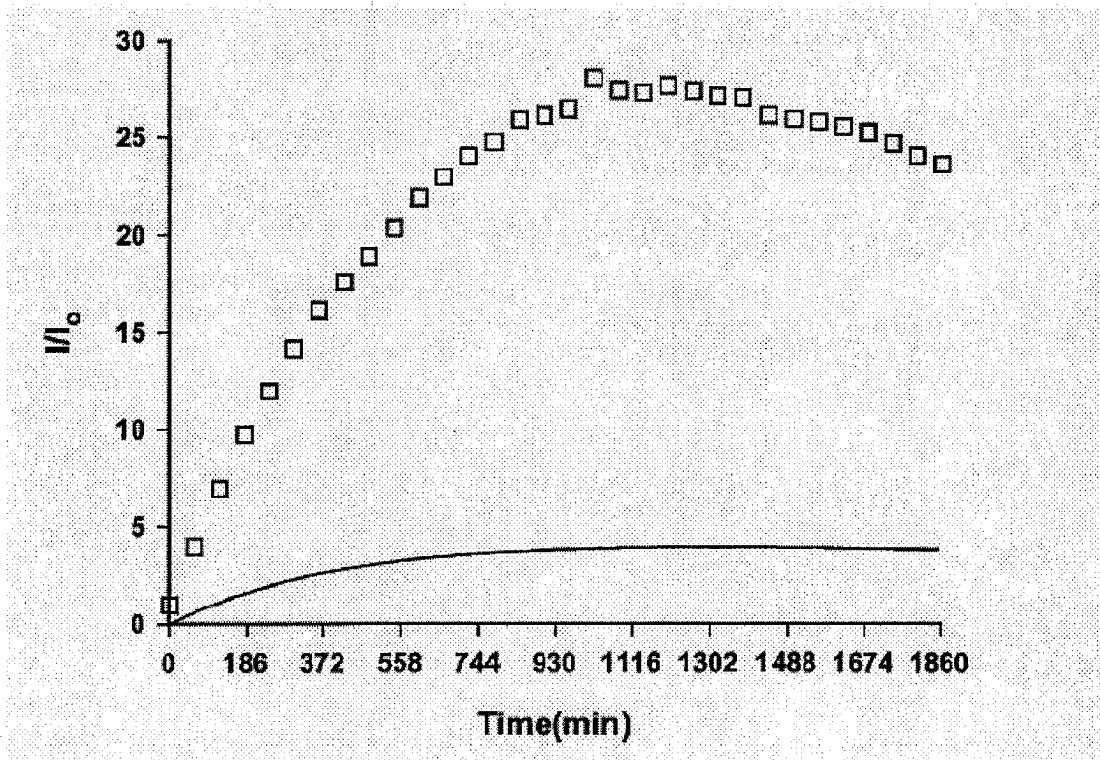


Figure 3.16. Kinetic trace and fit of AZM photolysis in acetate buffer (pH 3.0)

3.2.4. Identification of the Highly Fluorescent Intermediate and Relatively Non-fluorescent Final Photoproduct of Azinphos-methyl Photolysis

3.2.4.1. Comparison and Kinetic Results: Anthranilic Acid, Proposed Intermediate

It has been mentioned earlier (Section 1.5) that the fluorescence of AZM in basic solution is enhanced by a factor of 300 and this enhancement is a result of base hydrolysis producing the highly fluorescent compound, anthranilic acid (AA). Therefore, it was investigated whether the intermediate observed in the UV photolysis result might also be anthranilic acid, as it is a likely candidate.

In this current study, experimental results show that anthranilic acid itself is 11,000 times more fluorescent than AZM. To obtain this comparative fluorescence enhancement between AA and AZM, the fluorescence intensity of both unphotolyzed AA and AZM were measured in the fluorimeter. The concentration of AZM was 4.5×10^{-5} M, whereas the concentration of AA was 4.0×10^{-7} M. The 100 fold diluted concentration of AA relative to that of AZM was chosen because the measured fluorescence intensity of the higher concentrated solution of AA was off scale. The calculated ratio of the intensity of AZM and AA was 1:113. This gives the result that AA is 11,000 times more fluorescent than AZM.

To investigate the possibility that the highly fluorescent intermediate of AZM photolysis is indeed AA, the kinetics of AA photolysis was carried out. The result showed that (Figure 3.17) the decay rate constant ($k = 5.0 \times 10^{-3}$

min^{-1}) was very similar that of the AZM intermediate ($k_2 = 4.4 \times 10^{-3} \text{ min}^{-1}$) as shown in Figure 3.8. This provides support that anthranilic acid could be the intermediate photoproduct of AZM photolytic reaction.

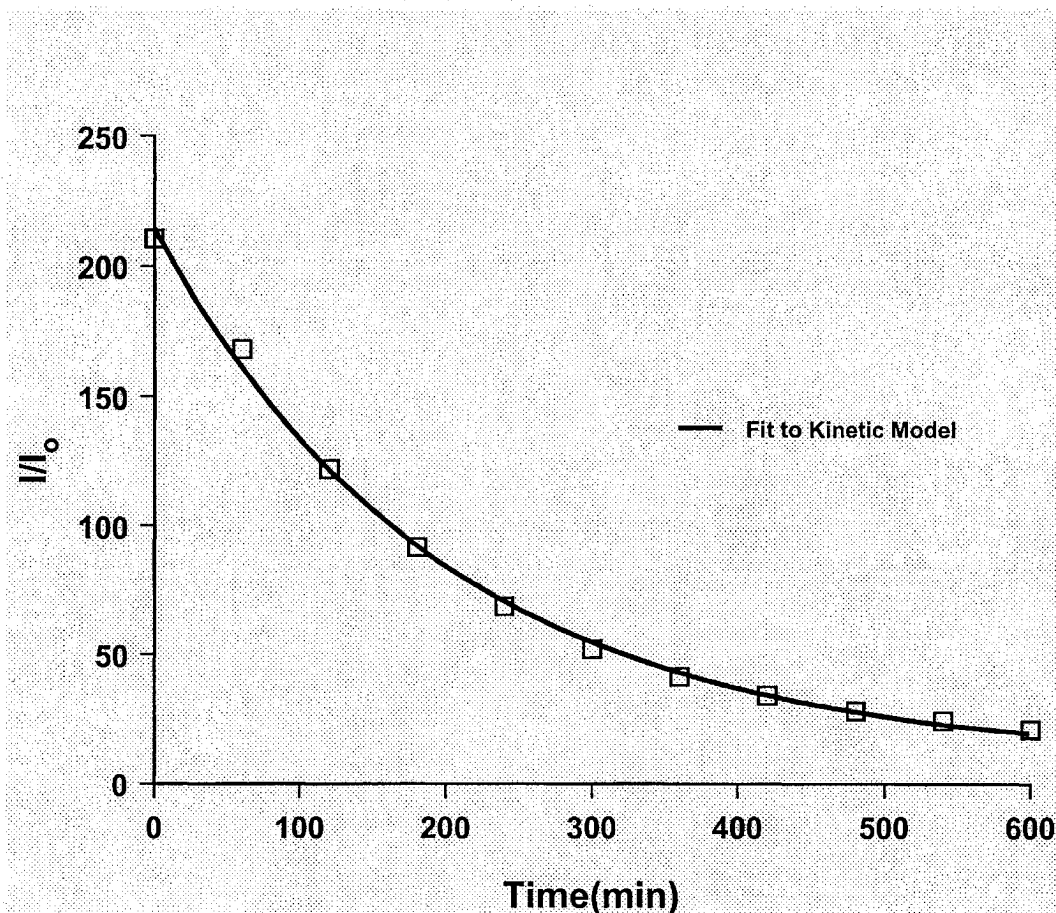


Figure 3.17. Kinetic curve for the anthranilic acid (concentration $1.0 \times 10^{-6} \text{ M}$)

These investigations were extended based on the literature³⁰ report that N-methyl anthranilic acid could also be a candidate as the intermediate. The comparison of the fluorescence intensity of AZM and NMAA was carried out. The concentration of AZM was $4.0 \times 10^{-5} \text{ M}$ and the concentration of NMAA was $1.0 \times 10^{-5} \text{ M}$. The concentration of NMAA was 4 fold diluted relative to that of AZM because of its higher fluorescence intensity. The

calculated ratio of the fluorescence intensity of AZM and NMAA was 1:33. Therefore, the fluorescence intensity of the NMAA was 130 times higher than that of AZM. This comparative result indicates that NMAA is indeed a potential candidate as the highly fluorescent intermediate (although it is not as fluorescent as AA). The photolysis of NMAA was therefore carried out in methanol. The kinetic result of NMAA showed (Figure 3.17) that the decay rate constant was $4.4 \times 10^{-3} \text{ min}^{-1}$, which, within the expected error, is the same as that of AZM ($k_2 = 4.4 \times 10^{-3} \text{ min}^{-1}$) shown in Figure 3.8. Thus it is also possible that NMAA is the intermediate.

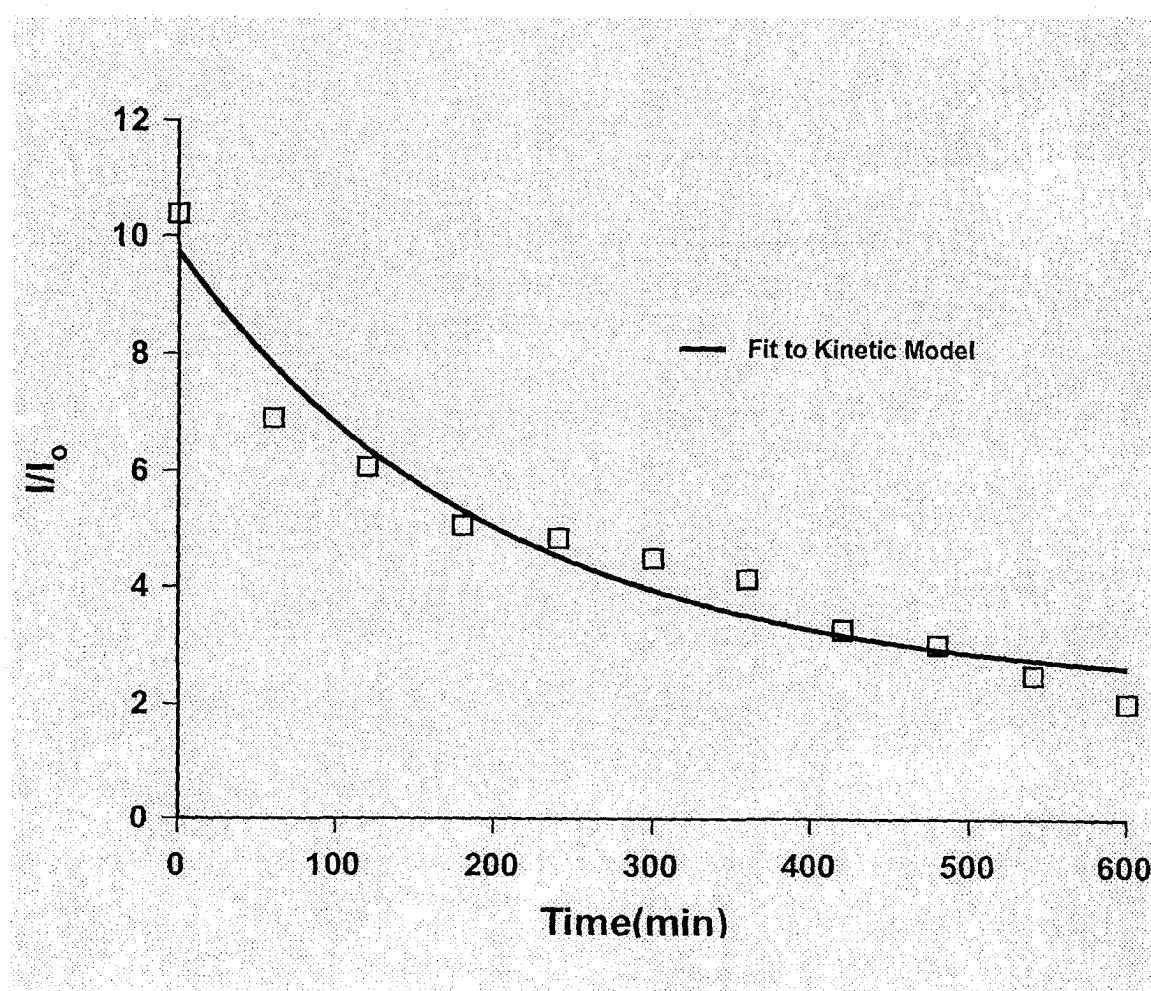


Figure 3.18. The kinetic curve of NMAA (concentration $1.0 \times 10^{-6} \text{ M}$)

Further investigations were performed to identify the highly fluorescent intermediate in the AZM photolysis, using fluorescence and NMR spectroscopy, as well as HPLC. These results will be mentioned in the following sections.

3.2.4.2. Normalization of the Fluorescence Spectra for the Identification of the Highly Fluorescent Intermediate Photoproduct of AZM

Since the kinetic traces of the decay of AA and NMAA both agreed well with that of the intermediate photoproduct of AZM photolysis, extended studies were done to identify and confirm the intermediate. The first approach was to compare the fluorescence spectrum of the intermediate to those of AA and NMAA. In order to do this, the fluorescence spectrum of the intermediate photoproduct of AZM (after a specific course of irradiation), anthranilic acid and N-methyl anthranilic acid from both water and methanol were normalized for direct comparison. The graphical results (Figure 3.19 and 3.20) showed that the spectra of NMAA and the AZM intermediate overlay each other extremely well, but this was not the case for AA. This was true for AA both in water and methanol. Therefore, the results from the fluorescence experimental measurement confirm that N-methyl anthranilic acid is the reactive intermediate photoproduct of AZM both in water and methanol solvents.

As the identification of the intermediate of AZM photolysis both in water and methanol was confirmed by the fluorescence technique, the kinetic experiment of AA and NMAA in water was not performed.

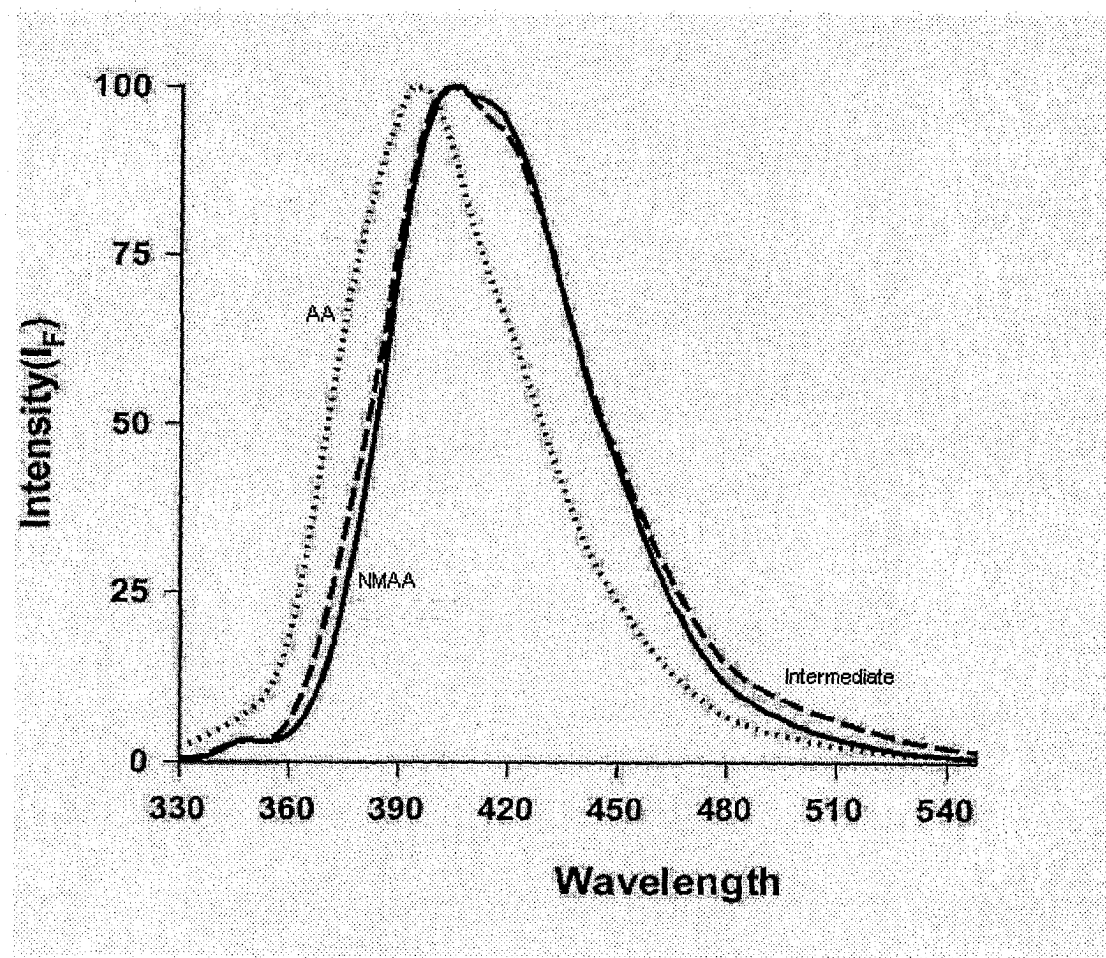


Figure 3.19. Normalized fluorescence spectra of AA (1.0×10^{-6} M), NMAA (1.0×10^{-6} M), and photolyzed (6 hours of irradiation) AZM (4.0×10^{-5} M) in methanol

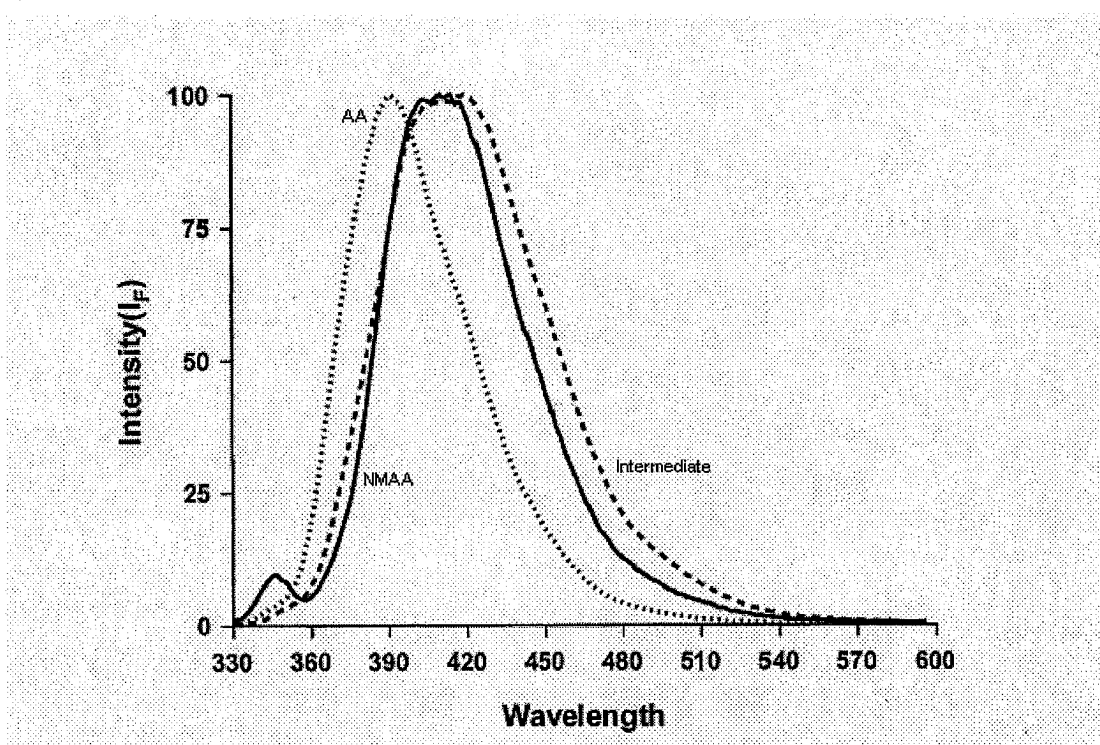


Figure 3.20. Normalized fluorescence spectrum of AA (1.0×10^{-6} M), NMAA (1.0×10^{-6} M), and photolyzed (6 hours of irradiation) AZM (4.0×10^{-5} M) in water

3.2.5. NMR Studies for the Determination of Intermediate and Final Photoproducts of AZM Photolysis

In order to confirm the fluorescence-based identification of N-methylanthranilic acid as the intermediate, and to identify the final product(s), ^1H NMR spectroscopy was performed on unphotolyzed and photolyzed AZM solution in deuterated methanol. The ^1H NMR spectrum was taken of the pesticide azinphos-methyl in deuterated methanol before any irradiation with UV-light (Figure 3.22). The concentration of the solution was 1.5×10^{-3} M, which was found to be suitable for both the NMR spectrum and the subsequent photolysis experiments. The spectrum given in Figure 3.22 showed two peaks at 4.84 ppm and 3.54 ppm that corresponded to the

deuterated methanol solvent. The bands at 8.35 ppm, 8.24 ppm, 8.11 ppm and 7.98 ppm represent the aromatic protons of AZM (labeled A to D in Figure 3.21). The other bands at 5.81 ppm and 3.76 ppm correspond to the non-aromatic protons (labeled E and F, respectively in Figure 3.21).

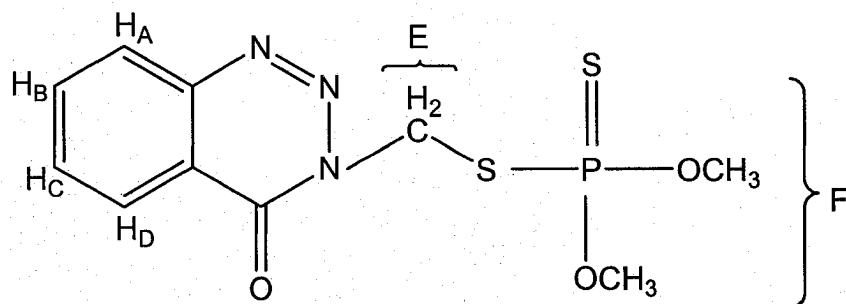


Figure 3.21. Structure of AZM showing different types of protons

The same concentrated solution was then exposed to 350 nm UV-A light in the photoreactor for 6 hours and the ^1H NMR spectrum was recorded again. This irradiation time was chosen based on the kinetic results for the photodegradation of AZM in methanol solution discussed in section 3.2 (maximum intermediate concentration indicated by the maximum fluorescence emission at this time).

After 6 hours of photolysis, the ^1H NMR spectrum (Figure 3.23) of the photolysis mixture showed a new peak (very weak) at 1.30 ppm. Other peaks were found at the same chemical shifts as in the case of the unexposed AZM. This peak did not match with any peak found for the spectrum of potential intermediate and products, namely anthranilic acid (Figure 3.25), N-methyl

anthranilic acid (Figure 3.26) and benzazimide (Figure 3.27), and at this point remains unidentified.

After 36 hours irradiation, the ^1H NMR spectrum of the photolysis mixture (Figure 3.24) showed that all peaks for the AZM band in the aromatic region disappeared, and new peaks had appeared at 8.32 ppm, 8.19 ppm, 8.09 ppm and 7.92 ppm. Thus, these correspond to the final product. In this case, the NMR spectrum matches very well to that of benzazimide, an observed final product in the previously discussed photolysis of azinphos-ethyl³⁴. The same peaks at 8.32 ppm, 8.19 ppm, 8.09 ppm and 7.92 ppm are identified in the spectrum of unexposed benzazimide showed in Figure 3.27. Other peaks at 5.80 ppm and 3.79 ppm could be from other unidentified final product(s).

Thus while, the ^1H NMR result of AZM exposed for 6 hours (Figure 3.23) did not show any trace of anthranilic acid (Figure 3.25) or N-methyl anthranilic acid (Figure 3.26) as an intermediate photoproduct, that exposed for 36 hours clearly showed (Figure 3.24) a significant amount of benzazimide (Figure 3.27) as a final product. The role of benzazimide as a stable product was further investigated by irradiating benzazimide solution for 12 hours; the resonance of the ^1H NMR spectrum for benzazimide did not change confirming that it is photochemically stable, and thus indeed a final product.

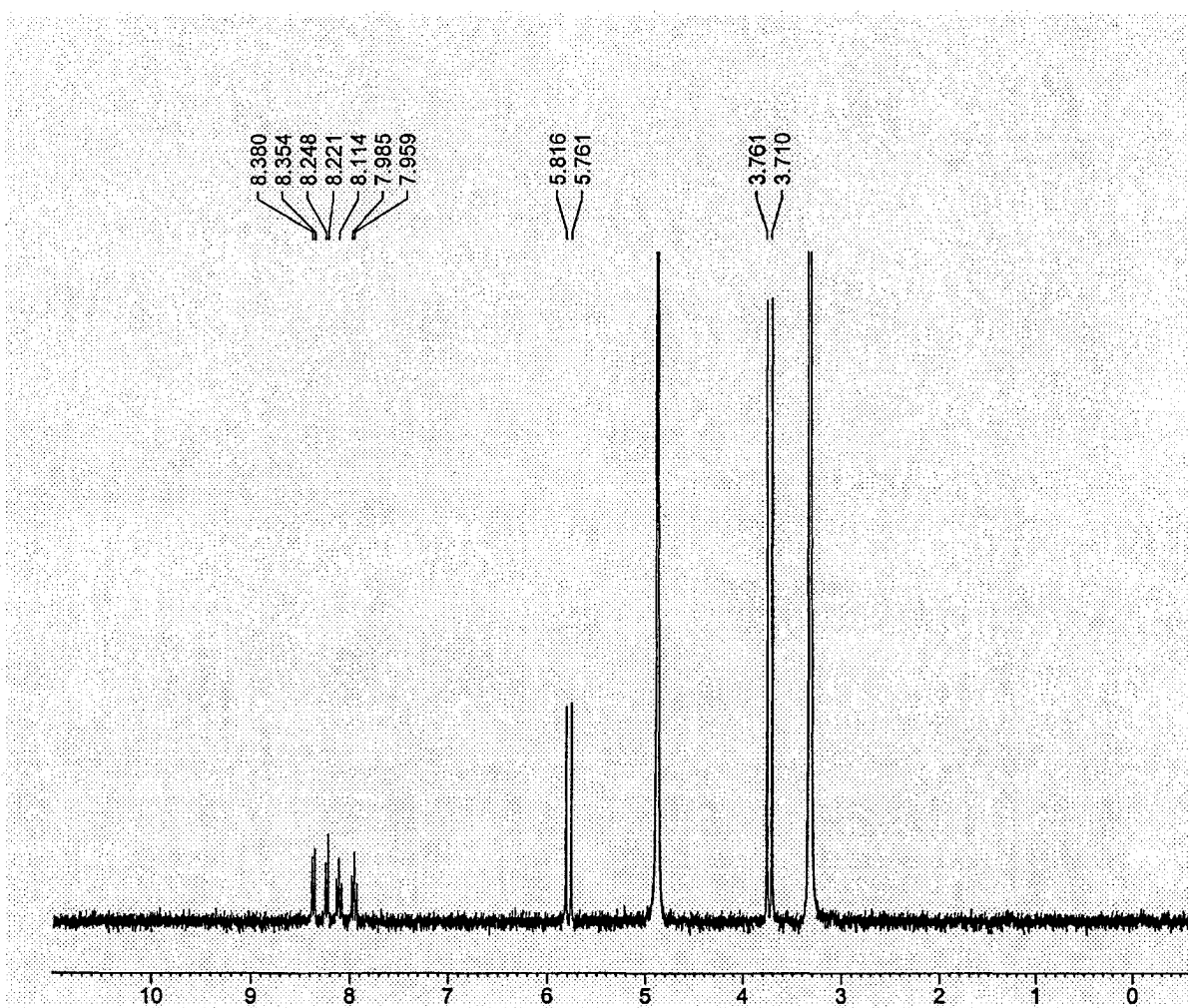


Figure 3.22. ${}^1\text{H}$ NMR Spectrum of AZM without any irradiation

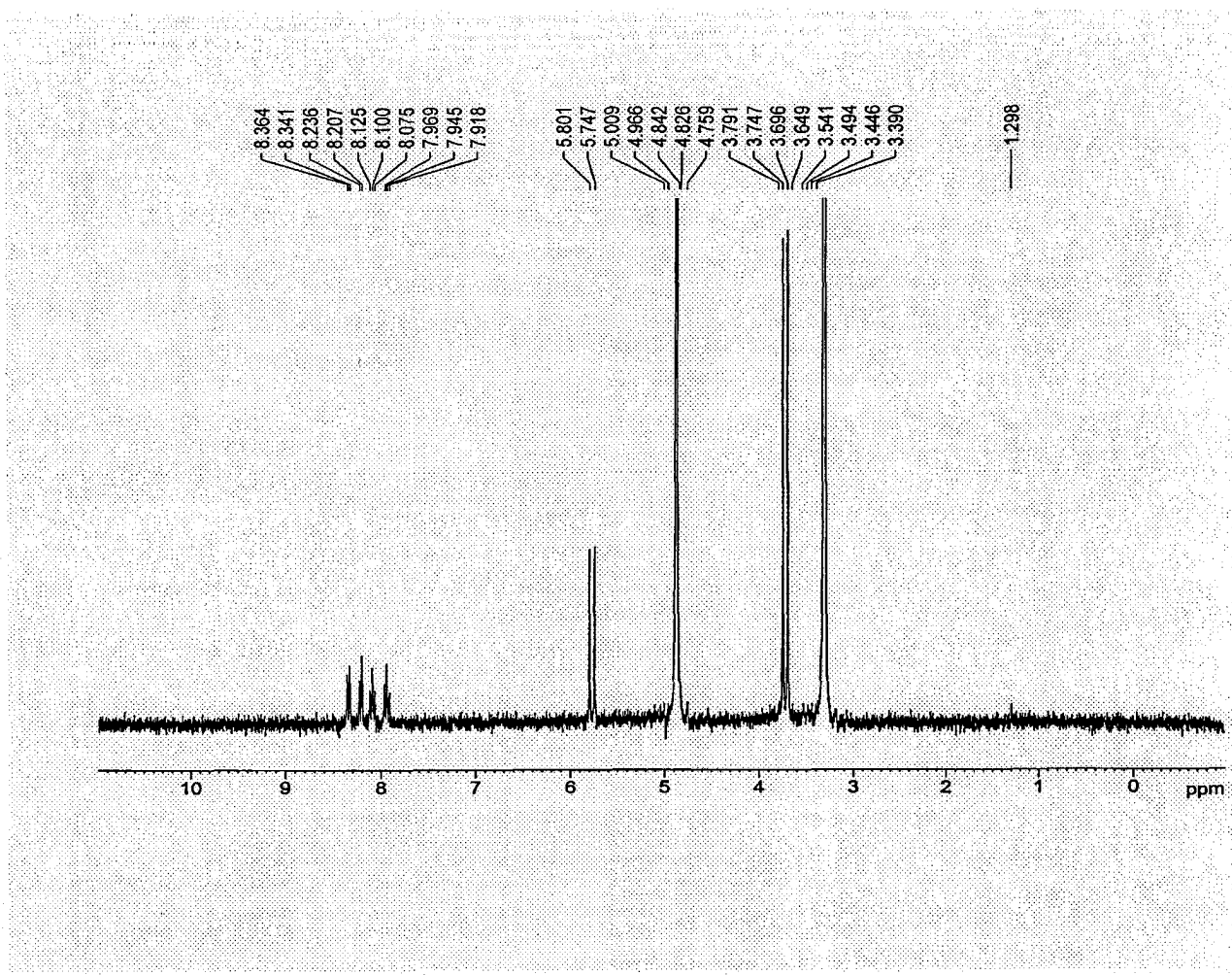


Figure 3.23. ^1H NMR spectrum after 6 hours irradiation

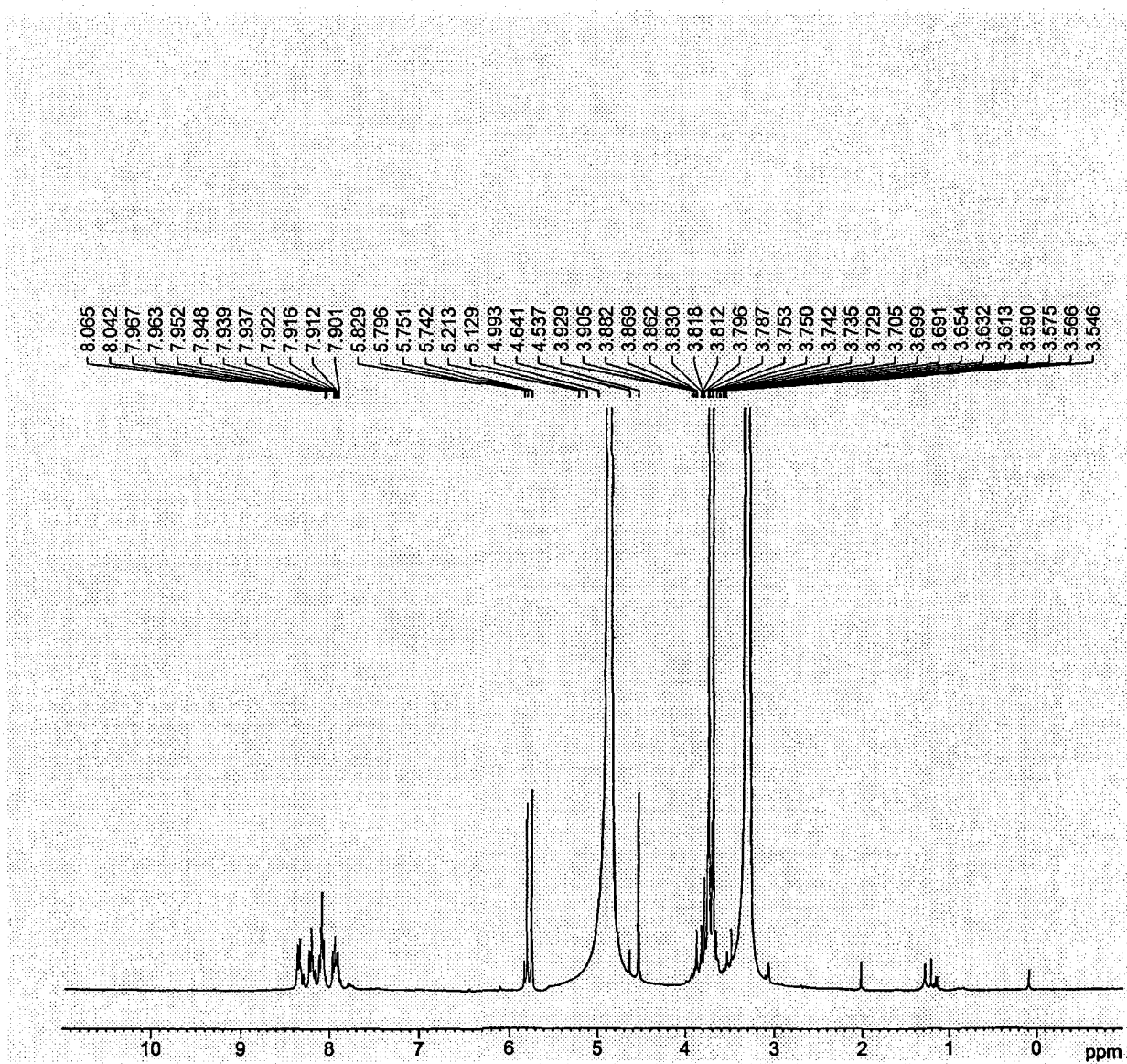


Figure 3.24. ${}^1\text{H}$ NMR spectrum after 36 hours irradiation

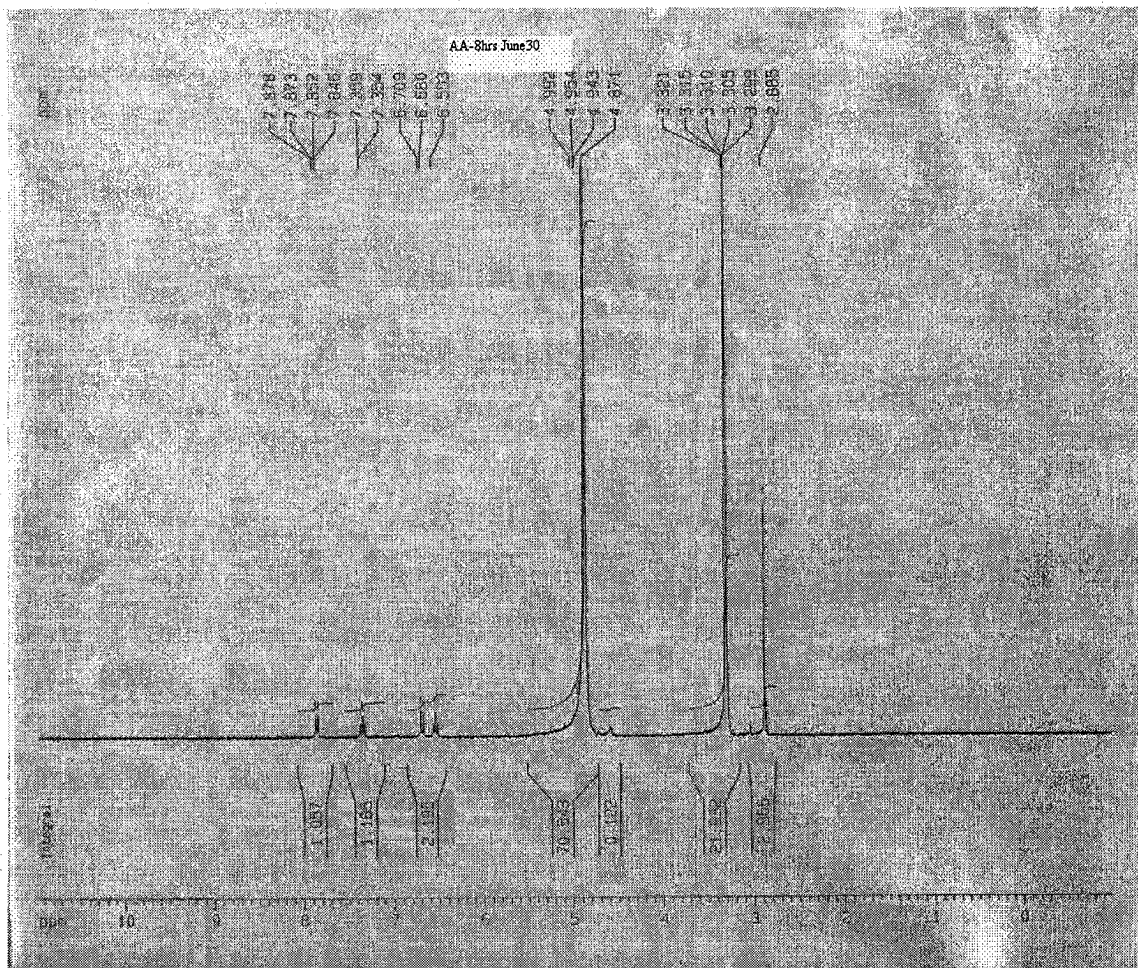


Figure 3.25. ^1H NMR for anthranilic acid without any irradiation

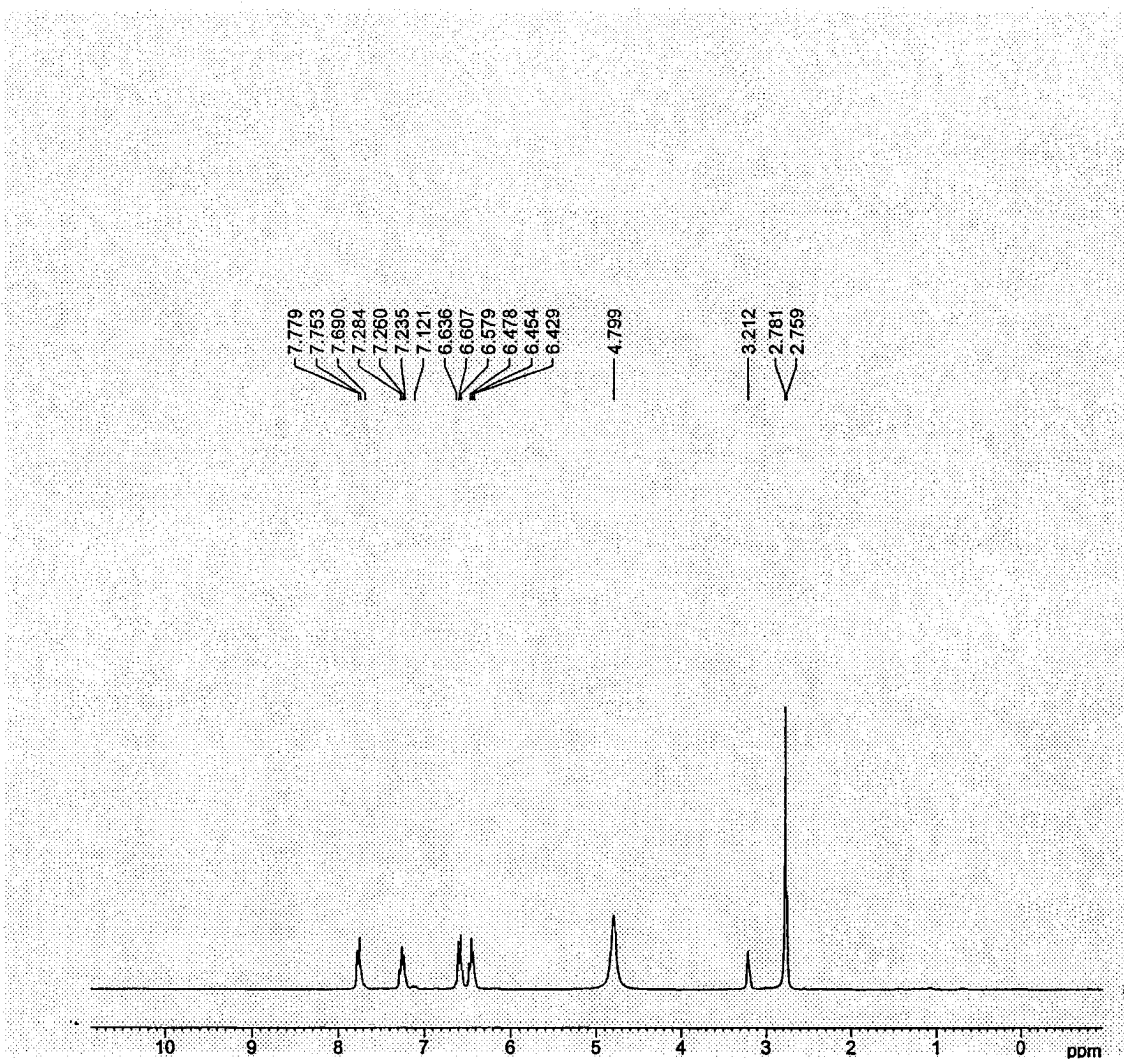


Figure 3.26. ^1H NMR for N-methyl anthranilic acid without any irradiation

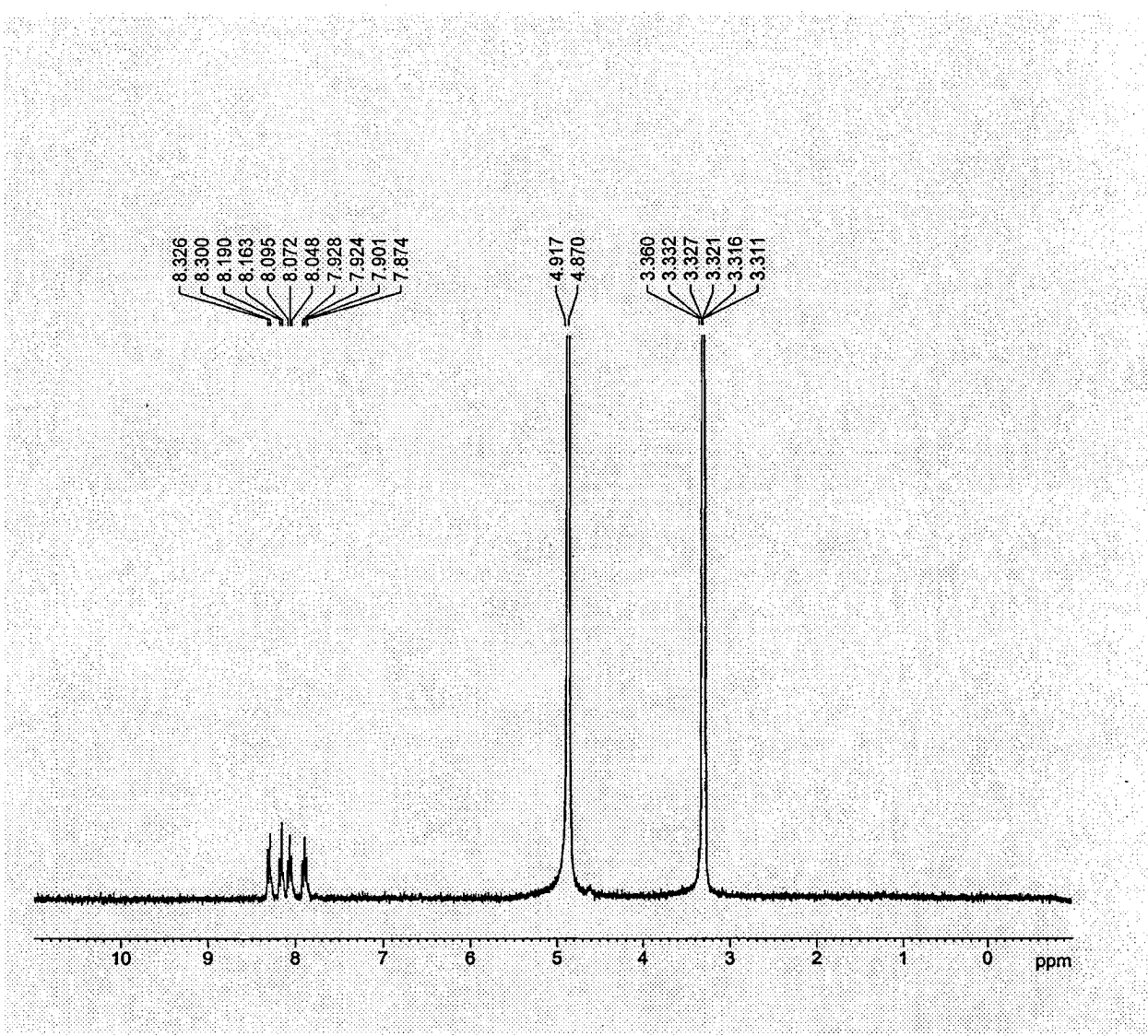


Figure 3.27. ^1H NMR for benzazimide without any irradiation

3.2.6. HPLC Studies for the Identification of Intermediate and Final Photoproducts of AZM

HPLC analysis was performed as another tool with the goal of identifying the intermediate and products of the AZM photolysis by separation using the column mentioned in the experimental section. In this experiment, the chromatograms of AZM (without any exposure to UV light), anthranilic acid, N-methyl anthranilic acid and benzazimide were obtained. The concentration of each of the four compounds (0.25mM) was the same.

Figures 3.28 to 3.31 show the chromatograms of AZM, AA, NMAA and BA.

A mixture of AZM, AA, NMAA, and BA solution was also run through the column to demonstrate the separability of the compounds, and establish the retention times of the compounds as standards. Figure 3.32 shows the chromatogram of the mixture of the four compounds. In Figure 3.32, the retention times of AA, NMAA and BA were very close, which matches with the chromatogram of those three in Figures 3.29-31. AA was eluted first, followed by NMAA and then BA. The peak of BA was very intense as compared to those of AA and NMAA. The peak of AA and NMAA were almost overlapped with each other. The peak at the retention time around 7.5 matches with the peak position of the parent AZM.

The same concentrated solution of AZM (0.25mM) was then exposed again to the UV light in the photoreactor for 8 hours. The HPLC method was used again, resulting in separation of the photoproduct. The run for mixed solution and the AZM irradiated solution were performed on two different days. Figure 3.33 represents the chromatogram of the photoproducts and the

parent material AZM. In Figure 3.33, the peak around 2.5 minute retention time matches with the peak of benzazimide in Figure 3.31. The peak around 7.5 retention time represents the parent material according to the chromatogram in Figure 3.28. Again, there was no clear evidence of AA or NMAA (Figure 3.33) as compared to the chromatograms of AA and NMAA shown in Figure 3.32. There are many small peaks positioned in between benzazimide and parent material AZM were obtained which were unidentified.

Thus, the HPLC experimental results provided more evidence that benzazimide is one of the photoproducts of AZM photolysis, in agreement with the ^1H NMR results. Since no trace of AA or NMAA was identified in photolytic reaction of AZM, HPLC technique did not provide information for the identification of the intermediate.

The lack of evidence of NMAA in either ^1H NMR or HPLC studies must be a result of its very low concentration as an intermediate, too low to be detected by these techniques. The fact that it could clearly be detected by fluorescence is a result of its extremely high fluorescence quantum yield compared to that of AZM (approximately 130 times more fluorescent, as determined above).

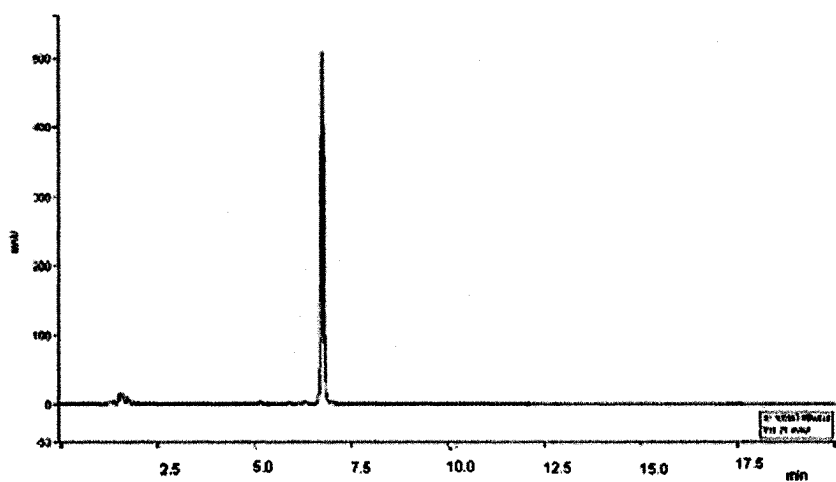


Figure 3.28. Chromatogram of unphotolyzed AZM (0.25 mM) in water-methanol (60/40)

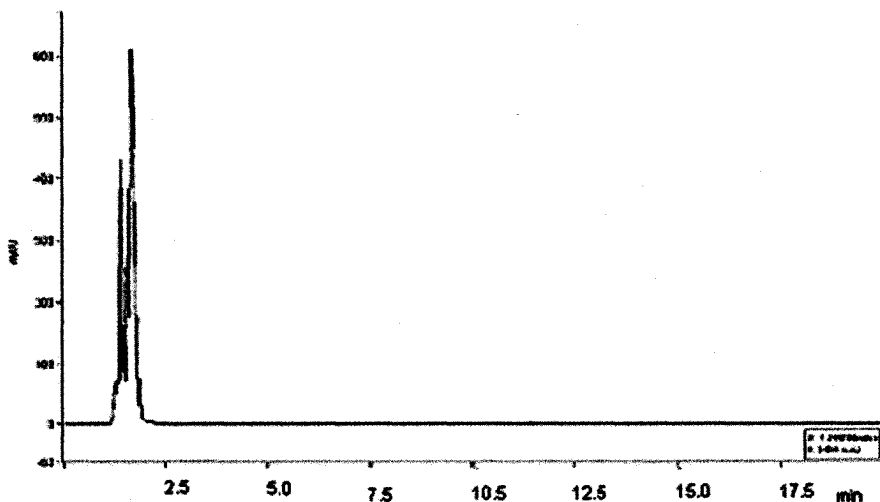


Figure 3.29. Chromatogram of unphotolyzed anthranilic acid (0.25 mM) in water-methanol (60/40)

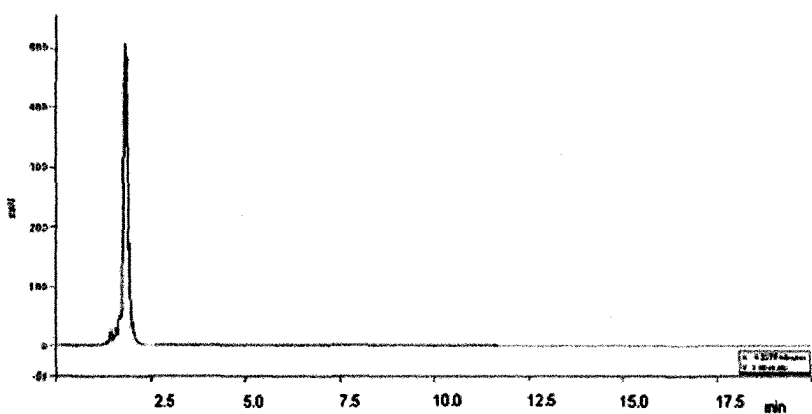


Figure 3.30. Chromatogram of unphotolyzed N-methyl anthralic acid (0.25 mM) in water-methanol (60/40)

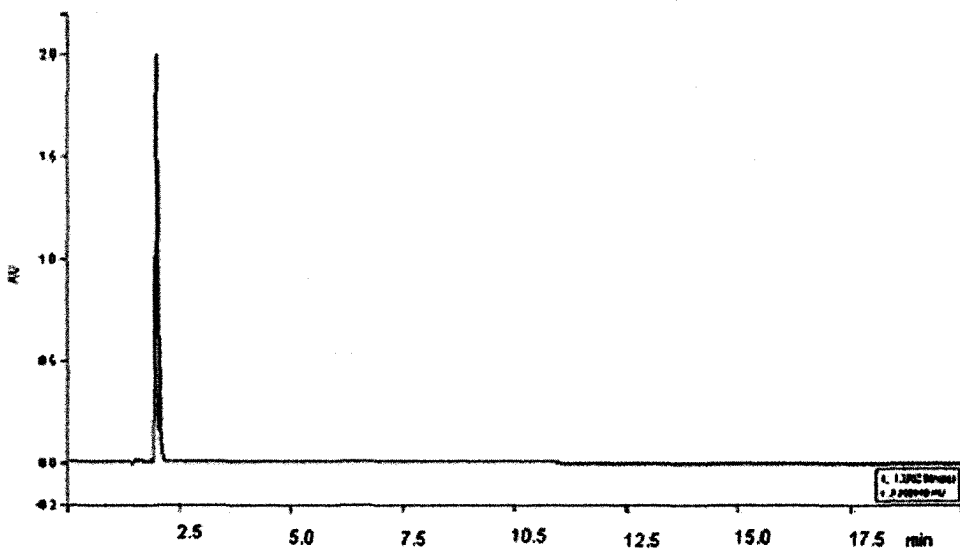


Figure 3.31. Chromatogram of unphotolyzed benzazimide (0.25 mM) in water-methanol (60/40)

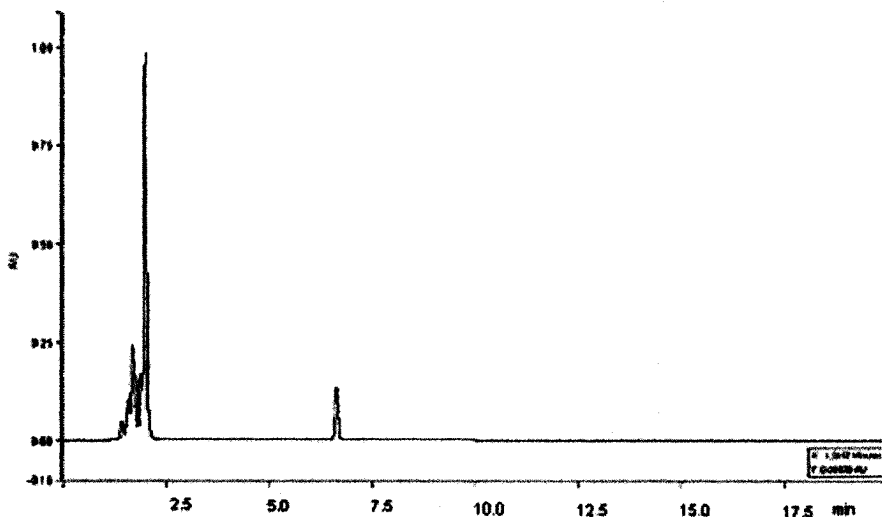


Figure 3.32. Chromatogram of mixture of unphotolyzed AA, NMAA, BA and AZM (0.25 mM) in water-methanol (60/40)

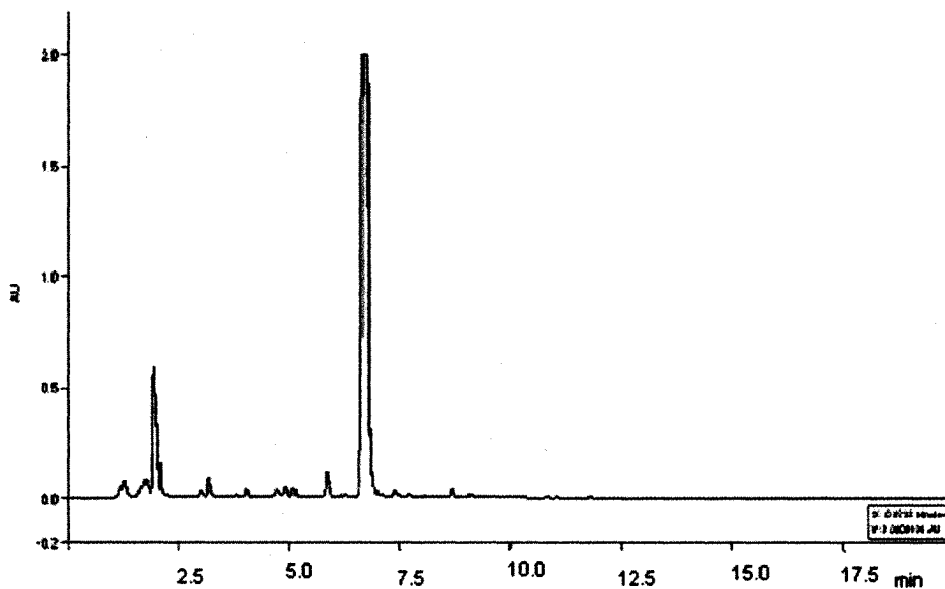


Figure 3.33. Chromatogram of photolyzed AZM (0.25 mM) in water-methanol (60/40) after 8 hours of irradiation

3.3. Laser Flash Photolysis Studies

Laser flash photolysis (LFP) provides a convenient experimental method for measuring the absorption spectrum of intermediates and products in photochemical reactions. Thus, samples of AZM and AA (our suspect as the intermediate at the time) were sent to Dr. Norman Schepp at Dalhousie University, who did the LFP experiments.

3.3.1. Azinphos-methyl Analysis

Azinphos-methyl dissolved in water and methanol was excited with 308 nm laser pulse. In both solvents no transient was seen under deoxygenated or oxygenated conditions (Figure 3.34). Therefore, the LFP studies show clearly that the intermediate and products of the photolysis of AZM absorb below 360 nm.

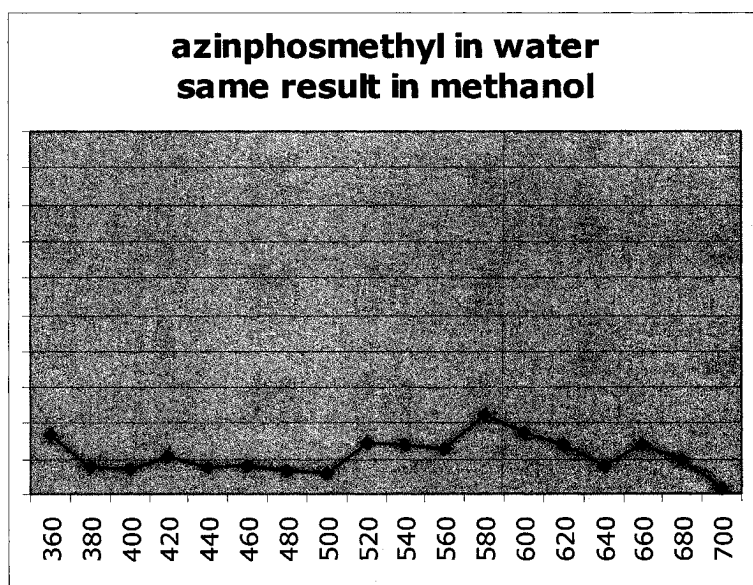


Figure 3.34. Transient absorption spectrum of photolyzed azinphos-methyl

This was an experimental limit of the LFP system for excitation at 308, and the region below 360 nm could not be investigated. Although these results are consistent with NMAA as the intermediate and benzazimide as the major product, they are not otherwise particularly useful.

3.3.2. Anthranilic Acid Analysis

It has already been mentioned that anthranilic acid could be a candidate for an intermediate degraded product of AZM (although subsequent fluorescence experiments identify the intermediate as NMAA, this was not known at the time of the LFP experiments). Studies with NMR and HPLC did not show any evidence for the formation of such a compound. To further our study, LFP was employed to examine its photolysis. In this case, the LFP result shows a transient with an absorption maximum at 420 nm. The kinetic trace at 420 nm shown in Figure 3.35 decreases in a first order manner, with a rate constant of $8.2 \times 10^5 \text{ s}^{-1}$. Thus, the life time of this intermediate is only 0.84 s. However, the decay does not proceed back to baseline, but to a significant absorbance above the baseline. This remaining absorption is very long lived, with no decrease on this time scale. This suggests the formation of very short-lived intermediate, which undergoes a first order reaction to a stable product, and that the intermediate and product have very similar absorption spectra. The anthranilic acid transient was not sensitive to oxygen (Figure 3.37). With methanol solution, the result was similar to that in water solution, although the signals were weaker than in water (Figure 3.36-37).

This intermediate would not be observed by any of the other experimental techniques, due to its extremely short lifetime. Thus, the LFP results were again not very useful.

As mentioned above, LFP studies of NMAA were not performed at that time (its identification as intermediate had not yet been made). Since very few useful results were obtained, it was decided not to have LFP experiments performed on NMAA.

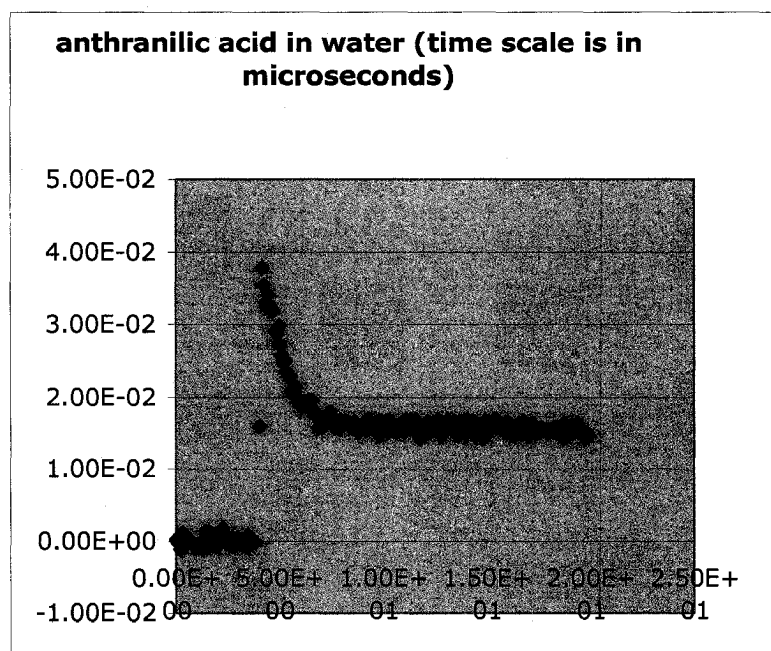


Figure 3.35. LFP kinetic trace of anthranilic acid at 420 nm

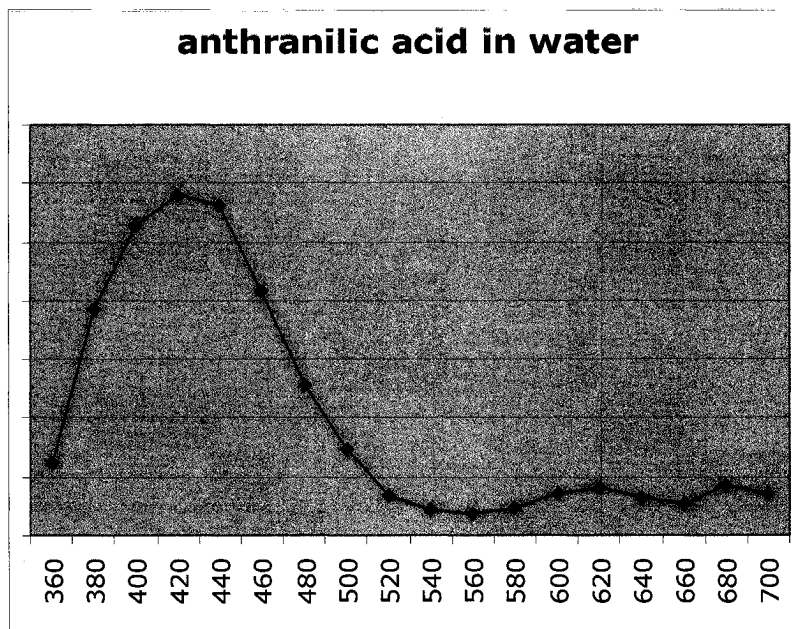


Figure 3.36. Transient absorption spectrum of photolyzed anthranilic acid

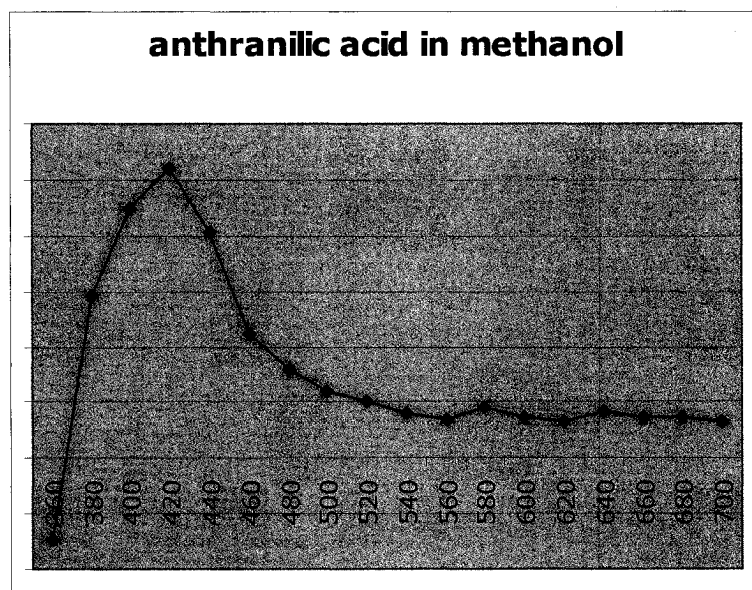


Figure 3.37. Transient spectrum of photolyzed anthranilic acid measured in deoxygenated solution

3.4. Photolysis Studies of Azinphosmethyl under Direct sunlight Using Natural Water

Among the different transformation processes (biotic and abiotic), photodegradation is an important factor influencing the fate of pesticides in the natural environment.⁴³ An important aspect of this project involved trying to approximate environmental conditions using sunlight as the UV source and natural water as the solvent. Although modeling pesticide behavior under laboratory conditions is a very useful tool for environmental studies, there is a need to conduct photodegradation studies in natural environmental conditions taking into consideration factors such as temperature variation, the daily and seasonal variation of natural sunlight intensity, dissolved organic matter in the solution.⁴⁴

The photochemical degradation of azinphos-methyl was investigated using natural stream water collected from a PEI stream under direct sunlight. The goal of this experiment was to investigate the photolysis of AZM in natural water in the environment.

AZM in natural water was exposed under direct sunlight with various cloudiness, and time of day, and variation in temperature. This was done by placing the fluorescence cuvette containing AZM in natural water at a concentration of 4.0×10^{-5} M on the balcony of the K.C. Irving Chemistry Center. The result showed that the pesticide azinphos-methyl photodecomposed when it was exposed under direct environmental sunlight (Figure 3.38). Since the intensity of the sunlight could not be held constant (clouds, elevation of the sun throughout the day), the results of these

experiments are considered to be qualitative. However, the experiment does provide an excellent qualitative model for photolysis of AZM in the environment, *i.e.* in natural water system under natural sunlight. It shows that UV from natural sunlight can photodegrade (Figure 3.38) the pesticide AZM which has found its way into natural water by agricultural run-off. For comparison, a dark controlled experiment was also carried out by keeping another cuvette of the same AZM solution inside a dark cupboard in the laboratory. The dark experiment (Figure 3.38) shows that AZM does not degrade in absence of any light source.

There is no report in the literature on the studies of the photodegradation of azinphos-methyl in natural water and in natural environment conditions.^{32, 33} However, such studies have been reported for other organophosphorus pesticides.⁴⁵⁻⁵⁰

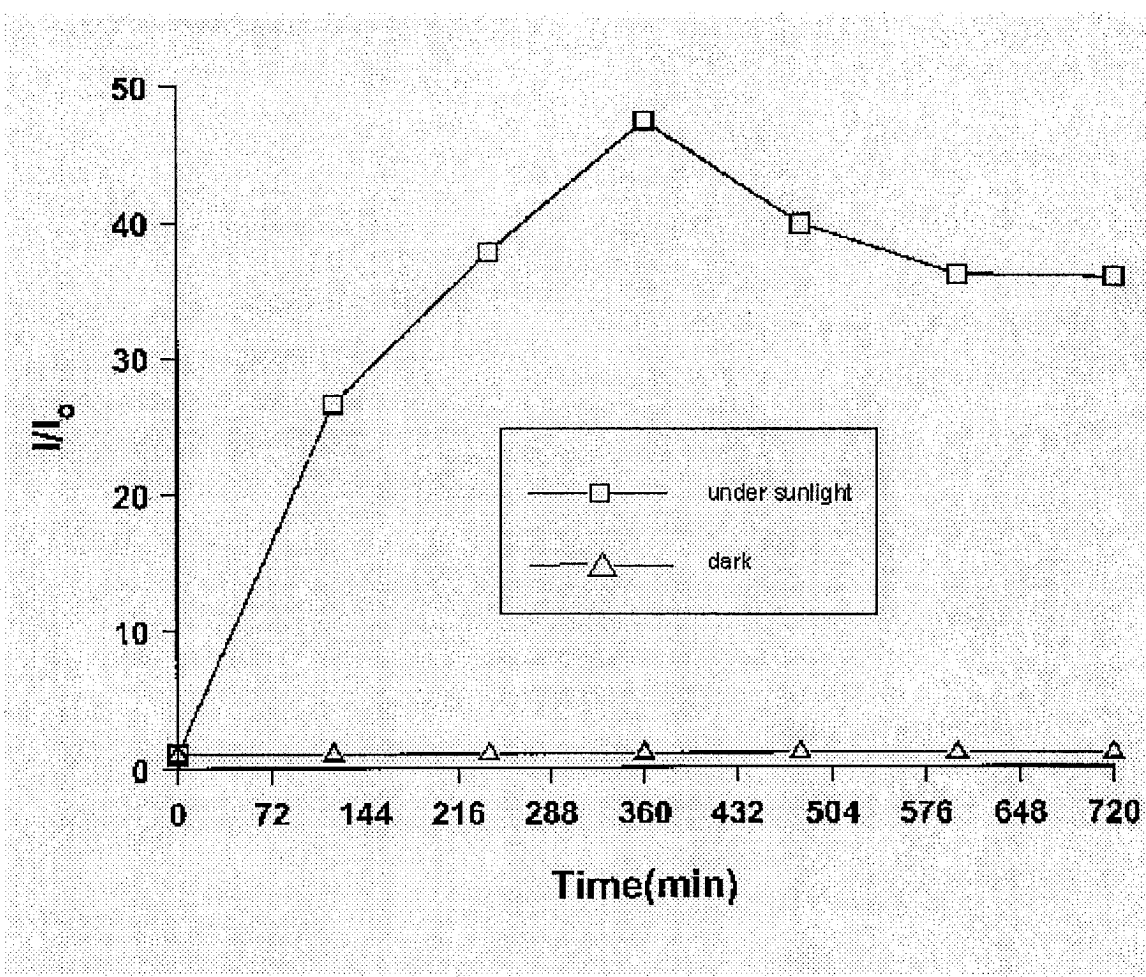


Figure 3.38. Photodegradation curve of azinphos-methyl in natural water under direct sunlight.

In the surface water (stream water) dissolved organic matter (DOM) and inorganic compounds, rather than the pesticide can absorb light and they can play an important role on the photochemistry of azinphos-methyl. Therefore, photodegradation of pesticides can occur by direct or indirect processes in aqueous media in the environment.^{19, 20}

Direct photodecomposition processes occur when organic pesticides absorb light sufficiently in the UV region (250-350 nm).⁵¹⁻⁵³ However, several factors often limit the efficiency of these photoprocess in aquatic

environments: the transparency of natural waters, pesticide molar absorptivity and water solubility, solar light absorption and pH value of water, which may shift the pesticide absorption maximum and produce significant effects on photodegradation of pesticide. For example, in the case of the direct photolysis of aromatic pesticides, the conversion yield has been shown to range from 18 to 99.5% for reaction times of 40-70 min, according to the molecular structure of compounds and the nature of the solvent.^{51, 52} On the other hand, during indirect photolysis light energy is absorbed by other constituents of the natural water.⁵⁴ The excited species can then either transfer the energy to the substance, undergo an electron transfer with the substance, or lead to the formation of reactive species, such as singlet oxygen or hydroxy radical, which enter into a series of reactions.^{26, 55, 56} However, a sensitization effect of humic and other substances of natural waters cannot be excluded. The sunlight absorbance by the DOM and other organic chromophores, such as riboflavin and flavin, could provide a rich variety of photochemical reactions.⁵⁷ The resulting excited states of the DOM, and reactive transients that were produced from DOM, could participate in energy transfer, electron transfer, and free radical reaction, which affect the fate of aquatic pollutants.⁵⁸

The results of the experiment show that AZM undergoes photolysis in natural water under direct sunlight in a very similar manner to that observed in distilled water in the photoreactor. In fact, the overall shape of the photodegradation curve in Figure 3.38 is similar to that observed in the

photoreactor experiments, indicating the photoproduction of a highly fluorescent intermediate, which in turn is photodegraded into relatively less fluorescent products. We propose that this occurs by the same mechanism found in the laboratory environment. This photodegradation of AZM in the environment is important in terms of its environmental fate and residue time. This work shows that this photolysis must be taken into account when predicting the effect of AZM run-off on fish populations, for example, especially in the case of relatively shallow, clear streams, such as those on Prince Edward Island. Photolysis by sunlight will clearly degrade this pesticide much faster than its decay predicted based on biotic and thermal degradation.

3.5 Proposed mechanism for AZM photolysis

On the basis of the experimental results of the photolysis of AZM both in water and methanol and in consultation with literature reports reviewed earlier proposed reaction pathways for the formation of the highly fluorescent intermediate and the relatively non-fluoresce final product(s) have been devised. The overall mechanism consists of two co-existing pathways of AZM photolysis, the first producing NMAA as an intermediate and aniline or N-methylaniline as the final products (Scheme 1A) and the other producing benzazimide as a final product (Scheme 1B). Scheme 1A is shown as two steps, which represent the formation of the highly fluorescent intermediate, NMAA (Step 1) which then undergoes further photodegradation to non-fluorescence final products (Step 2).

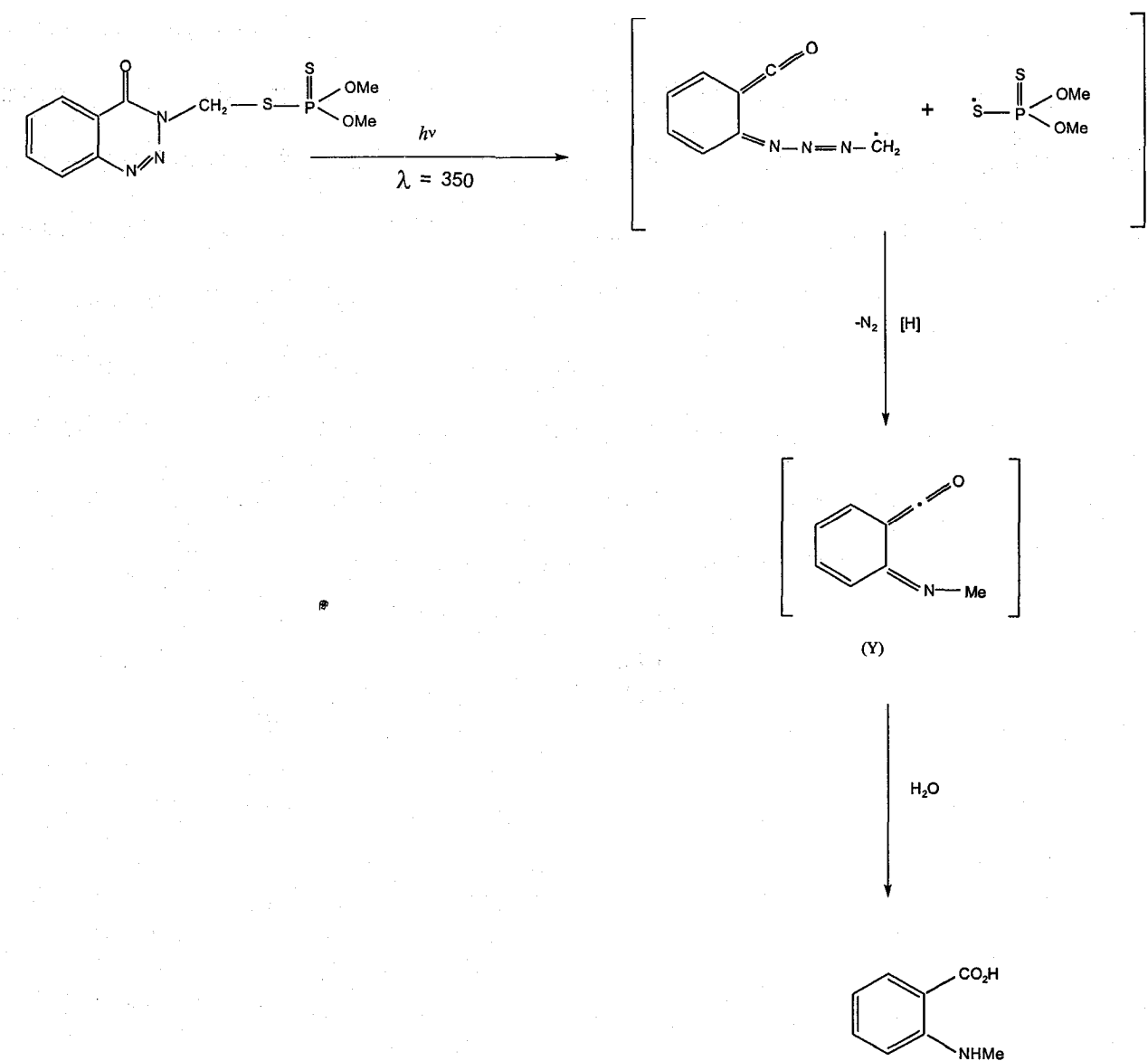
Again, it is emphasized that a separate pathway has been proposed for benzazimide as a final product, as shown in Scheme 1B. Thus, benzazimide is not the final product "C" in the consecutive first-order reaction model used to fit the kinetic results; in that $A \rightarrow B \rightarrow C$ model, A is AZM, B is NMAA, and C is either aniline, N-methylaniline, or some other unidentified final product. These separate concurrent mechanisms will be discussed individually in the following two sections.

3.5.1. Proposed mechanism for N-Methyl Anthranilic Acid as An Intermediate

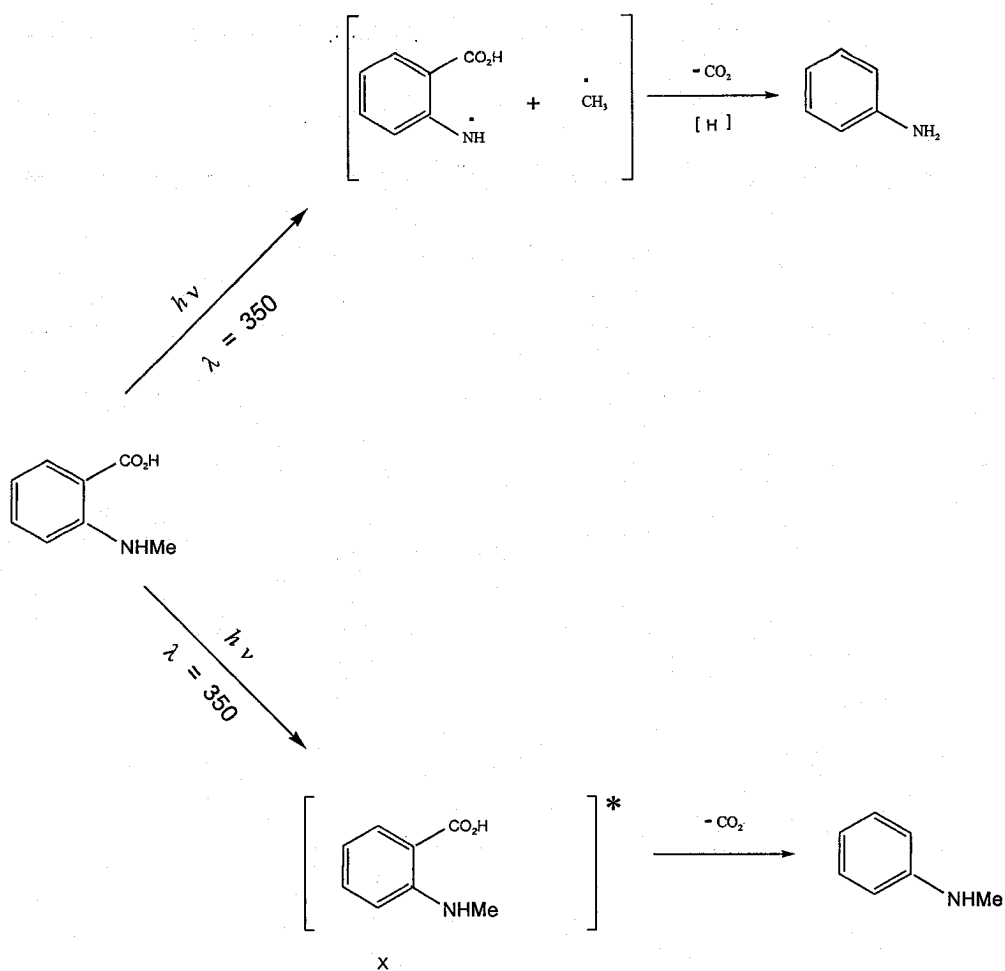
N-methyl anthranilic acid was identified as the highly fluorescent, photochemically unstable intermediate photoproduct (sections 2.3.5.4 and 3.2.4) of AZM. Step 1 in Scheme 1A proposes that during the exposure of AZM to UV light a homolytic cleavage of the C-S bond of the side chain results in the formation of a very short lived ketene.⁶⁰ In progression, another very short lived ketene (Y) is formed via hydrogen abstraction (presumably from solvent) and removal of N_2 . Reaction of this ketene with water produces the highly fluorescent intermediate NMAA. The mechanism for the formation of NMAA as a final product of AZE but not an intermediate was previously reported.³⁴ On the basis of our experimental results, a mechanism has also been proposed for this intermediate, NMAA that might undergo further photodegradation to produce relatively non-fluorescent photoproduct(s). These could include aniline and/or N-methyl aniline as shown in Step 2 in Scheme 1A. Due to time limitation, it was not possible to identify the further

photodegraded product(s) of the intermediate N-methyl anthranilic acid; these are likely to be produced in very low concentration.

In Scheme 1A Step 2, the mechanism of the further break down of the intermediate NMAA to produce other final photoproducts of AZM was rationalized. This breakdown may occur by photochemically induced chemical decarboxylation reaction followed by hydrogen abstraction to produce aniline. Another pathway for the degradation of NMAA could lead to the formation of N-methyl aniline via a photo-induced excited state intermediate X. Both of these products are stable to UV irradiation according to the literature reports.⁵⁹



Scheme 1A. Proposed reaction pathway 1 (Step 1: Formation of NMAA)

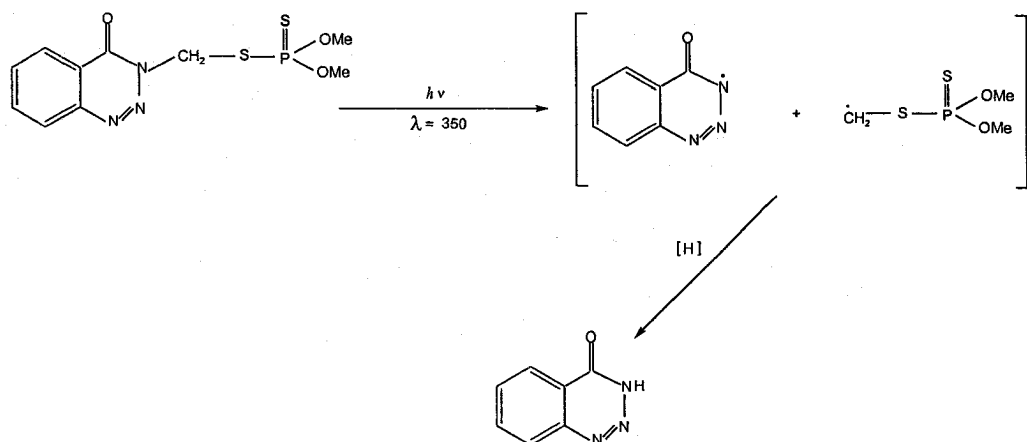


Scheme 1A. Proposed reaction pathway 1 (Step 2: photodegradation of NMAA)

3.5.2. Proposed Mechanism for Benzazimide as a Final Product

The experimental results showed benzazimide to be one of the final photodegraded products of AZM. The production of BA could be interpreted by Scheme 1B, in terms of the formation of very short-lived intermediate

radical due to homolytic cleavage of the C–N bond of the side chain. Then BA, the furnished product of the triazinone radical could be formed via hydrogen abstraction. This mechanism has been reasonably proposed in accordance with a previous report.³⁴ The NMR studies of photolysis of benzazimide confirmed that it was photostable against further irradiation to UV light.



Scheme 1B: Proposed reaction pathway 2 of AZM photolysis

Chapter 4. Conclusions and Future Work

In this project, photodegradation studies on the heavily used pesticide, azinphos-methyl, were carried out in the laboratory settings to model its environmental fate in the natural system as well as understand its photochemistry. The project as a whole can be divided into three phases. In the first phase, fluorimeter-based studies were carried out to determine the kinetics of the degradation reactions in methanol, water and water-methanol solvents with 300, 315 and 320 nm excitation wavelengths. On the basis of the experimental evidence water was added to methanol in various proportions in order to accelerate the photolytic reaction. Surprisingly, the degradation of the pesticide in methanol and water-methanol systems was very slow, whereas it was significantly faster in aqueous media. In this case, the photolysis was observed to be initiated within seven hours of irradiation. The frustrating outcome of these photolytic progressions in methanol and water-methanol media led to the use of a photoreactor ($\lambda = 350\text{nm}$) to do the photolysis study. In these experiments, a significant photodegradation of AZM was observed in all the solvents of interest, which followed first order reaction kinetics ($A \rightarrow B \rightarrow C$), where the generation of a highly fluorescent intermediate followed by further decomposition to relatively non-fluorescent end products was observed. The experimental results of solvent polarity effect on the photolysis of the pesticide in aqueous and organic solvents showed that the photochemically induced fluorescent enhancement with

irradiation time (growth of the highly fluorescent intermediate, k_1) followed no clear dependence on solvent polarity, but that a decent correlation of the rate constant for the further photolysis of the fluorescent intermediate (k_2) was observed. In acid buffer solution, the reaction was kinetically slow, indicating that it was not acid catalyzed. In this study, N-methyl anthranilic acid was identified as a highly fluorescent intermediate species that was found to photodegrade into relatively non-fluorescent photoproduct(s) basis on fluorescence spectrum analysis. A photostable compound, benzazimide was identified as one of the end products. UV-vis fluorescence spectrophotometer, NMR, HPLC and LFP techniques were employed for the investigation of the intermediate and the final photoproducts.

In the second phase, a model for the environmental fate due to agricultural use of the pesticide was investigated utilizing the experimental observations in the laboratory settings. Consequently, AZM in natural water was exposed under direct sunlight with various cloudiness, and time of day, and variation in temperature. The results showed that the species decomposed at a significant rate in a similar way to laboratory results, and in absence of UV light no evidence of photodegradation was observed. These results are significant, as they provide an excellent qualitative measure for the photolysis of the pesticide in natural environmental conditions.

Finally, in the progression of this project, a mechanism of AZM photolysis was proposed based on the experimental results and literature reports, which involved two reaction pathways. Pathway 1 described the

formation of the photoreactive and highly fluorescent intermediate, N-methyl anthranilic acid, which could further degrade to relatively non-fluorescent aniline and/or N-methyl aniline. In the second pathway, production of benzazimide via formation of a very short-lived intermediate was proposed.

Azinphos-methyl has entered an era of restricted use in the agricultural sector due to its threatening environmental effects since several fish killing incidents in PEI have come to light. However, it is a pesticide which has a great economic impact for agricultural growth, especially for the cultivation of potatoes. It is difficult to completely eliminate its use on PEI without an effective alternative, as PEI is the largest potato supplier through out all Canada and some parts of North America. Questions have been raised as to whether the pesticide should be totally banned or not. These findings show that the photochemical transformation to intermediate and final products results in the production of relatively less toxic compounds compared to the parent compound (AZM). This could help explain why the pesticide has been found to have only a very short-term effect (within 1 or 2 days) from a large surge of run-off field water into natural water systems just after an AZM field application (resulting in fish kills). It is not generally detected in natural water at a significant level at other times. More complete information on photochemical processes in the degradation of the pesticide in natural system would be important for understanding the fate determination of azinphos-methyl. In this context, a quantitative investigation should be taken as a major task and encouraged for the near future.

Further research is needed to fully confirm the proposed mechanism. This includes experimental observation of ketenes as intermediate (perhaps using time-resolved infrared spectroscopy⁶⁰), direct observation of NMAA by NMR or HPLC, and direct experimental observation of aniline or N-methyl aniline. Kinetic experiments in D₂O could be performed, to check for a deuterium isotope effect like that measured in methanol. In addition, the mechanism for AZM photolysis in other solvents also needs to be determined (although these are not significant in terms of environmental issues).

References

1. Fest, C.H; Schmidt K.J. In: Buechel KH (ed.) Chemistry of Pesticides. NY: John Wiley & Sons Inc., **1982**, 48-125.
2. McEwen, F.L.; Stephenson, G.R. The use and significance of pesticides in the environment. John Wiley & Sons Inc., New York, **1979**, 23-39.
3. Minton, N.A.; Murray, V.S.G. *Med. Toxicol.* **1988**, 3, 350-375.
4. Chemagro Division Research Staff. *Residue Rev.* **1974**, 51,123-180.
5. Mc Ewen, F.L.; Stephenson,G.R. The use and significance of pesticides in the environment. NY: John Wiley & Sons, Inc., 2nd Ed. **1989**, 43-61.
6. Federal Register **1989**, 54, 46082.
7. "Guthion and Imidan Hit Hard by FQPA", *The Fruit Growers News* , **2001**.
8. Azinphosmethyl: A Safe and Valuable Crop Protection Product for farmers," Letter from Bayer to the FQPA", **2001** available at: <http://www.panna.org/campaigns/caia/cropprofilebayer.dv.html>.
9. CBC news report: http://www.pei.cbc.ca/newsinreview/pei_fishkill.html.
10. Physical Chemistry, 5th ed, Ira N. Levine , McGraw-Hill, **2002**.
11. Wayne, C. E.; Wayne, R. P. Photochemistry, Oxford University Press, New York, **1996**.
12. Gilbert, A.; Baggot, J. Essentials of Molecular Photochemistry, Blackwell, Oxford, **1991**.
13. Wan, H.B.; Wong, M.K.; Mok, C.Y. *J. Agric. Food Chem.* **1994**, 42, 2625-2630.
14. Bossan,D.; Wortham, H.; Machlet, P. *Chemosphere* **1995**, 23, 21-29.
15. Kurtz, D.A., Long-Range transport of Pesticides, Lewis Press, Chelsea, MI, **1990**, 25-31.
16. Spencer, W.T.; Adams, J.F.; Shoup, T.D. *J. Agric. Food Chem.* **1980**, 28, 366-371.
17. Samsonov,Y.N.; Pokrovskii,L.M. *Atmos. Environ.* **2001**, 35, 2133-2141.

18. Baird, C. Environmental Chemistry, W.H. Freeman and Company , New York, 2nd ed. 1999.
19. Choughdry, G.G.; Webster,G.R.B. *Residue Rev.* **1985**, 96, 79-136.
20. Zepp, R.G.; Cline, D.M. *Environ. Sci.Tech.* **1977**, 11, 359-366.
21. Rosen,J.D. Environmental Toxicology of Pesticides, Academic Press, New York, **1972**, 435-447
22. Calvert, J. G.; Pitts, J.N. Photochemistry, Wiley, New York, **1966**, 1-830.
23. Kagan, J., Organic Photochemistry: Principles and Applications. Academic Press, London, **1993**.
24. Plane, J.M.C.; Zika, R.G.; Burns, L.A. *ACS Symp.* **1987**, 327, 250-260.
25. Zepp, R.G.; Baughman, G.L.; Schlotzhauer, P.F. *Chemosphere* **1998**, 10, 109-117.
26. Zepp, R.G.; Schlotzhauer, P.F.; Sink, R.M. *Environ. Sci. Tech.* **1985**, 19, 74-81.
27. Ross, R., Crosby, D.G. *Prep. Pap. Natl. meet.* **1975**, 15, 242-244.
28. Cook, W.; Otte, R. *J. Off. Agric. Chemists* **1959**, 41, 211-215.
29. Kurihara,N.H.; Crosby, D.G., Beckman,H.F. *Abstr. 152nd National Meeting, Amer. Chem. Soc., NY , secA*, **1966**, 47.
30. Crosby D.G. *Residue Rev.* **1969**, 25, 1-12 .
31. Schulz,K.R.; Lichtenstein,E.P.; Liang, T.T.; Fuhrmann,T.W. *J. Econ. Entomol.* **1970**, 63, 220-222.
32. Liang, T.T; Lichtenstein, E.P. *J. Econ. Entomol.* **1972**, 65, 315-321.
33. Liang,T.T; Lichtenstein, E.P. *J Agric. Food Chem.* **1976**, 24,1205-1210.
34. Abdou, W.M; Sidky, M.M; Wamhoff, H. *Z Naturforsch.* **1987**, 42b, 907-910.
35. Wagner, B.D. Fluorescence Studies of Supramolecular Host-Guest Inclusion Complexes. Chapter 1 in Hand book of Photochemistry and Photobiology, H.S. Nalwa, Ed., American Scientific Publishers, Stephenson Ranch, CA, **2003**, 1- 57.

36. Johnston, L.J.; Wagner, B.D. Physical Methods in Supramolecular Chemistry, Vol.8 of Comprehensive Supramolecular Chemistry, J.E.D. Davies, J.A. Ripmeester, Pergamon Press: Oxford, **1996**; Chapter 13.
37. Wagner, B.D. "Effect of Cyclodextrins On Guest Fluorescence", submitted Book chapter
38. Wagner, B.D.; Sherren, A. C.; Rankin, M. A. *Can. J. Chem.* **2002**, *80*, 1210-1216.
39. Spectrum Laboratories: Chemical Fact Sheet-Cas 86500;<http://www.speclab.com/compound/c86500.htm>.
40. Sherren, A.C. Honours Thesis, Investigations of Potential Fluorimetric Techniques for the detection of Azinphos-methyl in Natural Water Systems, UPEI, **2001**.
41. Laidler,K.J.; Meiser, J. H. Physical Chemistry, 2nd Edition, Houghton Mifflin Company, 1995.
42. Sanchez, F.G.; Gallardo, A.A. *Analyst* (Cambridge U.K.), **1992**, *117*, 195-198.
43. Felding, M.; Barcelo, D.; Heweg, A.; Galassi, S.;Torstensson, L.; Zoonen, P.V.; Wolter, R.; Angeletti, G. *In Water Pollut. Res. Rep.* **1992**, *27*, 1-136.
44. Chiron, S.; Abian, J.; Ferrer, M.; Sanchez-Baeza, F.; Messeguer, A.; Barcelo , D. *Environ. Toxicol. Chem.* **1995**, *14*, 1287-1298.
45. Mansour, M.; Thaller, S. ; Korte, F. *Bull. Environ. Contam. Toxicol.* **1983**, *30*, 358-364.
46. Wang, T.; Kadlac, T.;Lenahan, R. *Bull. Environ. Contam. Toxicol.* **1989**, *42*, 389-394.
47. Wang,T.C.; Hoffman,M.Z. *J. AOAC Int.* **1991**, *74*, 883-886.
48. Mikami,N.; Imanishi,K.,Y.; amada,H; Miyamoto,J. *J. Pestic. Sci.* **1985**, *10*, 263-272.
49. Freed, V.H.; Chiou, C.T.; Schmedding, D.W. *J. Agric. Food. Chem.* **1979**, *27*, 406-410.
50. Lee, P.W.;Fukuto,J.M.; Hernandez, H.;Steam, S.M. *J. Agric. Food. Chem.* **1990**, *38*, 567-573.

51. Coly, A.; Aaron, J. J. *Talanta*, **1994**, *41*, 1475-1480.
52. Coly, A.; Aaron, J. J. *Anal. Chim. Acta.*, **1998**, *360*, 129-141.
53. Patria, L.; Merlet, N.; Dore, M. *Environ. Technol.*, **1995**, *16*, 315-327.
54. Torrents, A.; Anderson, B.G.; Bilboulian, S.; Johnson, W.E. ; Hapeman, C.J. *Environ. Sci. Technol.* **1997**, *31*, 1476-1482.
55. Mill, T.; Hendry, D.G.; Richardson, V. *Science* **1980**, *207*, 886-887.
56. Haag, W.R.; Hoigne, J. *Environ. Sci. Technol.* **1986**, *20*, 341-348.
57. Rejto, M.; Saltzman, S.; Acher, A.J.; Muszkat, L. *J. Agric. Food Chem.* **1983**, *31*, 138-142.
58. Larson, R.A.; Weber, V. Reaction mechanisms in environmental organic chemistry. CRC Press, Boca Raton, FL **1994**, 359-413.
59. Sharshira, E.M. *Heterocyc. Commun.* **2003**, *9*, 527-534.
60. Wagner, B.D.; Arnold, B.R.; Brown, G.S.; Lusztyk, J. *J. Am. Chem. Soc.* **1998**, *120*, 1827-1834.